DESIGN AND DEVELOPMENT OF A

CONTROLLABLE WING LOADING UNMANNED

AERIAL SYSTEM

By

GARRET OAKLEY CASTOR

Bachelor of Science in Aerospace Engineering

Bachelor of Science in Mechanical Engineering

Oklahoma State University

Stillwater, Oklahoma

2017

Submitted to the Faculty of the
Graduate College of the
Oklahoma State University
in partial fulfillment of
the requirements for
the Degree of
MASTER OF SCIENCE
December, 2019

DESIGN AND DEVELOPMENT OF A

CONTROLLABLE WING LOADING UNMANNED

AERIAL SYSTEM

Thesis Approved:

Dr. Andy Arena

Thesis Adviser

Dr. Rick Gaeta

Dr. Kurt Rouser

ACKNOWLEDGMENTS

I must first start by saying that the work done to make this project successful was in no-way possible by one person. This project started with a team of 4 graduate students headed by Dr. Andy Arena, with many others joining along the way. I cannot take all the credit for this project as a whole.

I would like to thank Aron, Jeff, and Thomas, the other 3 of the original 4-man team. These 3 guys are responsible for making a wild idea turn into a fully functional and flight-proven aircraft. All 3 were heavily involved with all major decisions concerning designing, manufacturing, and testing the aircraft. I would also like to thank Marc Hartman who was the pilot willing to struggle with us along the way and fly our crazy, untested airplane.

I also have to thank 'The Don', Dr. Andy Arena, because he's the man that started this whole operation. Without his constant guidance, brilliance, and forgiveness when we made really dumb mistakes, we wouldn't have been able to pull it off.

Collin Boettcher is another man that deserves many thanks. I couldn't tell you exactly what his job description is, but he definitely had a hand in everything required to build and fly this airplane. Without Mr. Boettcher, we would have been hopelessly lost with things from trying to buy parts and jet engines to convincing the sponsors to keep funding the project.

Name: GARRET OAKLEY CASTOR

Date of Degree: DECEMBER, 2019

Title of Study: DESIGN AND DEVELOPMENT OF VARIABLE WING LOADING UNMANNED AERIAL SYSTEM

Major Field: MECHANICAL AND AEROSPACE ENGINEERING

Abstract: Vertical takeoff and landing (VTOL) unmanned aerial systems (UAS) offer all the benefits of wing borne flight without the need for conventional takeoff and landing (CTOL) infrastructure. There exists many effective VTOL UAS that utilize battery-powered rotors to provide vertical thrust. The problem with the existing UAS is that the VTOL capability is achieved at the sacrifice of speed, fuel/payload, and operational flexibility. Also, many of these UAS must transition from hover to horizontal flight which is both complex and risky.

The current research explores a new type of point launch and landing system that utilizes only liquid fuels, i.e. no electric powered rotors. Instead of exposed rotors, the new configuration has a turbojet engine mounted vertically inside the fuselage to provide vertical thrust. With the turbojet being 'hidden' from the freestream air, it mitigates the drag seen from the other configurations' rotors, allowing a higher top speed. Also, the new configuration bypasses the hover and transition phases of flight.

The vertical turbojet effectively changes the weight of the aircraft which allows it to have controllable wing loading (CWL), and therefore variable stall speed. With the jet at full power, the aircraft weighs virtually nothing and can takeoff from the launchpad with almost no airspeed. Likewise, on landing, the aircraft can slow to almost zero airspeed and land with little to no rollout. The CWL configuration has proved it possible to have approximately a 95% reduction in landing distance.

This paper describes the study, design, manufacturing, and testing of the point launch and landing CWL configuration. Two commercial off the shelf (COTS) UAVs were retrofitted with a CWL system to test the validity of the idea and the necessary systems. Following the proof of the idea, a composite UAS with a maximum takeoff weight of 50 lb. was designed, manufactured, and flown. It successfully demonstrated both a point launch and point landing while being capable of reaching speeds of up to 100 mph, more than double the top speed of some other VTOL UAS in its weight class.

TABLE OF CONTENTS

CHAPTER PAGE

CHAPTER PAGE

CHAPTER PAGE

LIST OF TABLES

TABLE PAGE

LIST OF FIGURES

FIGURE PAGE

FIGURE PAGE

FIGURE PAGE

CHAPTER I

INTRODUCTION

THE development of aircraft with vertical takeoff and landing (VTOL) capabilities has been of interest and consideration since the development of reliable, high thrust-to-weight jet engines in the late 1940s and early 1950s [1]. Being able to take off and land like a helicopter while also being able to fly as long and as fast as fixed-wing aircraft would benefit both the military and civilian sector [2]. Jay Gundlach, the author of *Designing Unmanned Systems*, provides a more scientific definition of VTOL by saying, “VTOL vehicles use vertical thrust to provide the lifting force during takeoff and landing operations. Vertical takeoff and vertical landing may be dynamic maneuvers, though most VTOL vehicles are also capable of hovering flight. VTOL platforms are generally able to operate with zero forward airspeed, which necessitates lift through means other than the wings” [3, p. 462].

While true VTOL and short takeoff and landing (STOL) are different, they share many performance requirements. To accommodate this, all further discussion will refer to vertical or near-vertical takeoff and landing aircraft as vertical/short takeoff and landing (V/STOL). One of the main reasons that V/STOL is so difficult to achieve in fixed-wing aircraft is that the vertical/short takeoff and landing “is not to be accomplished at a sacrifice in the cruising performance of the aircraft” [4, p. 1]. This means that even though there is added weight and complexity, the aircraft still needs to be able to perform similarly to other aircraft in its class. VTOL aircraft can also be defined as "aircraft with vertical takeoff and landing capabilities and cruising speeds equal to those of ordinary fixed-wing aircraft […]" [4, p. 4]. This speed requirement along with the "conflicting requirements of compressibility effects and retreating blade stall" prevents helicopters, autogyros, multicopters, and other rotorcraft from being considered as V/STOL aircraft.

The development of full-scale V/STOL aircraft began in the late 1940s and early 1950s, shortly after the advent of turbojet engines; whereas the development of V/STOL unmanned aerial vehicles (UAVs) has only just begun within the last 10 years. This recent development is due to modern advances in UAV technology. Components like electric motors, batteries, miniature turbojet engines, and small, reliable flight control computers have never been as affordable and efficient as they are today. This advancement in UAV technology has stemmed from an increase in the interest of UAVs from the military that wants a mission-specific aircraft and the everyday hobbyist looking for the next cool thing. The market for point launch and recovery UAVs is rapidly expanding because they offer all the advantages of conventional takeoff and landing (CTOL) aircraft while having a much smaller ground operations radius. Instead of needing a smooth runway, the aircraft only need a small, open space free from overhead trees, power lines, and other obstructions. The commercial sector has also seen a large increase in interest with V/STOL UAVs. Companies like DHL and Amazon are developing delivery systems that hinge on the use of V/STOL UAVs. Also, Walmart is developing a system that will allow UAVs to shuttle products between different departments inside the store [5].

There are many specific requirements and complex systems and integration issues that stand in the way of making V/STOL UAVs widely used. This introduction will serve as means to weigh the pros and cons of V/STOL, explain the basics of V/STOL aerodynamics, discuss the required controls and systems, compare the different configurations, and list the requirements to achieve V/STOL.

Benefits of V/STOL

The first and most obvious reason to design and develop a V/STOL aircraft is the reduction in ground operations radius. Coinciding with a reduced ground operations radius is a reduction in the required ground infrastructure. Not only can the need for a runway be eliminated, but so can all the money, time, security, and maintenance that a runway requires.

Aircraft designed for V/STOL do not need the wings to be sized for takeoff and landing, since they only require a small amount, if any, of aerodynamic lift for these stages of flight. This reduces the overall size of the wing planform which reduces parasitic drag and weight.

For UAVs, the concept of V/STOL opens the possibility of point launches and landings. Depending on the size of the UAV, it could be launched, on the go, from the back of a truck or the deck of a small ship. This would be beneficial in combat, extreme weather tracking and forecasting, or any other situation where data must be collected on the move.

Drawbacks of V/STOL

The implementation of V/STOL capability into an aircraft greatly increases its design complexity. Many existing V/STOL aircraft, both full-scale and unmanned, use multiple propulsion systems. One system is used to provide vertical thrust for takeoff and landing while the other system is used to provide thrust for horizontal flight. Having multiple propulsion systems means having multiple, sometimes different, fuel systems, which leads to a weight penalty [3, p. 463]. Also, the pilot not only has to control multiple engines, but multiple engines providing thrust in different directions. For single propulsion system V/STOL aircraft, the design complexity stems from having to vector the thrust. Thrust vectoring is especially difficult for the transition mode of VTOL which will be discussed later.

Along with increased design complexity, there is an increase in integration complexity. Aircraft, especially UAVs, are already low on available space and V/STOL requires the integration of secondary propulsion systems with their accompanying fuel systems and/or the integration of thrust vectoring controls and ducting. The integration problems arise from having to add support structure for the additional systems and having to include more wiring and plumbing while also maintaining appropriate thermal management and center of gravity (CG) location.

Another drawback of V/STOL is that at the low forward speeds seen during takeoff and landing, the aircraft cannot utilize its aerodynamic controls that are so heavily relied upon during forward flight. This raises the need for an alternative control and stabilization system.

V/STOL Configurations

Since the development of V/STOL technology, more than 60 years ago, scientists and engineers have come up with many different configurations to achieve vertical takeoffs and landings. Below is a short description of the five main configurations. This is not an exhaustive list and each configuration has variations within itself.

Tail-Sitter

The tail-sitter configuration is where the aircraft sits on its tail with the thrust axis being orthogonal to the ground. This allows the aircraft to take off vertically while using the same propulsion system for horizontal flight. An example of a tail sitter is the Convair XFY Pogo shown in Figure 1.1.

Figure 1.1 Convair XFY Pogo [6]

Tilt-Wing

The tilt-wing configuration functions by rotating the entire wing, with engines mounted to it, slightly more than 90^0 while the fuselage remains horizontal in a level flight attitude. An example of a tilt-wing is the Hiller X-18 shown in Figure 1.2.

Figure 1.2 Hiller X-18 [7]

Tilt-Rotor

The tilt-rotor configuration functions similarly to the tilt-wing but instead of rotating the entire wing, only the engines are rotated. In this configuration, the aircraft and the wing remain in a horizontal level flight attitude. A well-known and currently in service example of the tilt-rotor configuration is the V-22 shown in Figure 1.3.

Figure 1.3 Bell Boeing V-22 [8]

Submerged Fan

In this configuration, fans are horizontally submerged in the wings. The wing can act like a duct around the fan which increases static thrust. Once enough forward speed is gained, a cover slides over the fans to regain the lost wing area. The Ryan XV-5 is an example of the submerged fan configuration and can be seen in Figure 1.4.

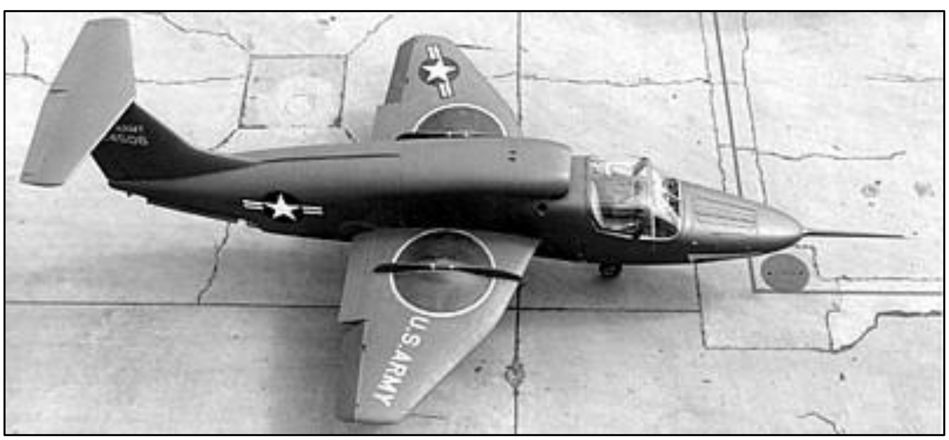

Figure 1.4 Ryan XV-5 [9]

Direct Thrust

In the direct thrust configuration, engines provide vertical thrust by either thrust vectoring or being oriented vertically. This configuration has three sub-configurations: lift/cruise, direct lift, and composite. Schematics of the sub-configurations can be seen in figure 1.5. The lift/cruise configuration uses the same engines for horizontal thrust as for vertical thrust. The engines can rotate to allow the aircraft to transition to horizontal flight. The direct lift configuration is where there are separate engines for vertical thrust and horizontal thrust. Normally, the vertical thrust engines will be turned off once enough forward speed is gained to provide sufficient aerodynamic lift. Lastly, the composite configuration is a combination of both lift/cruise and direct lift. In this configuration at least one of the engines can rotate to provide vertical and horizontal thrust while the other engines only provide vertical thrust. Figure 1.6 shows the F-35B, an example of the composite direct thrust configuration.

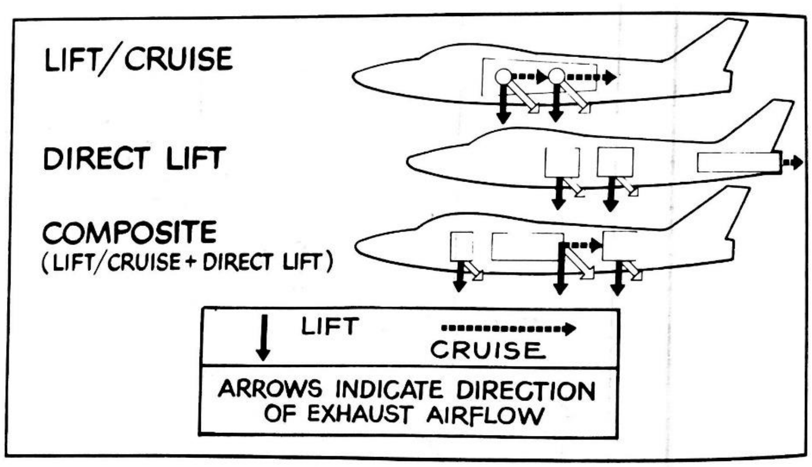

Figure 1.5 Direct Lift Configuration [10]

Figure 1.6 Lockheed Martin F-35B [11]

V/STOL Requirements

Giving an aircraft the ability to take off and land vertically or near vertically requires adding new requirements. The first and most important requirement is that the aircraft must have a thrust to weight ratio greater than one. Most non-V/STOL aircraft with a thrust to weight ratio greater than one are designed for supersonic flight. All that excess thrust is necessary to accelerate the aircraft through the speed of sound which shows how much extra energy is required for V/STOL. Generally, it is desirable to have a thrust-to-weight ratio greater than one with the minimum acceptable ratio being 1.05 [12]. The excess thrust is necessary to allow the aircraft to climb off the deck. While the acceptable ratio is 1.05, it is desirable to have a thrust-to-weight ratio of 1.3 to give some cushion in case of an emergency and to allow some of the thrust to be diverted to help with control.

Unlike CTOL aircraft, V/STOL aircraft cannot utilize aerodynamic controls during takeoff and landing due to lack of forward airspeed; therefore, the attitude of the aircraft has to be controlled by thrust modulation. The two main types of thrust modulation used for control during takeoff and landing are reaction control systems (RCS) and thrust vectoring (TV). An RCS passes bleed air from the main engine[s] through small thrusters pointing downward in the wings and/or nose and tail [12, p. 769]. A TV system is an adjustable nozzle at the exit of a jet engine that can divert the engines' thrust to counteract any unwanted pitching or rolling.

Another V/STOL requirement is having to carry extra fuel for landing. Conventional aircraft normally land with their engine[s] at a low power setting whereas V/STOL aircraft land with their engine[s] at or near full power. This, along with the thrust modulation system, adds to the overall propulsion system weight. Also, the additional required systems need space, which increases the internal volume requirement of the aircraft, which makes it heavier [12, pp. 771-772].

Implementation Problems

There are several problems encountered when trying to achieve vertical/short takeoffs and landings and each must be addressed or at least acknowledged. The three fundamental problems are weight, thrust matching, and balance. Another issue is the transition from vertical to horizontal flight and vice versa for landing. Some other issues that mostly apply to the jet direct lift configuration are hot gas ingestion (HGI), suckdown, fountain lift, foreign object debris (FOD), and ground erosion.

The necessity for a much higher than normal thrust-to-weight ratio in V/STOL designs forces the reduction of aircraft weight to be much more crucial than with CTOL designs. There are three notable points to make about V/STOL designs in terms of the weight problem:

1) The lower than usual structure fraction, which reflects deliberate structural reductions to help lower weight.
2) The higher than usual powerplant fraction, which reflects the considerably higher installed thrust to weight ratio.
3) The lower than usual fuel fraction, which reflects the relative lack of volume available for fuel […] [13].

Aircraft designers are already always pushing for maximum weight reduction. Designing a V/STOL aircraft means adding more weight through additional propulsion and control systems while also needing to reduce the weight even more to achieve a higher thrust-to-weight ratio.

Thrust matching is difficult because the thrust to weight ratio for V/STOL aircraft needs to be greater than one. This requirement means that the engines would be oversized for cruise where they would be operating away from the maximum efficiency point, meaning higher fuel consumption and having to carry excess engine weight. For this reason, many V/STOL designs incorporate separate lift engines [12, p. 755]. Utilizing separate lift engines means that the cruise engine can be sized and optimized for conventional, wing-borne flight, which extends the aircraft's range and endurance due to a more efficient specific fuel consumption (SFC).

Balancing an aircraft during vertical or near-vertical takeoffs and landings is a complicated problem. The only way to avoid the necessity of having multiple points of vertical thrust is to put the source of vertical thrust at the aircraft’s CG which creates an inverted pendulum problem. If the single source of vertical thrust is not at the CG, then there will be a net moment on the aircraft causing it to pitch or roll. This net moment must be balanced by another point of vertical thrust which means ducting from the main engine[s] or a separate engine altogether. Either choice adds weight and complexity to the design. Figure 1.7 depicts the balance problem.

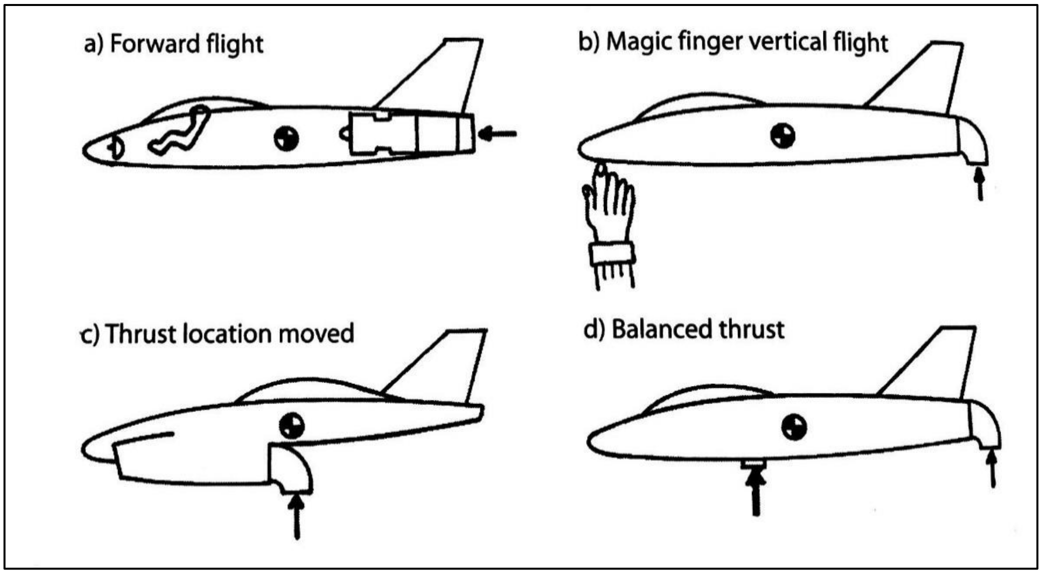

Figure 1.7 The Balance Problem [12]

For all aircraft, FOD can be a dangerous problem if not managed properly but V/STOL aircraft must be especially careful since they have some component of vertical thrust acting straight at the ground. The management of FOD is even more difficult for designs that utilize a vertical thrust turbojet because the hot gas impinging on the ground creates a wall jet region with a shear stress distribution great enough to move solid objects and erode the surface of the ground [14]. If the wall jet picks up dirt, rocks, and/or pieces of asphalt and recirculates them into the engine, it could ruin the engine and potentially the whole aircraft. The effect of the hot, fast-moving exhaust gas eroding the surface is called ground erosion. Although ground erosion must be considered, it can be easily and effectively dealt with. Generally, small translational velocities can cause drastic reductions in ground erosion effects. Also, if takeoffs and landings are limited to concrete or other solid platforms, there are almost no ground erosion effects [15]. The hot gas can also set fire to vegetation. A ground fire could be dangerous to the aircraft, ground crew, and ground facilities so precautions must be taken to prevent and manage a ground fire. A visual representation of ground erosion and ground fire can be seen in Figure 1.8.

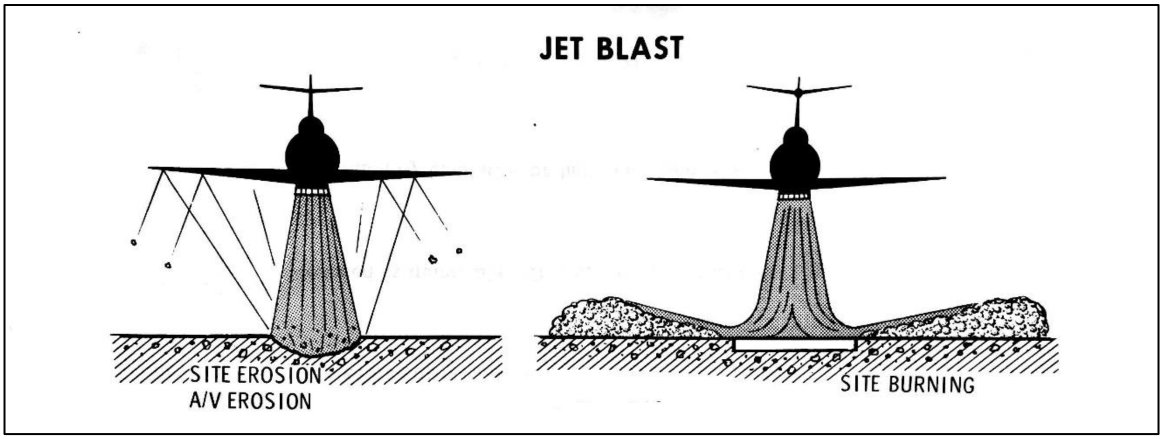

Figure 1.8 Ground Erosion [16]

Paralleling the concern for FOD ingestion is the concern for recirculation and HGI. “Recirculation describes the motion of air around a jet lift V/STOL aircraft when hovering in ground effect” [14]. There are three main contributors to recirculation: buoyancy effect, impingement of multiple wall jets, and the interaction of wall jets with relative wind. Since the jet exhaust is at a much higher temperature than ambient air, there is a natural tendency for the hot gas to rise, i.e. the buoyancy effect. If the rising gas is re-ingested into the engine, there will be a reduction in engine performance; another reason to have a thrust-to-weight ratio of 1.3 or higher.

The effect of relative wind piggybacks on the buoyancy effect because the relative wind can push the rising hot air back towards the intake which increases the amount of hot gas that gets re-ingested. Figure 1.9 depicts the different modes of recirculation and HGI.

The impingement of multiple wall jets can cause a fountain effect that pushes the hot air upwards, which increase the amount of hot gas that is ingested. Also, this hot air underneath the aircraft should be carefully monitored since it could cause undesirable heating.

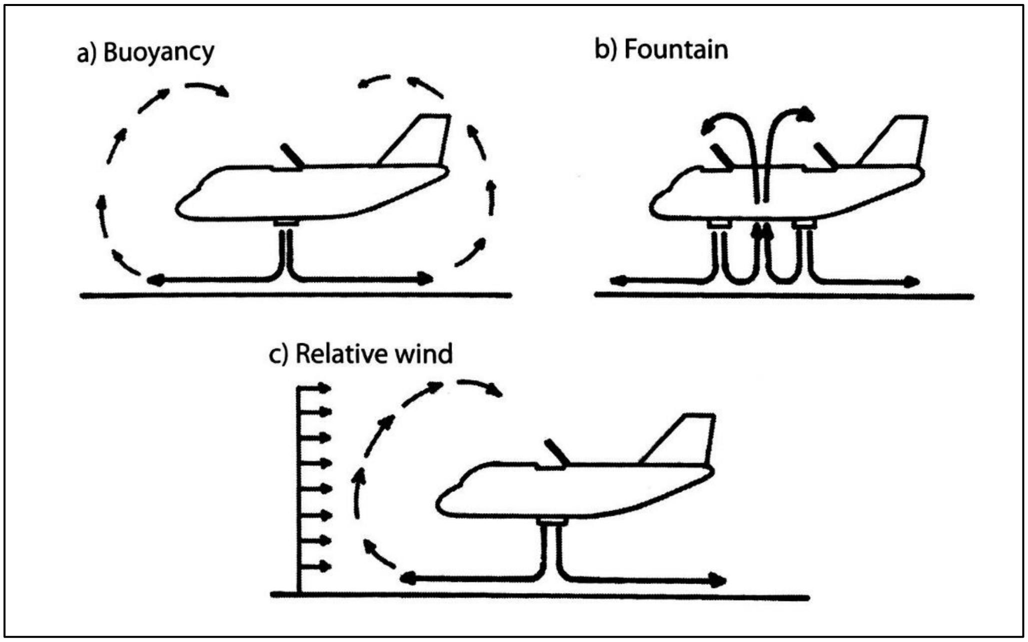

Figure 1.9 Recirculation and HGI [12]

Two more phenomena that can happen when using a lift jet for V/STOL are suckdown and fountain lift. The jet exhaust that provides vertical lift also entrains some of its surrounding air. This entrained air pulls air from around the aircraft and accelerates it downward. Due to viscous effects, this downward accelerating air creates a vertical drag force known as suckdown, which requires more thrust to get off the ground.

Aircraft with multiple lift jets can sometimes experience the opposite of suckdown. As the wall jets from multiple engines impinge on each other under the aircraft they can push up on the aircraft creating a net upward force known as fountain lift. This fountain lift is small relative to the amount of lift provided by the jet, but it can be enough to cancel out the suckdown. Not only can suckdown and fountain lift alter the net vertical thrust, they can also increase the instability of the aircraft while in ground effect. As the aircraft gets higher, the fountain lift effect decreases which changes the effective vertical thrust, which, if not accounted for, can cause the pilot to lose control of the aircraft or cause pilot induced oscillations (PIO). The opposite can happen on landing. As the aircraft approaches the ground there is an increase in effective vertical thrust which could trick the pilot into altering the throttle setting and thus potentially causing loss of control or PIO. A visual representation of suckdown and fountain lift can be seen in Figure 1.10.

Achieving vertical or near-vertical takeoffs and landings has many advantages but is also a very complicated design problem. Each of these problems needs to be understood and the designers need to know how these problems affect the aircraft's dynamics and performance during takeoff and landing.

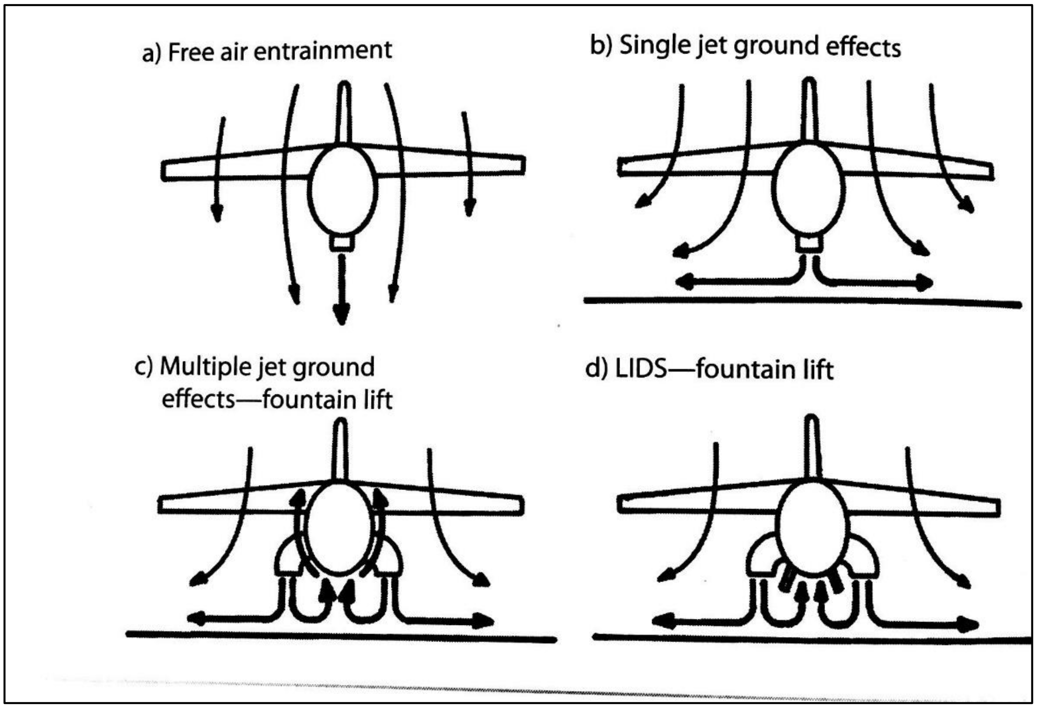

Figure 1.10 Suckdown and Fountain Lift [12]

Full-Scale V/STOL Aircraft Study

The early 1950s saw the first attempts at jet-powered VTOL aircraft. The Ryan X-13 test rig, Figure 1.11, was basically a vertically oriented jet engine with some VTOL controls strapped to it. In 1951 it made its first free hovering jet flight that was controlled remotely and in 1953 it made its first piloted hovering jet flight. Neither of the flights actually flew conventionally but they proved the possibility of using a jet engine to power vertical takeoffs and landings [17, p. 71].

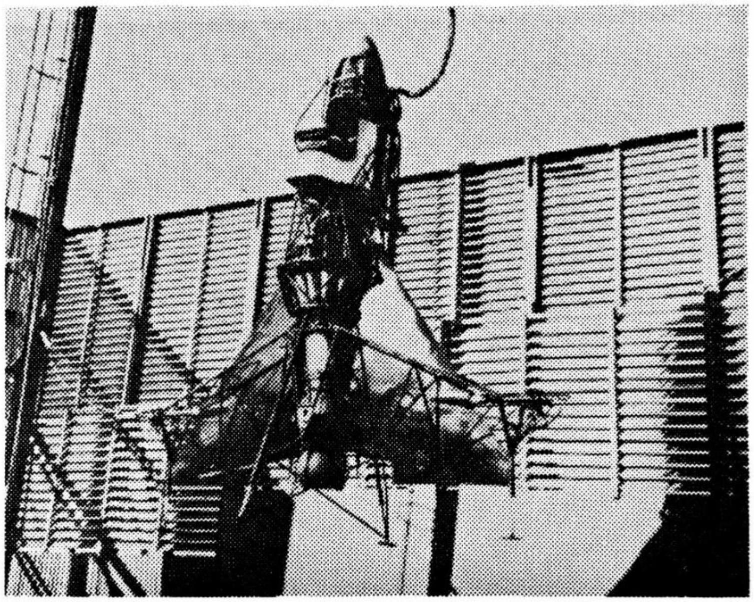

Figure 1.11 Ryan X-13 Test Rig [10]

Since then, there have been many different prototype aircraft designed to demonstrate different configurations and systems. In 1958, Bell's X-14, Figure 1.12, completed a transition from vertical to horizontal flight. This fully realized the possibility of an aircraft that could fly like a jet and take off and land like a helicopter.

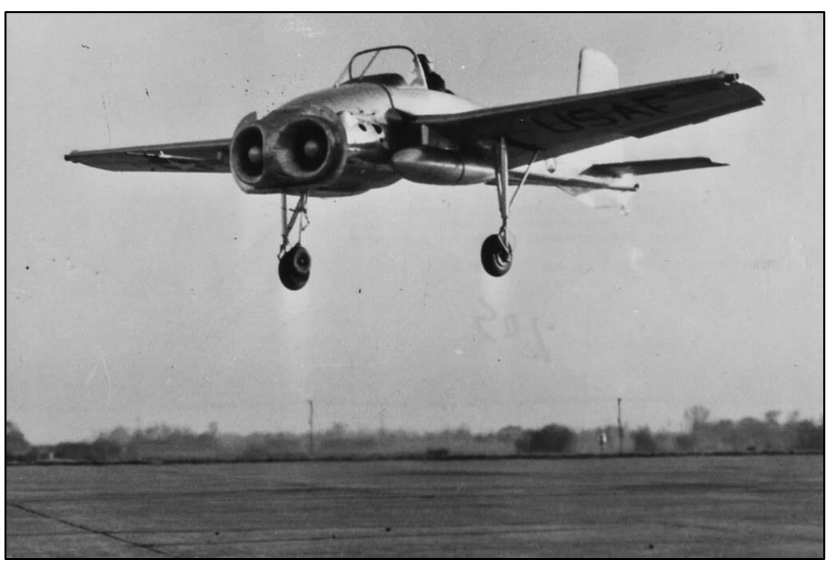

Figure 1.12 Bell X-14 [18]

The success of the X-14 encouraged Hawker to develop the P.1127 shown in Figure 1.13. "The P.1127 is a turbofan-powered deflected-thrust type VTOL aircraft utilizing a single BS 53 Pegasus engine" [17, p. 80]. It deflected thrust from the engine through two nozzles on each side of the aircraft. Each nozzle could rotate to deflect thrust downward and aft. It demonstrated its complete vertical to horizontal flight transition in 1961.

Figure 1.13 Hawker P.1127 [19]

The Hawker P.1127 is the predecessor to the well-known McDonnell Douglas (now Boeing) AV-8B Harrier II, nicknamed the Harrier Jump Jet. The AV-8B II, shown in Figure 1.14, was the first fully operational jet V/STOL aircraft. Its first successful flight was in 1981 and it entered service with the United States Marine Corps in 1985 [20]. Its vertical lift system is pretty much identical to the P.1127 with some minor changes that increased stability. The AV-8B II proved the viability of the lift/cruise V/STOL configuration which then led to the development of Lockheed Martin's F-35B, shown in Figure 1.15.

Figure 1.14 McDonnell Douglas AV-8B Harrier II [21]

The F-35 is a 5th generation, multi-role, supersonic fighter with the ‘B’ variant having short takeoff and vertical landing (STOVL) capabilities [22]. It is arguably the most advanced fighter aircraft in the world due to its stealth characteristics and advanced avionics and sensor packages. It has many attributes that make it a high-tech superior fighter but, for this research, the most interesting attribute is its STOVL capability. Like the P.1127 and the AV-8B II, the F-35B is set up in the lift/cruise configuration. It utilizes a single Pratt & Whitney F135 engine with a Rolls-Royce LiftSystem. The Rolls-Royce LiftSystem is comprised of a lift fan that is shaft driven by the F135 engine and a thrust vectoring nozzle that allows the jet exhaust to be deflected downward [23]. The lift fan is in front of the CG of the aircraft and the jet nozzle is aft of the CG and they work together, with reaction control jets in the wings, to achieve short takeoffs and vertical landings.

Figure 1.15 Lockheed Martin F-35B [24]

UAS V/STOL Aircraft Study

As mentioned earlier, the development of fixed-wing V/STOL UAS has only begun within the last 10 years, as did the development of small UAS sized turbojet engines. Ten years is not much time for projects to develop and ideas to get passed along. The lack of existing jet V/STOL UAS demonstrates the infancy of the concept. There are many UAVs that utilize the tilt-wing, tilt-rotor, or hybrid direct thrust configuration but almost all of them are electric or hybrid-electric. Table 1.1 shows a list of some of these UAVs.

Company	Aircraft	MTOW [lb]	Wingspan [ft]	Max Payload [lb]	Cruise Speed [mph]	Max Speed [mph]	Endurance [hr]	VTOL Endurance [min]	Configuration
Quantum Systems	Trinity F90	11	7.5	1.5	38		1.5	N/A	Tilt-rotor
DHL	Parcelcopter 3.0	31	N/A	N/A	43		0.17	N/A	Tilt-wing
Alti	Transition	39.7	9.8	3.3	45		12	3	Hybrid: boom rotors and pusher
NorthSea Drones	STOVL UAV	55	6.5	3.3	155	217.5	N/A	2	Direct Lift (requires launcer)
L3	FVR-90	117	N/A	8-22	75		12-22	N/A	Hybrid: boom rotors and pusher
Israel Aerospace Industires	Panther	143	N/A	18	80		6	N/A	External Direct Lift
Arcturas	Jump 20	210	18.5	60(incl. fuel)	83		9-16	N/A	Hybrid: boom rotors and tractor
Drone Tech	AV-1 Albatross	300	17.7	77(incl. fuel)	77	86	12-18	2.5	Hybrid: boom rotors and tractor/pusher
ULC	VTOL Drone	N/A	10	10	50		1.5	N/A	Hybrid: boom rotors and pusher
Aurora Flight Sciences	Excalibur (P.O.P. hover only)	720	10	N/A	N/A	23	N/A	3	Direct Lift

Table 1.1 V/STOL UAS

Some of the cells in Table 1.1 are marked with ‘N/A’ due to the lack of available information. Many of these UAVs are still in development or not widely sold so their listed specifications are sparse.

Electric V/STOL aircraft have been proven to work successfully at the sacrifice of speed, excess weight, and efficiency. Most of the successful V/STOL UAVs are fixed-wing aircraft with booms and rotors attached to them like the Alti Transition in Figure 1.16. These booms and exposed rotors cause a drag penalty during forward flight which reduces the overall speed and efficiency of the aircraft. Another issue with the fixed-wing rotor configuration is excessive battery weight. For example: if the aircraft uses half of its battery life for takeoff, it still has to fly with those now useless and heavy batteries unless it has an alternator which adds more weight. The configurations that use liquid fuels lose weight during takeoff due to fuel burn which increases their cruise efficiency.

Regardless of the configuration, V/STOL comes with a weight penalty. The fixed-wing rotor configuration comes at a higher weight penalty than the direct lift-jet type due to its many extra systems. The direct lift-jet type only requires an engine, fuel, fuel pump, fuel tank, and a TV unit; whereas the fixed-wing rotor typed requires additional booms, four electric motors, four electronic speed controllers (ESC), four propeller, extra batteries, and extra wiring.

Figure 1.16 Alti Transition [25]

Another drawback of the fixed-wing rotor configuration is low wind tolerance. Most of the aircraft with booms and rotors cannot take off if there is a crosswind due to the rotors not being able to stabilize the aircraft, which limits them to stationary, low-wind takeoffs [26]. However, the direct thrust configuration aircraft, like the F-35, have better takeoff and landing performance if there is wind. With these aircraft, the V/STOL propulsion systems are buried within the aircraft which means they do not cause increased drag and instability with an increase in wind speed. Also, the direct lift type aircraft spend as little time as possible in hover and try to transition to wing-borne flight as soon as possible. With greater wind, the aircraft sees a higher net airspeed which reduces their hover time and helps them achieve wing-borne flight faster.

With the fixed-wing rotor configuration, there is little room for configuration change unless the booms are easily detachable. Even still, many of these aircraft do not have the type of landing gear capable of CTOL which limits them solely to V/STOL. The direct thrust configuration aircraft usually have CTOL capable landing gear which allows for a multi-platform airframe. For instance, the V/STOL systems could be removed to allow for additional payload and/or fuel for extended missions.

Throughout the literature that was searched, there were only two UAVs that utilized a turbojet engine to provide vertical thrust. The first of which was Aurora Flight Sciences' Excalibur. The Excalibur, shown in Figure 1.17, was a proof-of-principle (POP) vehicle that demonstrated a successful vertical takeoff and landing on June 24th, 2009 for the Defense Advanced Research Projects Agency's (DARPA) VTOL X-Plane project [27] [28] [29]. It utilizes a turbojet on a swivel with three lift fans to provide vertical thrust for takeoff, hover, and landing. The turbojet can rotate from vertical to horizontal for transition to horizontal flight. The POP vehicle never made a horizontal flight; its purpose was to test and validate the VTOL system.

Figure 1.17 Aurora Flight Science Excalibur [30]

The other UAV that uses a turbojet for vertical lift is North Sea Drones' STOVL Drone, shown in Figure 1.18. The information about this aircraft was limited to a short fact sheet provided by North Sea Drones and a few news articles. The STOVL Drone was very similar to the Excalibur in terms of propulsion system but both designs varied largely in scale and overall shape. The STOVL Drone utilized a turbojet on a swivel and three lift fans: one in each wing and one in the nose. It was launched from a launcher for takeoff and then the hatches covering the lift fans were jettisoned before the turbojet rotated into a vertical position for landing [31] [32]. Both UAVs have demonstrated the feasibility of using a turbojet to provide vertical thrust in the composite configuration (lift/cruise + direct lift). Also, both designs rely heavily on electric fans for landing. So, as of the current date, there does not exist a UAV with V/STOL capabilities that relies solely on hydrocarbon fuels for propulsion (to the best of my knowledge).

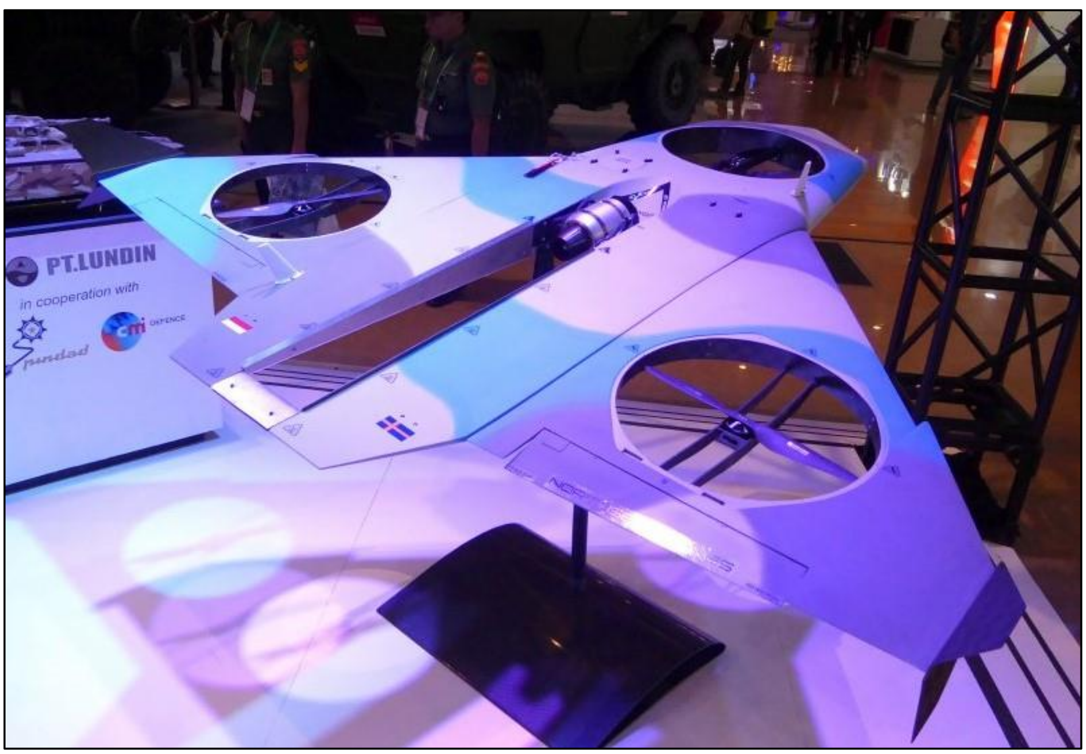

Figure 1.18 North Sea Drones STOVL Drone [33]

The fixed-wing rotor configuration is a proven configuration with high endurance, but it has many performance losses due to the attached booms and rotors. For this reason, the current research will explore the use of the direct lift configuration using only liquid fuels for the propulsion systems with the vertical propulsion system embedded in the fuselage.

Research Goals

There are many benefits that can be obtained from having a UAV with V/STOL capabilities once all the accompanying V/STOL problems are solved. Many successful V/STOL designs exist but most of them rely heavily, if not entirely, on electric power. The problem with electric power is that batteries have a low energy density relative to that of liquid hydrocarbons which makes a heavier aircraft. Also, many of the existing UAVs utilize the boom-rotor configuration which causes extra drag and lowers top speed and efficiency.

The goal of this project is to develop a low drag, high speed, point launch and recovery UAS that uses only liquid fuels and can operate in wind speeds of up to 50 mph. Most UAS that are capable of high speeds are not capable of point launches and landings, and most UAS that are capable of point launches and landings are not capable of high speeds. This research goal was created to bridge the gap between high speed and point launch and recovery UAS.

The conceptual design is a UAV that utilizes the direct lift V/STOL configuration while it is not a true V/STOL aircraft. Since hovering costs a great deal of fuel and stabilization effort; and the transition from vertical to horizontal flight is difficult and risky [34], the conceptual design will skip the hover and transition phases altogether. The aircraft will instead immediately begin flying with almost zero airspeed by utilizing a lift turbojet to provide vertical thrust to decrease the effective weight of the aircraft. With the jet changing the effective weight, the aircraft has a controllable stall speed due to the *Controllable Wing Loading (CWL).* At almost zero weight, the stall speed is almost zero which means the aircraft can begin wing-borne flight with little forward velocity.

In addition, the conceptual design will benefit from a non-zero wind because a non-zero wind results in a perceived airspeed which will give the aircraft more lift. The wind will be even more advantageous during landing because the extra drag will help slow the forward motion while also increasing lift which will help allow point landings.

This aircraft will also be capable of being used in multiple configurations. The CWL system can be removed to allow room for more fuel and/or payload when there is a suitable runway for conventional takeoffs and landings. Also, when there is access to a runway, the aircraft could be ‘overloaded’ to where its vertical thrust-to-weight ratio is less than one. This configuration would prevent point launches but would still give it STOL or STOVL capability.

The overall design will center around a miniature turbojet jet engine mounted vertically in the fuselage to provide vertical thrust for takeoff and landing with an internal combustion (IC) engine providing thrust for forward flight. A turbojet was chosen over a ducted fan for is high thrust-to-weight ratio and its ability to expend weight through burning fuel during use.

For takeoff, the aircraft will be tethered to a launch platform where both the main internal combustion (IC) engine and the lift-jet will be producing the required takeoff thrust. When ready, the aircraft will be released and will immediately begin climbing at a roughly 45^0 angle until its forward airspeed is greater than its no-lift-jet stall speed. At this point, the aircraft could fly on aerodynamic lift without the need for the jet and the pilot could then turn off the jet and fly the mission. For landing, the pilot will restart the jet and fly a predetermined pattern to reach the appropriate airspeed and altitude. With the jet at nearly full throttle, the aircraft will effectively only weigh a few pounds so it will approach the ground well below its no-lift-jet stall speed.

Right before landing, the pilot will flare, with full flaps, and try to point land with minimal rollout.

Outline

The subsequent sections of this paper will explain the design, manufacturing, and testing of the aircraft. Chapter 2 details the design of the aircraft including the proof of concept vehicle, aerodynamic sizing, propulsion systems, electronics systems, landing gear, and structural configurations. Chapter 3 explains the launch and recovery methods as well as the launch system and the ground control station. Chapter 4 follows by providing a detailed explanation of the whole manufacturing process from the fabrication of tooling to the final aircraft assembly and component integration. Chapter 5 explains the testing procedures of the individual components and the full aircraft, and the results from the flight tests. Finally, Chapter 6 lists the conclusions of the project and recommendations for further research.

CHAPTER II

DESIGN OF THE LOCUST

The development of Locust began when Oklahoma State University (OSU) approached the head of the UAV design and development program with a new VTOL project. The project required the rapid development of a VTOL capable, group two UAV. Group two UAVs are classified as having a maximum takeoff weight (MTOW) of less than 55 lbs. and a maximum speed of less than 250 kts. Its main mission was to have the ability to be rapidly deployed in any type of terrain to allow military personnel to calibrate radars for the detection and tracking of small, fast-moving UAVs. Since UAV technology is becoming more readily available and reliable, the military now has a greater interest in threats from UAVs. One of the problems with current radar systems is being able to detect and track small, fast UAVs. The proposed design will help military personnel be able to tune their radars and accompanying systems to be able to detect, track, and eliminate small, fast UAVs.

Initial Design Requirements

The customer had thirteen specific operational and performance requirements. The hardest and most complicated requirement to realize was that the aircraft had to be capable of point launches and landings. The rest of the thirteen requirements were:

1) Point launch and landing capable

2) Maximum airspeed of at least 100 mph (87 kts)

3) Cruise flight time of at least 60 minutes

4) Rapid deployment time of 60 minutes or less

5) Payload of at least 3 lb.

6) Launch/deployment system and aircraft must fit in the bed of a pickup truck

7) No capture/recovery system

8) Mission operations require at most 5 personnel

9) Propulsion systems must be fueled by liquid hydrocarbons (batteries only for avionics)

10) Return to loiter (RTL) capable in case of loss of telemetry

11) Maximum takeoff weight (MTOW) of 50 lb. or less

12) Autonomous flight capability

13) Carry two, 6 in. radar reflector prisms (fore and aft)

Mission

Locust's primary mission is to fly patterns to calibrate radar systems for the detection and tracking of small, fast-moving UAVs. The V/STOL requirement stems from the radar systems being on terrain that is not always suitable for conventional takeoffs and landings. Figure 2.1 shows a basic concept of operations (ConOps) for Locust. Once the aircraft is fully developed, the middle section of the ConOps could vary drastically while keeping the highly beneficial CWL capability. Also, the CWL system could be taken out and replaced with fuel to increase mission time or additional payload to perform various functions.

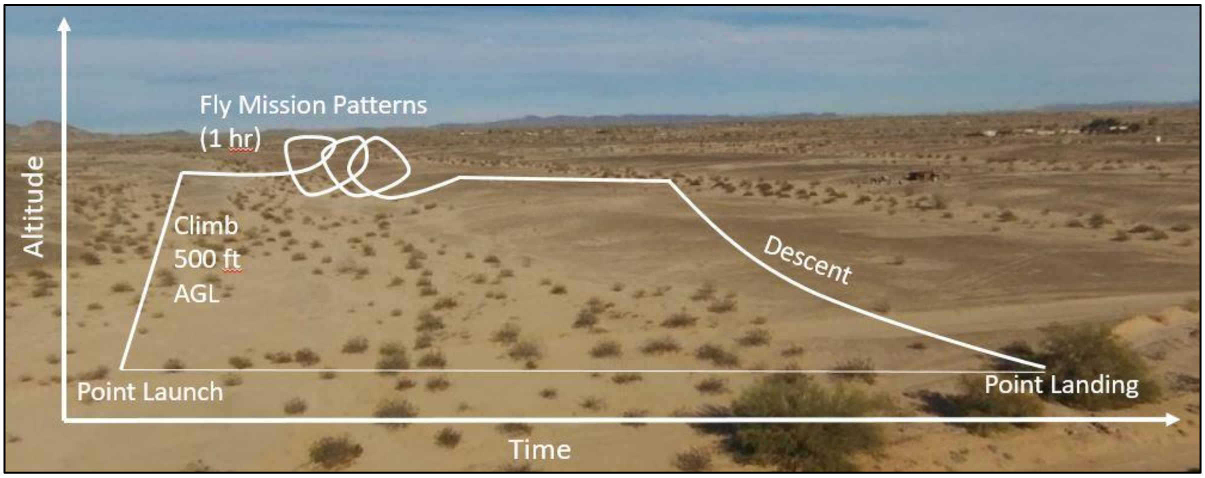

Figure 2.1 Locust CONOPS

With high speed being one of the primary mission requirements, there was a need to minimize the aircraft's drag as much as possible. This is one of the reasons that the internal lift jet was chosen over the boom-rotor configuration. Since drag increases as a function of velocity squared, the exposed booms and rotors create much higher drag at the high speeds that inhibit fuel efficiency. The aircraft could be designed to reach the required top speeds with the booms and rotors, but it would need a larger main engine which would increase weight and fuel consumption, making the overall system less efficient.

Initial Design Configuration

The most impactful design decision was to utilize the direct lift configuration: a fixed orientation turbojet providing vertical thrust and an IC engine providing thrust for horizontal flight. A turbojet was chosen for vertical lift due to its high thrust-to-weight ratio and relatively compact size. The propulsion systems will be discussed in depth in the Propulsion Systems section. The direct lift configuration was chosen over the lift/cruise configuration due to the weight restriction. The lift/cruise configuration would require a strong, mechanical system of brackets, hinges, and motors that could rotate an engine producing 50 lb. of thrust. It would also require a network of ducting to divert the jet exhaust for the different phases of flight. Keeping the GTOW below 50 lb. meant keeping the airframe as small as possible to minimize skin and structure weight. These constraints simply did not allow for the necessary weight and volume that the lift/cruise configuration requires.

Also, the high-speed mission requirement pushed the airframe design to be as sleek and light as possible. Figure 2.2 shows Locust on a plot (diamond shape) with other V/STOL UAVs. From the plot, it can be seen that Locust's top speed will be roughly double that of other V/STOL UAVs in its weight class.

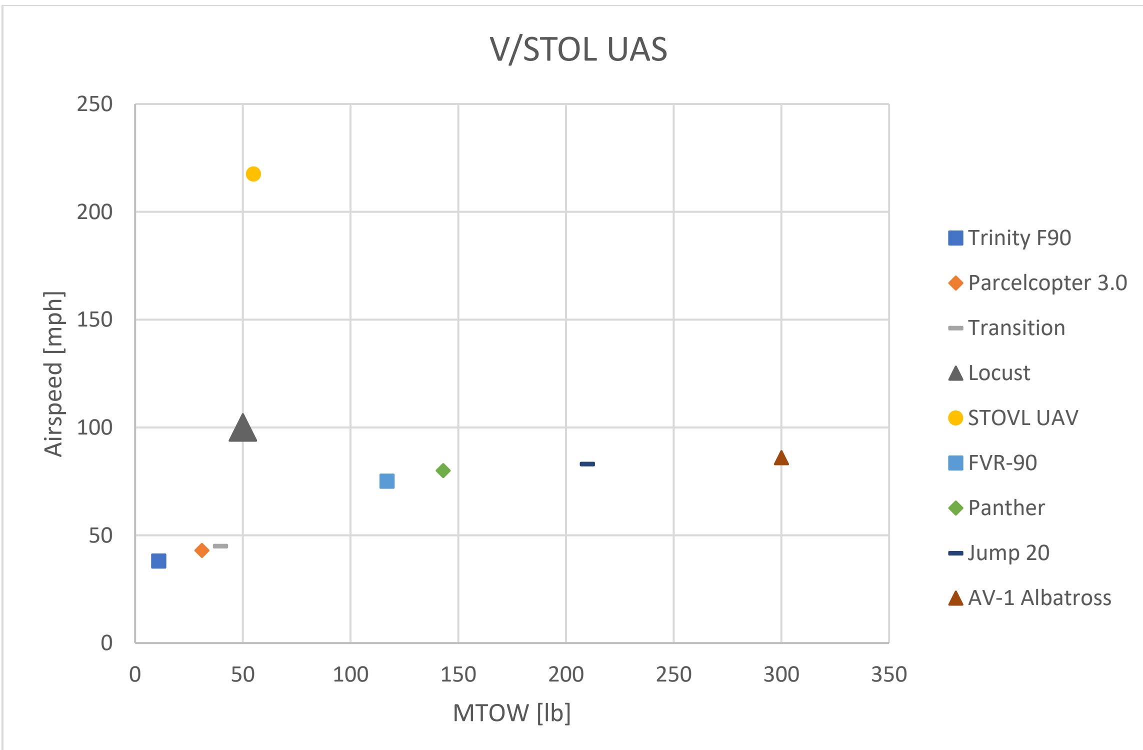

Figure 2.2 V/STOL UAS Weights and Airspeeds

The weight and volume limitations also prevented the use of RCS for takeoff and landing stabilization. An alternative stabilization system was developed using a lightweight thrust vectoring (TV) nozzle at the exit of the jet. The TV nozzle, shown in Figure 2.3, was controlled by two servos that could actuate the nozzle to augment pitch and roll stability. The thrust vectoring system was controlled by an Eagle Tree Guardian; an inertial stabilization sensor that senses deviations from a wings-level attitude. When the Guardian sensed an unwanted roll or pitch motion, it sent a signal to the thrust vectoring system to correct the aircraft back to a wings-level attitude.

Figure 2.3 Thrust Vectoring Nozzle Jet Pipe

The basis of the initial design was that a turbojet would be vertically mounted to provide vertical thrust with a thrust vectoring nozzle controlled by a rate gyro to provide stabilization. Horizontal thrust would be provided by a gasoline-powered IC engine and a propeller mounted at the front of the aircraft. The initial design sketch can be seen in Figure 2.4.

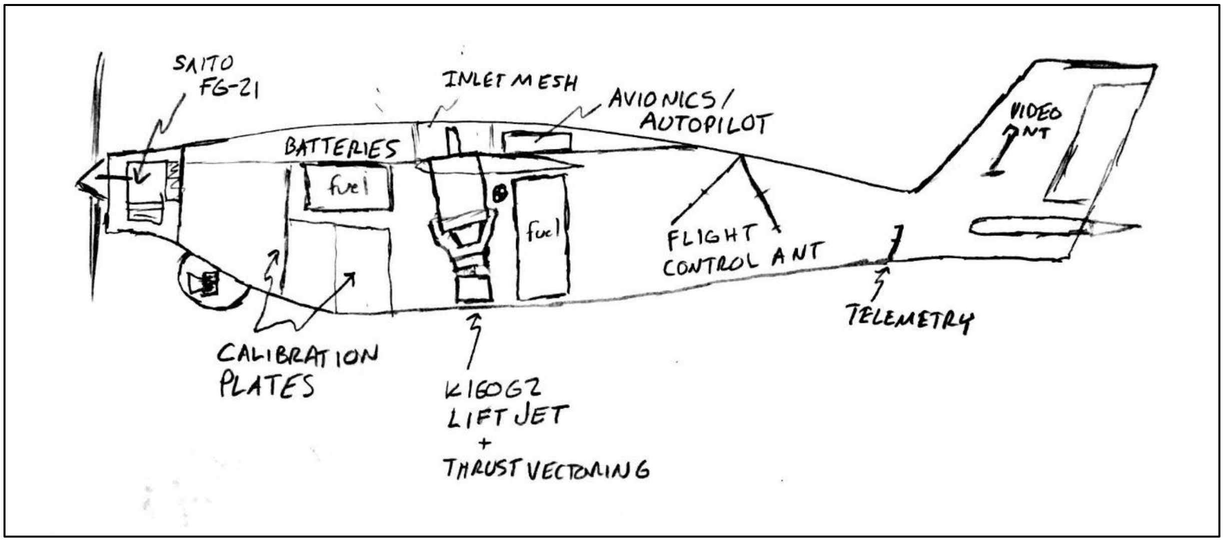

Figure 2.4 Locust Initial Design Sketch

Proof of Concept

In order to test the validity of the initial design, a commercial off the shelf (COTS) UAV airframe was retrofitted with a CWL system to be a rough representation of the initial design configuration. The 65 in. Turbo Bushmaster was roughly 1/3rd the size of the proposed aircraft. In the VTOL chapter of Raymer's Aircraft Design book, he states that "one of the simplest ways of providing VTOL capability is to add lift engines to an essentially conventional aircraft" [12]; and that is exactly what was done. Instead of going through the rigor of designing an airplane from scratch, the Bushmaster was overhauled and fitted with a CWL system. Figure 2.5 shows the unmodified 65 in. Bushmaster. The modified Bushmaster was name Grasshopper for its ability to begin wing-borne flight with no rollout.

Figure 2.5 Turbo Bushmaster 65

The retrofit process was very involved and took weeks of design and development. First, the aircraft’s landing gear system had to be converted from tail-dragger configuration to a tricycle configuration. The original gear was removed, and support structure was added for the attachment of the rear main gear of the tricycle configuration. The nose gear system consisted of a custom, 3-D printed mount that could support the front motor and the Robart nose gear strut. The aircraft did not come from the manufacturer with an airspeed sensor, so a Jeti MSPEED EX airspeed sensor and pitot-static tube were installed in the starboard wing as shown in Figure 2.6.

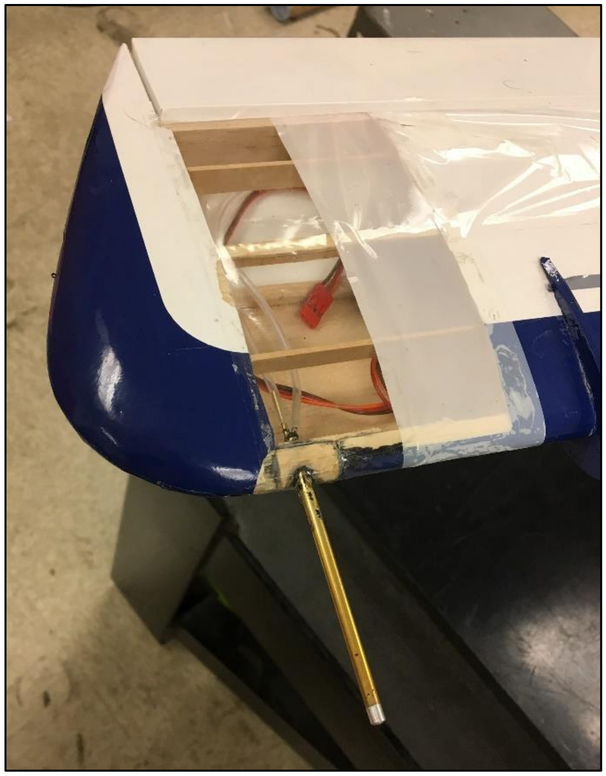

Figure 2.6 Grasshopper's Airspeed Sensor

The interior of the aircraft was completely removed along with some of the structure, which was replaced by modified structure to accommodate a KingTech K-70 jet engine and additional systems hardware. As seen in Figure 2.7, the top of the aircraft had to be cut away to allow airflow to the jet and a hole had to be cut in the bottom of the fuselage to allow the jet exhaust to escape. A thrust vectoring nozzle was installed to the to bottom fuselage bulkhead, directly below the jet’s nozzle as in Figure 2.8. The TV nozzle was controlled by two Futaba S3172 servos (one for pitch and one for roll). These servos, including the rest of the aircraft’s servos, were controlled through a Jeti Duplex, 12 channel telemetry receiver. The Duplex had an auto-leveling feature that was allowed to have control over the TV servos. The auto-leveling feature allowed the aircraft to correct its attitude by diverting the jet exhaust to counteract unwanted pitch and/or roll motion. Along with the thrust vectoring system, the aircraft also featured standard aircraft control surfaces: ailerons, flaps, elevator, rudder, and steerable nose wheel. For horizontal thrust, a Jeti Elite 15cc electric motor was mounted to the forward engine mount. The modified front cover in Figure 2.7 was made to reduce drag and provide protection for the avionics bay while the top was kept open to allow airflow to the jet.

Figure 2.7 Grasshopper

Figure 2.8 Grasshopper's Thrust Vectoring Nozzle

With all of the avionics in the fore area of the fuselage and the jet directly at the CG, roughly the quarter chord of the wing, the only place for the extra fuel tank was directly behind the jet. The fuel bay was modified to support two 16 oz. Sullivan slant tanks. Using a set of Xicoy three-point CG scales and the nose wheel as the datum, the aircraft was weighed empty and full of fuel to check the distance of CG travel. The travel needed to be within the bounds of the TV nozzle so that it would add minimal horizontal thrust while not creating an unwanted pitching moment. The travel was 10 mm which is less than the diameter of the TV nozzle which meant that the CG would stay directly in line with the jet nozzle for the duration of the flight. The final, gross takeoff weight (GTOW) of the aircraft was 13.1 lb., and with the K-70 engine producing up to 15 lb. of thrust at full throttle, the aircraft had a thrust-to-weight ratio of 1.14.

Table 2.1 shows Grasshopper's CWL components and its overall CWL system weight fraction. The 31% is significantly higher since its structures weight fraction is much lower. While there isn't an exact number, its airframe is made of light-weight balsa bulkheads covered in very light-weight MonoKote.

Component	**Weight [lb]**
K-70 Engine	1.7
TV Nozzle	0.1
ECU	0.1
Thrust Vector Servos	0.1
Fuel	1.2
Fuel Tanks	0.3
Fuel Pump w/valve and filter (K-70)	0.3
Battery	0.4
Total	**4.1**
GTOW	13.1
CWL Fraction	31%

Table 2.1 Grasshopper CWL Weight Fraction

Flight tests with Grasshopper were carried out at the OSU UAS airfield in Stillwater, OK. The flight test procedure consisted of performing a specific list of pre-flight checks, mission briefing, and launch and landing. The pre-flight procedures used for Grasshopper were very similar to the procedures used for Locust which are shown in the appendices. After completing the pre-flight checks, Grasshopper was tethered to its portable launch pad. With both engines at their takeoff power levels, the pilot signaled the ground crew member to pull the release cord, which allowed the aircraft to take off and climb at roughly a 45^0 angle. Figure 2.9 is a burst set of photos that shows Grasshopper's takeoff. After flying the mission, the pilot flew the aircraft in a specific landing set-up pattern to achieve the correct speed and altitude targets for a spot landing. Figure 2.10 shows a burst set of photos of Grasshopper's landing. The last photo in the set is of it on the ground after its roll-out which was only about 10 feet. Once Grasshopper had demonstrated successful takeoffs and landings, the CWL was validated and Locust was ready to be designed.

Figure 2.9 Grasshopper Takeoff

Figure 2.10 Grasshopper Landing

Locust Internal Layout

Since the pre-prototype was dubbed Grasshopper, for its ability to jump straight into wing-borne flight, it was decided that the main, group two aircraft should be called Locust, a larger member of the grasshopper family. The design of Locust started with pre-sizing the primary flight components. With the 50 lb. or less weight restriction and the direct lift V/STOL configuration, the main lift engine had to produce at least 50 lb. of thrust to achieve the required thrust-to-weight ratio of one. For this, the KingTech K-260 turbojet engine was chosen for its maximum static thrust of 51.5 lb., which would give the aircraft a thrust-to-weight ratio of 1.03. While not ideal, a thrust to weight ratio of 1.03 is sufficient.

The forward thrust IC engine and propeller were required to produce enough thrust for a maximum airspeed of at least 100 mph while also being efficient enough to cruise for at least one hour. Using a custom engine sizing program, the forward engine was required to provide at least 8 HP. To meet that power requirement, a DA-120 IC engine was chosen. The propulsion systems will be discussed in much greater detail in the Propulsion Systems section.

The fuel tanks were sized based on fuel consumption, available space and weight, and available COTS tank sizes. From initial testing, it was determined that 120 fl. oz. of gasoline was needed for the DA-120 and 60 fl. oz. of jet fuel was needed for the K-260 to fulfill the mission requirements.

To fulfill the design requirement of having autonomous flight capability and to have a similar flight deck setup as other military UAVs, a Pixhawk II autopilot system was used as the primary flight control system. The Pixhawk II would work in conjunction with a Jeti Duplex telemetry receiver where the Jeti would receiver pilot input and send it to the Pixhawk, which would re-route the signal to the corresponding systems. The avionics and electronics system will be discussed in detail in the Electrical System section.

Coinciding with the avionics and electronics, the customers gave the desired payload equipment: a DL 500 (GPS) and a TS 4000 (radio modem), so that they could be weighed and modeled for the full aircraft CAD assembly.

With the majority of the large components decided upon, a CAD model of every component was developed. While the individual CAD models were being created, so was a weight and balance spreadsheet where every component had a weight and a location in the aircraft measured from a datum (the firewall). A condensed system weight break-down can be seen in Figure 2.11 while the full weight and balance spreadsheet can be seen in the appendices. Once the CAD models were complete, they were used to create the full aircraft CAD assembly.

Ideally, the fuel would be placed directly at the CG to minimize CG travel during flight; however, there was not enough room since the whole design was centered around having the K-260 and accompanying jet pipe and TV unit directly at the CG. With the area fore of the CG being filled avionics and electronics, the only place for the fuel was directly behind, but as close as possible to the CG.

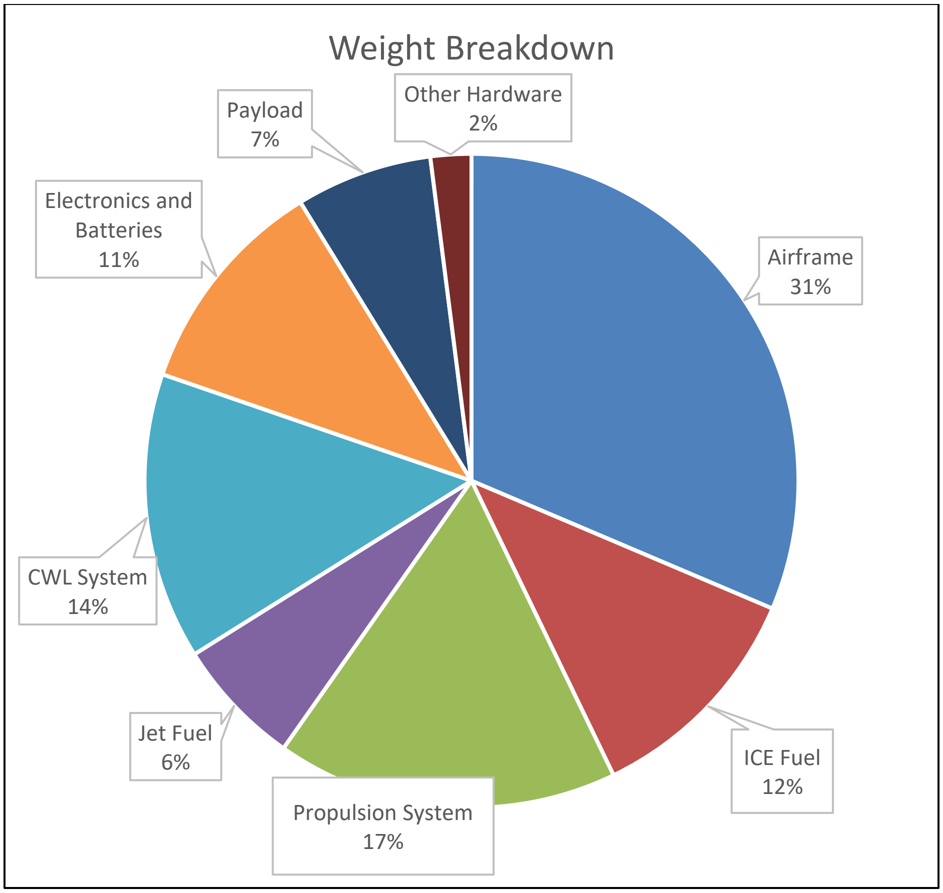

Figure 2.11 System Weight Breakdown

As mentioned in the previous paragraph, the jet engine required a jet pipe. The jet pipe was needed for three reasons: to safely divert the hot exhaust gas, to support the TV unit, and to increase the moment arm. Since the aircraft did not have the volume allocations for a reaction control system, the jet pipe and TV unit were designed to have as much leveling effect as possible by maximizing the pitch and roll moment. With thrust being constant, the only adjustable variable was the moment arm. From the initial CAD drawing shown in Figure 2.12, it would appear that the jet pipe would fit beneath the jet; however, the jet pipe in the model was only an estimate and it was found that a jet pipe that small could not be purchased and the smallest one available would not fit. To accommodate the lack of room, a ventral pod was added to increase the vertical height and volume to fit the jet pipe and TV unit which can be seen in Figure 2.18. A pod was chosen over simply increasing the fuselage size to help save weight. When developing a V/STOL aircraft, weight savings are pursued more aggressively than with a CTOL aircraft. A normal, tube-shaped fuselage would have been more aerodynamic and lighter, but weight was being eliminated wherever possible.

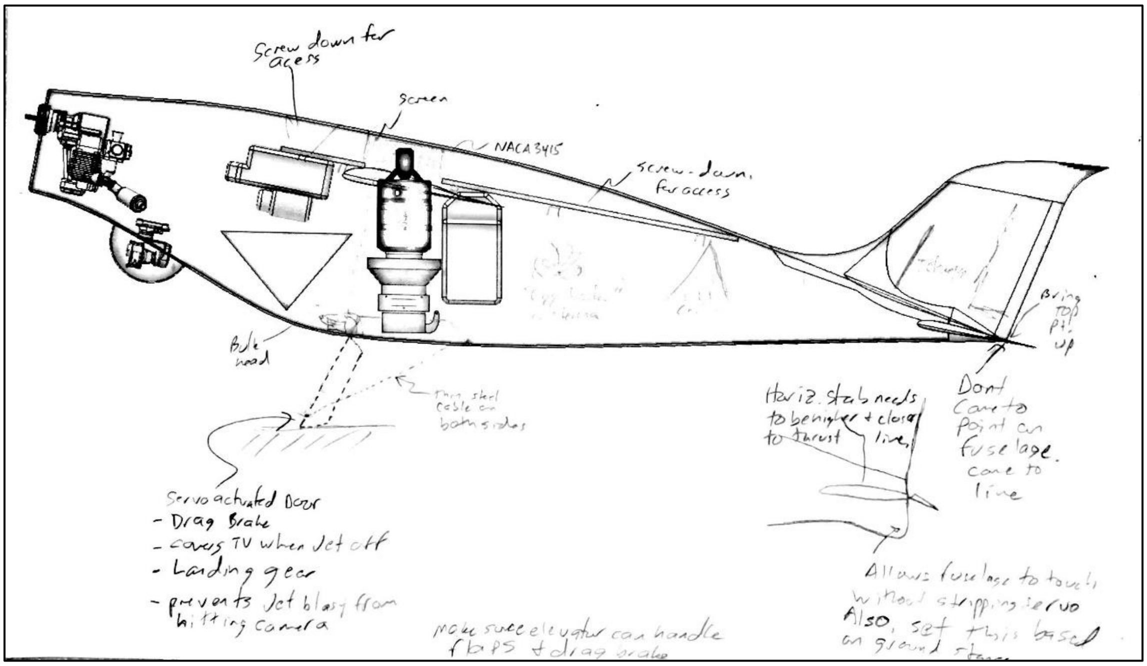

Figure 2.12 Locust Preliminary CAD Model

Propulsion Systems

Main Engine

The direct lift VTOL configuration requires two separate propulsion systems: one for vertical thrust and one for forward thrust. As previously stated, one of the design requirements was that all propulsion systems use liquid hydrocarbons (gasoline, diesel, jet A, nitro, etc.) as the fuel, which basically meant no electric motors. The preliminary engine sizing was done using a proprietary program called VorProp. VorProp uses Goldstein’s vortex theory to predict propeller performance. It takes inputs of propeller data, engine data, and aircraft data to output engine performance, endurance, and range estimates. Initially, a Desert Aircraft DA-85 was chosen as the primary forward thrust engine because it met the required thrust and fuel flow parameters. However, after preliminary tests, it proved to be too weak to reach the maximum speed of 100 mph. Also, it was found that the DA-85 caused significant vibrations, more than most of the other DA engines. For these two reasons, the DA-85 was replaced by a DA-120, a 121 cc 2-stroke, UAV engine with an engine speed range of 1300 – 6900 RPM. It uses a 40:1 fuel to oil mixture with 'Premium' 91 to 93 octane gasoline and Red-line Two-Stroke Racing Oil. The DA-120 can be seen in Figure 2.13.

Figure 2.13 DA-120 Engine

Aircraft drag estimates for the engine sizing program were obtained using SolidWorks' computational fluid dynamics (CFD) analysis. The results of the CFD drag analysis can be seen in chapter 5 in Figure 5.11. Figure 2.14 shows the required thrust from the CFD drag estimates along with the available Thrust from the DA-120 with the 3-blade Beila 26x12 propellor. The drag estimates show that flying at 87 kts. (100 mph) would require at least 11 lb. of thrust. Multiple propellers were tested in VorProp until one was found to give the appropriate amount of thrust while requiring less than the DA-120's maximum power output (8 hp). A 3-blade Beila 26x12 with the DA-120 proved to provide enough thrust to fly at the required top speed.

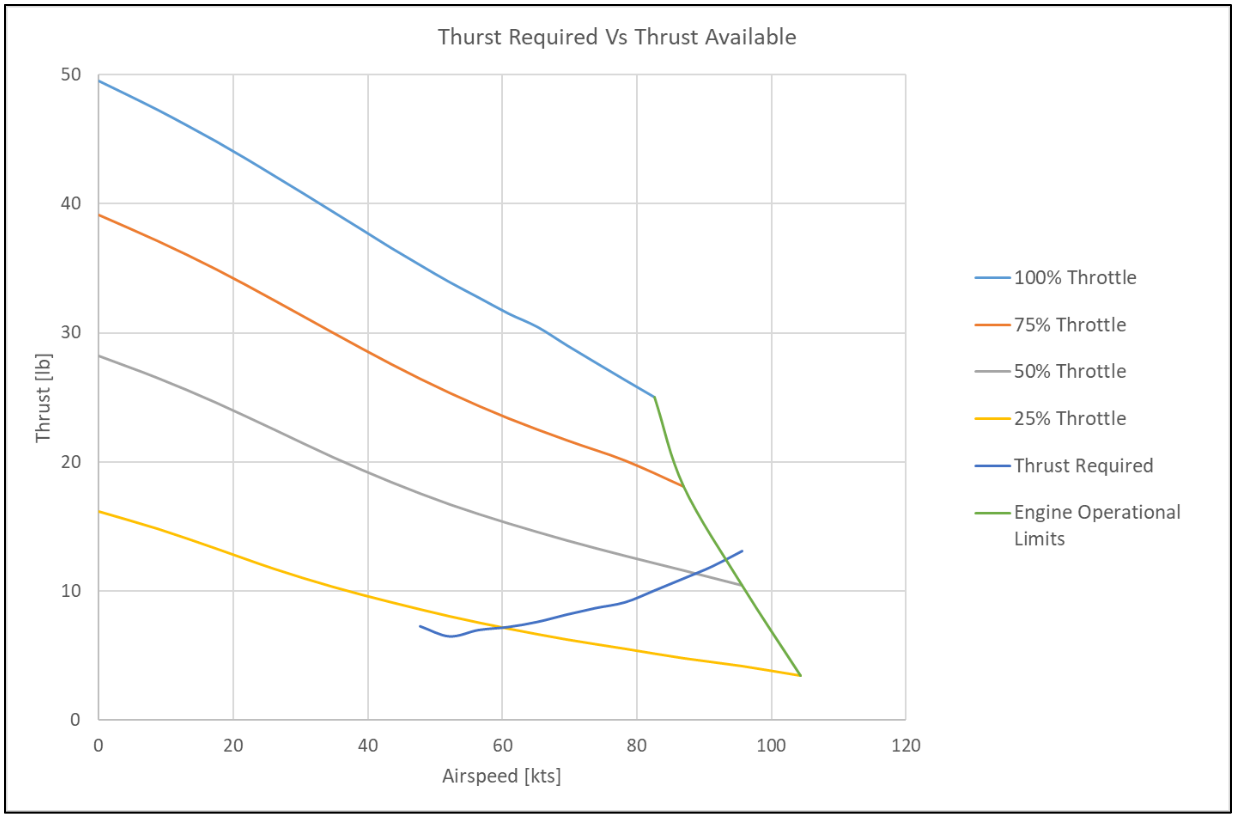

Figure 2.14 Locust Thrust Curves

In its normal, CWL configuration, Locust has an estimated maximum endurance of 1.6 hours. However, if the jet and its equipment were removed and replaced with fuel, Locust could have a maximum endurance of about 5 hours. Table 2.2 depicts the possible endurances as a function of the throttle setting and the initial amount of fuel. The values shown in Table 2.2 were calculated by dividing the initial weight of fuel by the measured fuel consumption at a given throttle setting.

Endurance [hr]				
Weight of fuel [lb]	Throttle %			
	100	75	50	25
2.8	0.38	0.49	0.7	1.6
5.7	0.8	1	1.4	3.3
8.5	1.2	1.5	2.1	5

Table 2.2 DA-120 Endurance

In the initial design, the front of the fuselage skin could have been kept to act as a cowling; but, since the DA-85 was replaced by the DA-120, which has 2 side-mounted heads, the sides of the cowling had to be cut away so much that it was decided to remove the cowling entirely.

Lift Jet

The sizing of the jet was much simpler than the sizing of the IC engine. Basically, the vertical thrust engine had to produce at least as much thrust as the plane weighs. Since the maximum engine thrust was the only driving factor, the engine selection was based on factors of merit such as weight, cost, size, reliability, system compatibility, and familiarity. With limited options of miniature jet engine suppliers and even fewer options of jets producing near 50 lb. of thrust, the only reasonable engine was the K-260.

The K-260, shown in Figure 2.15, is a small, turbojet engine manufactured by King Tech Turbines. It weighs in at only 5 lb. while producing a maximum of 51.5 lb. of thrust, giving it a thrust-to-weight ratio of 10.3. Although miniature turbojet engines have greater losses and are less efficient than full-scale jets, they still have very high thrust to weight ratios packed into a small size. The K-260 can use diesel, kerosene, or Jet A with a 20:1 fuel to oil mixture. Initially, the diesel was used for the break-in and thrust testing. However, when experimenting with the engine in a vertical position, it was almost impossible to get the fuel to ignite. Many hours were spent reading about and experimenting with the different engine settings but it still would not light consistently. After all the failed attempts, it was decided to try Jet-A for its slightly lower flash point than diesel 2-D (100^0F and 126^0F respectively) [35]. The jet fuel lit almost immediately as the burner was turned on during the engine start-up cycle.

The engine was tested many times both vertically and horizontally using a custom jet test stand, and it was found that the jet fuel ignited much more consistently than diesel. The engine testing will be discussed more in the Component Ground Testing section.

Figure 2.15 K-260 G2 Engine

After deciding to use jet fuel, the static thrust test was redone which showed the previously stated uninstalled thrust of 51.5 lb. The static fuel consumption test was also repeated, and it was found that, at 100% throttle, the K-260 consumed 28 fl. oz./min. Using two of the 60 fl. oz. tanks for the test flights gave a little less than 4.5 minutes of the jet at full throttle. The fuel consumption data is shown in Table 2.3 and Figure 2.16.

Jet Endurance											
Throttle %	0	23	31	42	50	58	65	73	81	92	100
Thrust [lb]	2.4	7.7	13.7	18.0	21.5	27.5	30.9	36.9	42.1	45.4	51.2
Fuel Burn [fl oz/min]	4.9	8.4	13.0	13.0	14.3	16.7	18.5	19.3	22.7	24.6	28.1
Endurance [min]	24.5	14.3	9.2	9.2	8.4	7.2	6.5	6.2	5.3	4.9	4.3

Table 2.3 K-260 Fuel Consumption

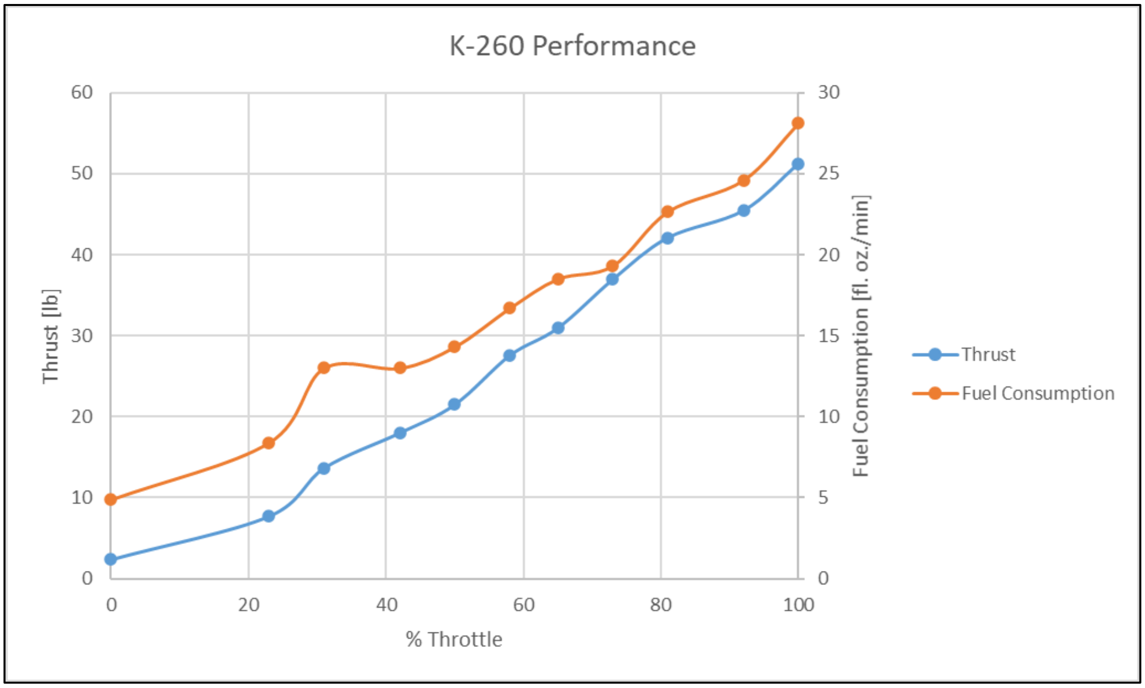

Figure 2.16 K-260 Performance

Thrust Vectoring Control System

One of the problems with V/STOL designs (and the CWL design) is attitude control at low forward speeds as mentioned in the V/STOL Requirements section. At low speeds, the traditional aerodynamic control surfaces have little to no control authority which is the driving reason for the TV system. Locust TV system functions similarly to an inverted pendulum where the aircraft's CG is synonymous with the pendulums center-of-mass and the TV nozzle with the pivot point. The inverted pendulum is an unstable system on its own which is why the inertial stabilization system necessary.

The TV system provides control assistance about the longitudinal (roll) axis and the lateral (pitch) axis. For longitudinal control, the TV system diverts the jet exhaust gas to either the port or starboard to counteract roll disturbances. For example: if the aircraft has port roll disturbance, the TV nozzle diverts exhaust gas to the starboard to create a counter moment to offset the unwanted roll. Figure 2.17 shows a graphical representation of the longitudinal control where the red rotation arrow is the roll disturbance and the black rotation arrow is the TV correction.

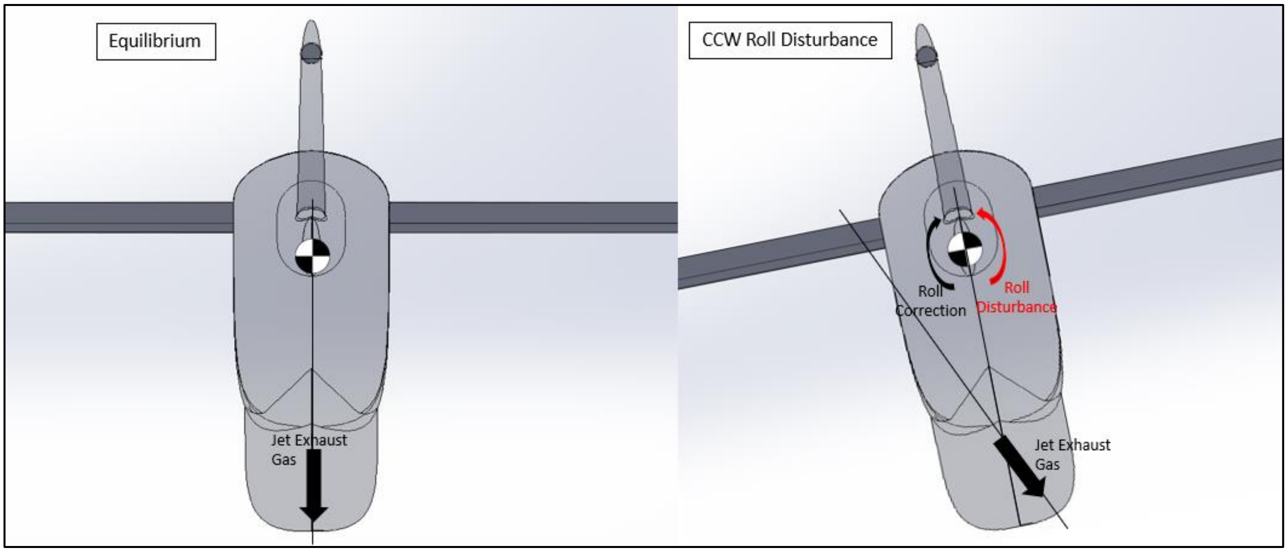

Figure 2.17 TV Roll Control

The TV control works similarly for lateral control where if there is an unwanted pitch up motion, the TV nozzle diverts exhaust gas forward to offset the pitching motion. Also, the nozzle is oriented such that it is angled slightly forward when the aircraft is at a wings-level attitude. This was done to provide some reverse thrust (red arrow in Figure 2.18) to help slow the aircraft during landing. From Figure 2.18, this small angle does not create a pitching moment since the thrust line of action passes directly through the CG.

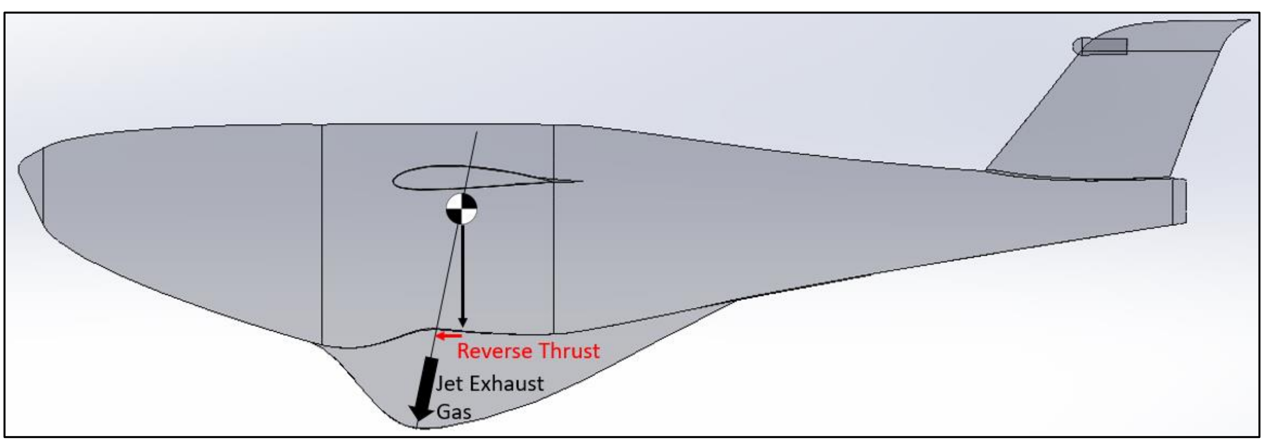

Figure 2.18 TV Reverse Thrust

Aerodynamics and Sizing

Static Stability

Once the initial configuration and layout were roughly designed, the sizing of the aircraft and control surfaces followed. The basic shape of the aircraft was made by placing the components in a SolidWorks assembly and orienting them such that their weights would balance the aircraft at roughly the quarter-chord of the wing. Using SolidWorks' lofting feature, sketches were made to enclose the components in the fuselage and then lofted together. The sketches hugged the internal components as close as possible to minimize the surface area of the skin to help reduce overall weight. Figure 2.12 shows the initial aircraft shape.

Sizing the wing played a critical role in the aircraft's layout and stability. The wing was sized for 3 main design points: minimal drag at cruise, reasonable conventional landing speed i.e. less than 50 mph (43.5 kts), and high thickness for increased bending strength, torsional rigidity, and internal volume. The airfoil for the main wing was the NACA 3415, which was chosen for its relatively high lift coefficients and its 15% thickness. The maximum thickness of the wing was designed to be 1.5 in. to house the control servos, other electronics, and the main carry-through spar while still being as small as possible to minimize drag. With the maximum thickness being 1.5 in, and the NACA 3415 airfoil's thickness is 15% of the chord, the chord had to be 10 in. Since the chord was set at 10 in, the span of the wing was then set to 85.5 in. to allow for minimal angle of attack at 100 mph. The tips of the wings were swept back for an added aesthetic appeal dubbed 'sexy tips'; Figure 2.19 shows the wing with the sexy tips.

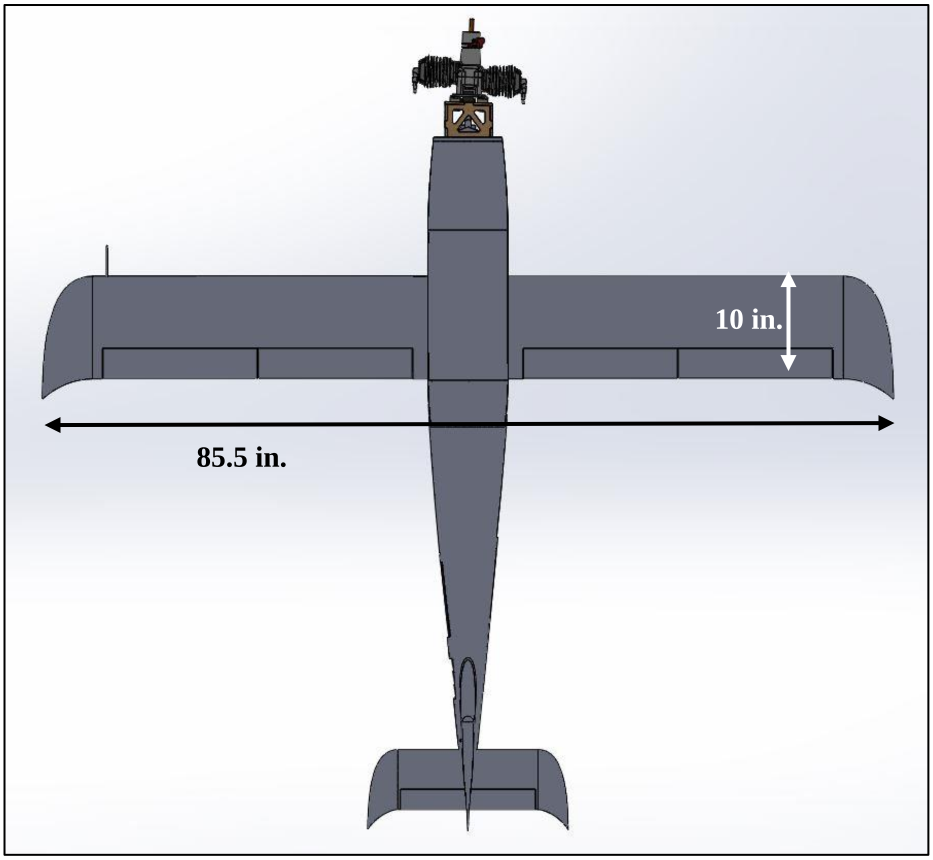

Figure 2.19 Locust Top View

With the general wing shape, fuselage shape, and weights and balance known, a basic longitudinal static stability analysis was performed using the Multhopp Method, a systematic body build-up. The first step in the stability analysis was to calculate the wing's contribution to the pitching moment of the aircraft. This was done by summing the moments about the CG. Non-dimensionalizing the summation by dividing by $\frac{1}{2}\rho V^2 S\bar{c}$ and assuming the small-angle theory is used, the moment equation reduces to

$$C_{m_{cg_w}} = C_{m_{ac_w}} + C_{L_w}\left(\frac{x_{cg}}{\bar{c}} - \frac{x_{ac}}{\bar{c}}\right)\cos(\alpha_w - i_W) - C_{d_w}\frac{z_{cg}}{\bar{c}}(\cos(\alpha_w - i_w) \tag{1}$$

Assuming the vertical contribution is negligible, equation 1 reduces to

$$C_{m_{cg_w}} = C_{m_{ac_w}} + C_{L_w}\left(\frac{x_{cg}}{\bar{c}} - \frac{x_{ac}}{\bar{c}}\right) \tag{2}$$

Where

$$C_{L_w} = C_{L_{0_w}} + C_{L_{\alpha_w}}\alpha_w \tag{3}$$

Applying the condition for static stability $\left(\frac{dC_m}{d\alpha} < 0\right)$ yields

$$C_{m_{\alpha_w}} = C_{L_{\alpha_w}}\left(\frac{x_{cg}}{\bar{c}} - \frac{x_{ac}}{\bar{c}}\right) \tag{4}$$

The horizontal tail's contribution to pitching moment was calculated following the wing's. The only fixed value for the horizontal tail was its distance from the CG. The variables such as chord, span, and incidence were left floating so that when the fuselage contribution was finished, the tail size could be iteratively changed to offer the best stability characteristics. Like the wing's pitching moment, the horizontal tail's pitching moment was calculated by summing the moments about the CG. If the summation is non-dimensionalized by dividing by $\frac{1}{2}\rho V^2 S\bar{c}$, the small-angle theory is used, and it is assumed that $C_{L_t} \gg C_{D_t}$, the moment equation reduces to

$$C_{m_t} = -V_H \eta C_{L_t} \tag{5}$$

Where $V_H = l_t S_t / S\bar{c}$ is called the horizontal tail volume ratio.

See *Flight Stability and Automatic Control* [36, pp. 42-52] for a more detailed explanation of the wing and tail contributions.

After the horizontal tail, the fuselage was analyzed to determine its contribution to the pitching moment. Multhopp's method for analyzing the fuselage's contribution consists of dividing the fuselage into segments and determining the contribution of each, then summing them together. For the full process and equations, see *Flight Stability and Automatic Control* [36, pp. 52-55].

Since the fuselage's outer mold line (OML) was fixed due to the internal components, the only 'rubber' part of the aircraft for longitudinal static stability was the horizontal tail. Using the Multhopp method, the 'rubber' variables of the horizontal tail were adjusted until the aircraft had the desired pitching characteristics, shown in Figure 2.20, and a static margin of 14%.

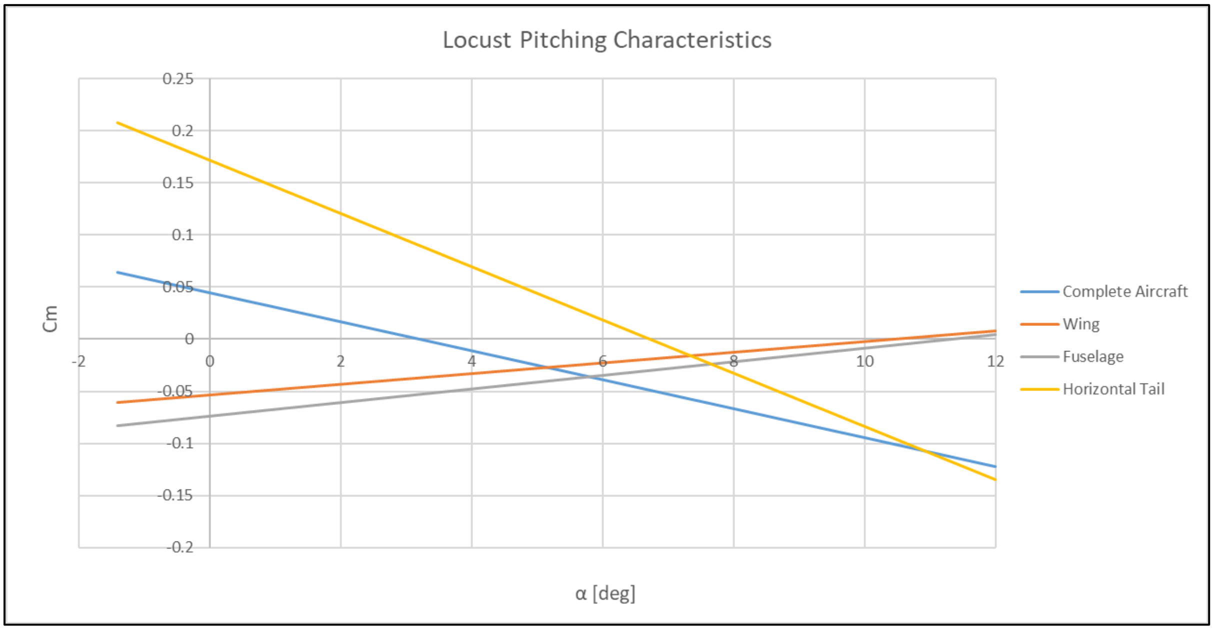

Figure 2.20 Locust Pitching Characteristics

The directional static stability was performed in a similar manner as the longitudinal static stability in terms of dividing the aircraft into its main directional components: wing, fuselage, and vertical tail. Generally, the contribution of the wing is very small relative to the contribution of the fuselage if the angle of attack is not large; therefore, the wing and the fuselage are lumped together. A full explanation of the method is in *Flight Stability and Automatic Control* [36, pp. 73-77]. The overall yawing moment, C_{n_β}, was calculated by adding the wing-fuselage contribution to the vertical tail contribution. With the actual value calculated, the span, root chord, and tip chord of the vertical tail were iterated upon until the aircraft had the desired directional stability characteristics.

However, after the CFD analysis, discussed in the CFD Static Stability section, the original buildup method was checked and found to have an error. Figure 2.21 shows a plot with the original (incorrect) C_{n_β}, the corrected value, and the value if the vertical tail volume was doubled. From the plot it can be seen that the original value showed that the aircraft was directionally stable ($C_{n_\beta} > 0$), and the corrected value was unstable ($C_{n_\beta} < 0$). The implemented fix of doubling the vertical tail volume will be discussed later.

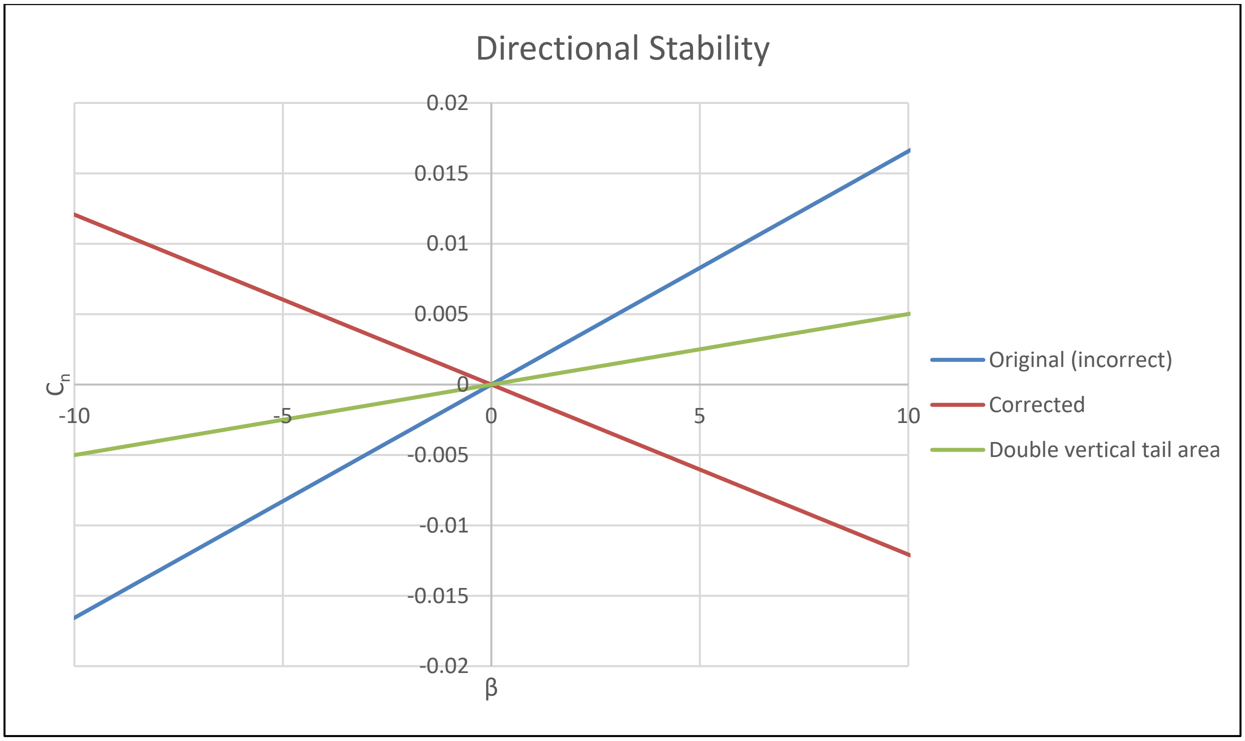

Figure 2.21 Locust Directional Stability

Control Surface Sizing

Like most aircraft, Locust has the traditional aerodynamic controls: ailerons, elevator, rudder, and flaps. The sizing of Locust's control surfaces was much less rigorous than that of full-size aircraft because uncertified UAV's do not have to comply with the Federal Aviation Regulations (FAR).

The ailerons and flaps for Locust were not quantitatively sized, but rather from the OSU aerospace design personnel's many years of practical experience building UAVs. Each wing had 31 in. of useable length for control surfaces so it was decided to split that length evenly between the flaps and ailerons for manufacturing simplicity and consistency. The chord length of flaps and ailerons is generally 30% of the wing chord for this size of UAV. Following the 30% convention, the flaps and ailerons had a 3 in. chord, which left plenty of room in the rest of the wing for the airspeed sensors, telemetry receiver, and control surface servos. The rudder was sized in the same manner as the flaps and ailerons. The elevator, however, was sized quantitatively using XFOIL. This was done by running the horizontal tail's airfoil, the NACA 0012, with different elevator chords at different deflection angles and comparing their effect on pitching moment with the previously mentioned longitudinal static stability. It was seen that an elevator with a chord of 20% of the horizontal tail chord and a deflection angle of 15^0 provided ample elevator control authority. The elevator effectiveness data is shown in Figure 2.22.

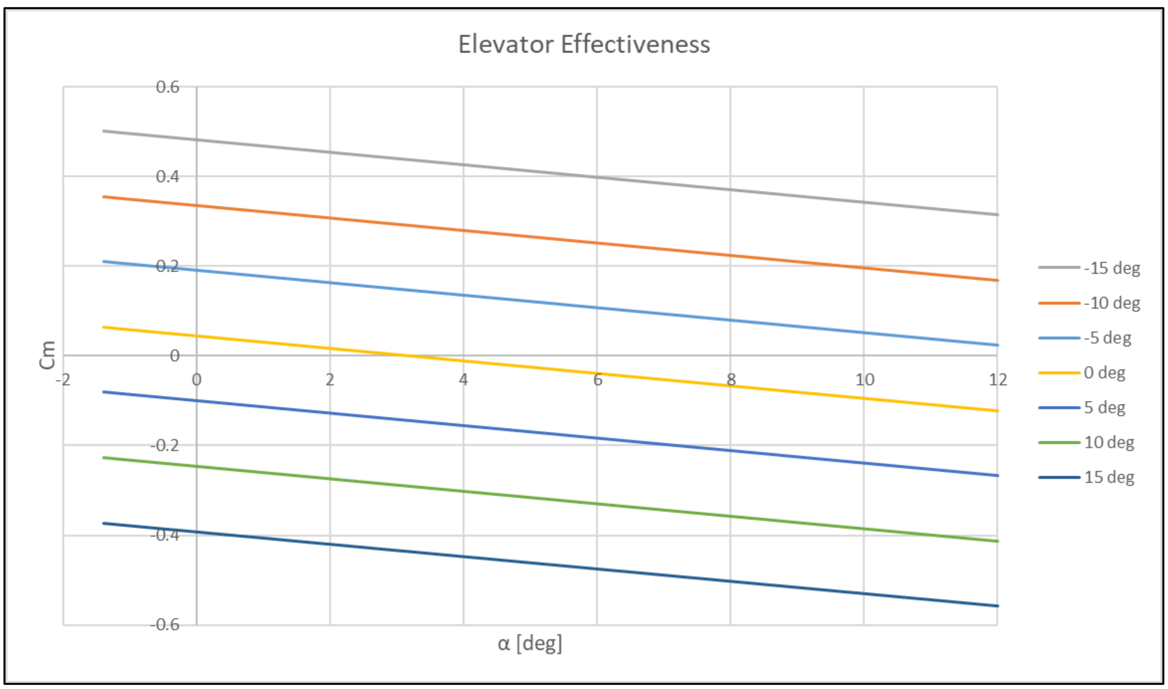

Figure 2.22 Elevator Effectiveness

These control surface sizes, however, were not permanently fixed. Changing the size of the control surface can easily be done during the manufacturing process. So, if the pilot feels that the aircraft needs more authority in pitch, roll, or yaw, the corresponding control surface could be increased in size up to about 40% chord on the next aircraft.

CFD Static Stability

After the body build-up static stability analysis, another static stability analysis was performed on the final CAD model using SolidWorks' CFD. This was done because one of the underlying assumptions of the Multhopp method is that the fuselage is relatively cylindrical whereas Locust's fuselage is tall and narrow. The study was set up to calculate the center of pressure about the vertical (directional) axis to determine the aircraft's directional stability characteristics. Also, the study was repeated with different configurations such as fuselage only, fuselage and wing, and others shown in Table 2.4.

From Table 2.4 and Figure 2.23, it can be seen that the aircraft's directional center of pressure is fore of the CG without the ventral tail. The directional center of pressure being in front of the CG causes directional instability by producing a destabilizing yawing moment at a given sideslip angle. This was problematic because the fuselage molds had already been fabricated, and molds of that size and complexity are too expensive to simply throw away and make new ones.

Directional Center of Pressure		
Datum		Tip of Nose (0)
Components		Z_{CP} [in]
	CG	30.6
1	Fuselage + Wing	-9.4
2	Fuselage	0
3	Fuselage + Wing + Vertical Tail	21.5
4	Fuselage + Vertical Tail	31.8
5	Fuselage + Wing + Vertical Tail + Ventral Tail	35.2

Table 2.4 CFD Directional Center of Pressure

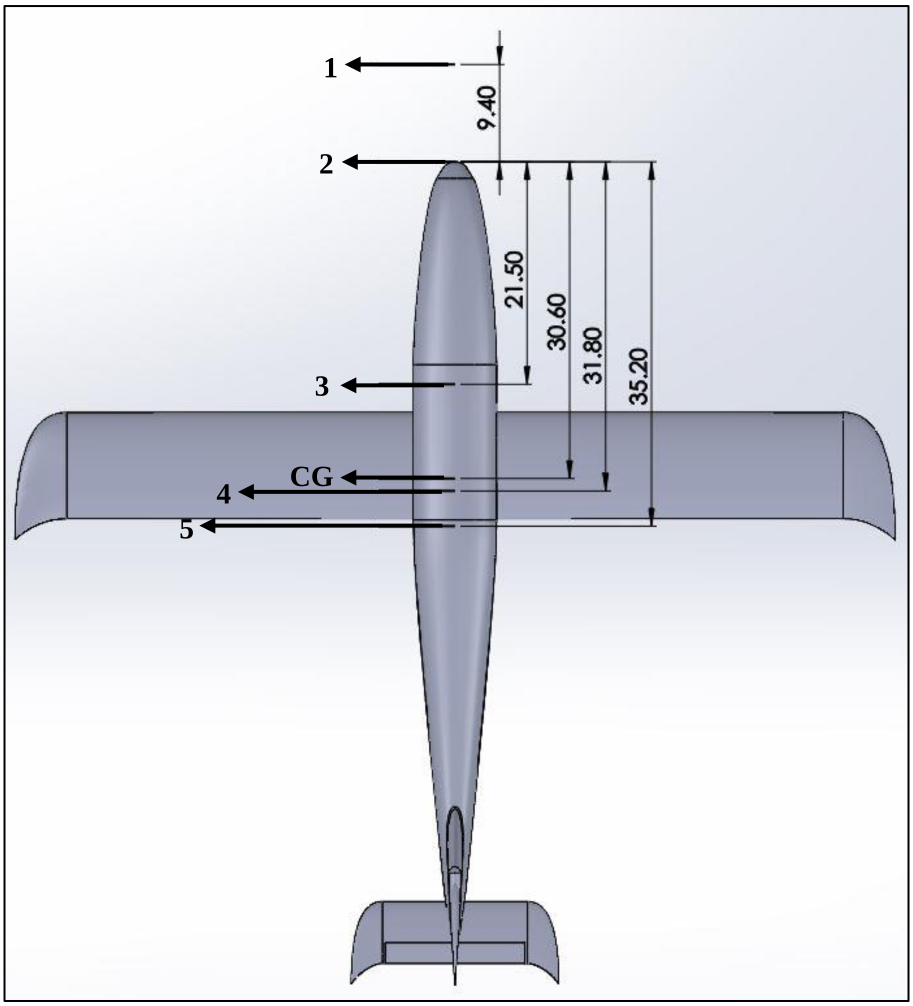

Figure 2.23 CFD Directional Center of Pressure

The aircraft being directionally unstable was mainly a cause of the fuselage being tall and narrow, causing the vertical stabilizer to be too small to compensate for the fuselage’s adverse yawing moment. If the molds hadn’t already been fabricated, the vertical tail could have easily been resized in the CAD model to achieve directionally stability.

To achieve directional stability without changing the OML, a ventral tail was added. This was done by essentially copying the vertical tail and placing it upside down on the bottom side of the fuselage as shown in Figure 2.24. This was both a time and cost-effective solution because it required little additional design work and no additional tooling. The method of making and attaching the ventral tail will be discussed in the Post Processing section.

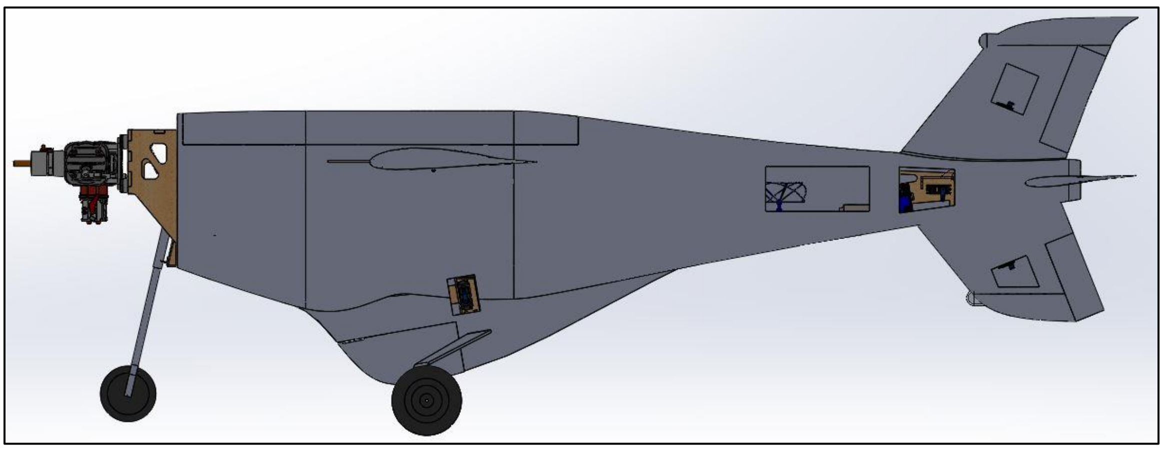

Figure 2.24 Locust Side View of Ventral Tail

Although adding a ventral tail added weight and manufacturing complexity, it ended up being more of a benefit than a detriment. Before the ventral tail, with the initial tail-dragger configuration, the aircraft sat at an extreme angle that had to be mitigated by a special support stand on the launch pad. The ventral tail served as a stand that helped the aircraft sit closer to a wings-level attitude. Also, it helped to decrease the aircraft's overall footprint. Since the top of the vertical tail is the tallest part of the aircraft from the ground, it would only have gotten taller had the vertical tail been resized. Now, the aircraft’s footprint is such that it can fit in the back of a full-size SUV.

CFD Drag Study

To quantitatively describe the boom rotor configuration's impact on drag, a CFD study was performed on the three Locust CAD models shown in Figure 2.25. The first was the aircraft clean without the belly pod, the second was the normal configuration with the belly pod, and the third was the clean aircraft with booms and rotors. The rotors were locked in-line with the flow to minimize their contribution to drag. The study was performed at a simulated airspeed of 60 mph and an angle of attack (AoA) of 9^0. This speed and AoA were chosen for steady level cruise at Locust's best endurance speed.

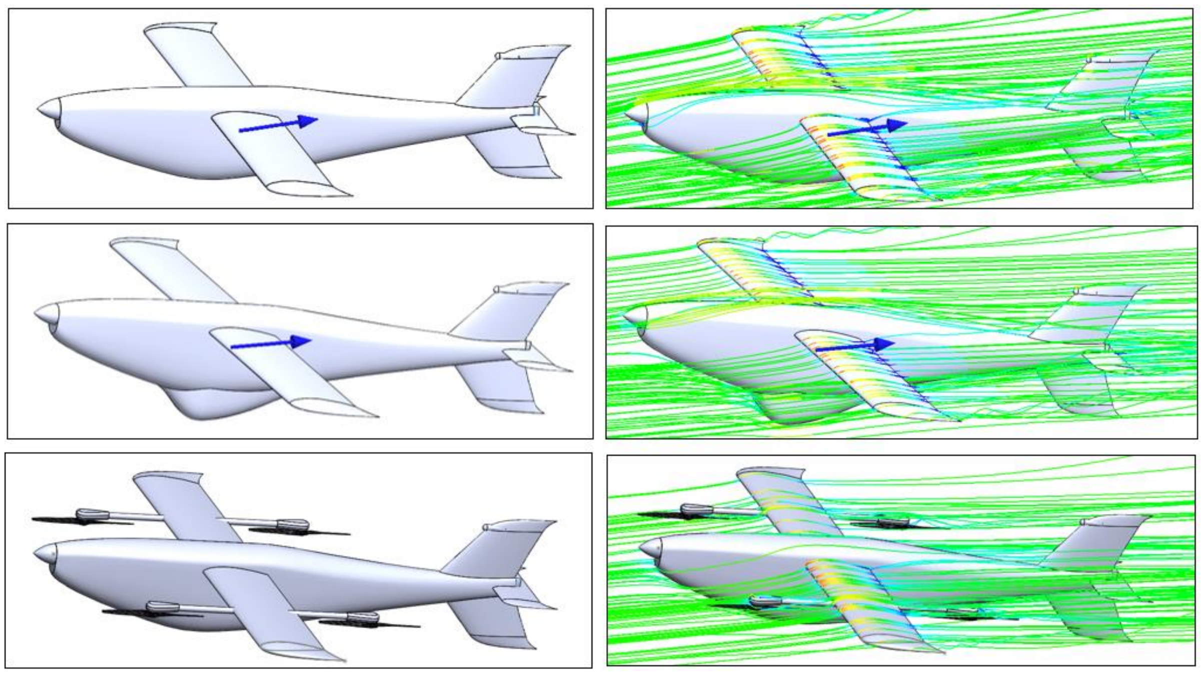

Figure 2.25 Configuration Drag Comparison

The results shown in Table 2.5 show that the booms do increase the drag as predicted. Comparing the boom configuration to the clean configuration, the booms and rotors cause a 7% increase in drag. Table 2.5 also shows, incorrectly, that the belly pod decreases drag. This is a slight error due to the varying lift values. If the clean configuration and the belly pod configuration were producing the same amount of lift, it would show that the belly pod does slightly increase the drag. This drag study validates the previous assumptions that the boom rotor configuration has a non-negligible drag increase.

Configuration	Lift [lb]	Drag [lb]	Airspeed [mph]	AoA [deg]
Clean	56.2	4.2	60	9
Belly Pod	50.3	4.1		
Booms and Rotors	57.0	4.5		

Table 2.5 Configuration Drag Comparison

Wing Spar Sizing and Testing

The minimal weight and rapid deployment requirements were the main drivers when designing the wing spar. Since the aircraft's mission is to fly patterns without high g maneuvers, it was deemed that the spar only needed to support a 4 g load which, with the aircraft's 50 lb. maximum weight roughly translates to a 1900 lb. in. moment at the root of the wing. The moment calculation was estimated by assuming a constant lift distribution across the wing with the resultant lifting force acting at mid-span. Assuming a constant lift distribution yields a conservative moment approximation because the actual resultant force is slightly more inboard. This method was chosen to quickly approximate the aerodynamic loads while also having an additional factor of safety. Equation 6 shows the moment calculation based on Figure 2.26.

$$M = 4\left(\frac{1}{2}W_A\right)X_{midspan} = 4 * 0.5 * 50 * 19.25 = 1925 \qquad (6)$$

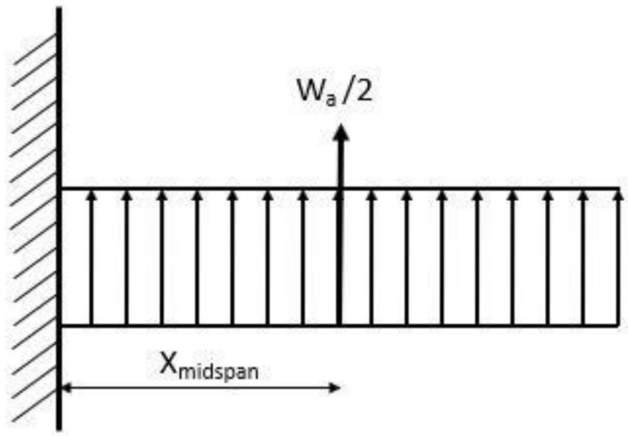

Figure 2.26 Assumed Constant Lift Distribution

The design constraints were to support a 1925 lb. in. moment, be as light as possible and have a maximum outer diameter of 0.875 in. The outer diameter was set by the availability of COTS tubes and to be as thick as possible while allowing room for support structure between it and the wing skins. Multiple COTS tubes made of 4130 steel, 6061-T6 aluminum, GT6030 carbon fiber, and GT608 carbon fiber were tested. The wall thickness of these tubes varied but the outer diameter was set to 0.875 in. Testing the spar tubes was done by applying a load at the end of the spar with a hydraulic engine hoist (cherry picker) while the other end was fixed to a table. Figure 2.27 shows the testing set up. An in-line hanging scale was placed between the lift and the spar tube to measure the applied load. The steel and aluminum spars were loaded until plastic deformation occurred and the carbon fiber spars were loaded until failure. The maximum loads, with the distance from the mount to the loading point, were then used to calculate the bending moments. From the results shown in Table 2.6, the GT6030 carbon fiber tube was by far the strongest and the lightest, so it was chosen to be the main wing spar.

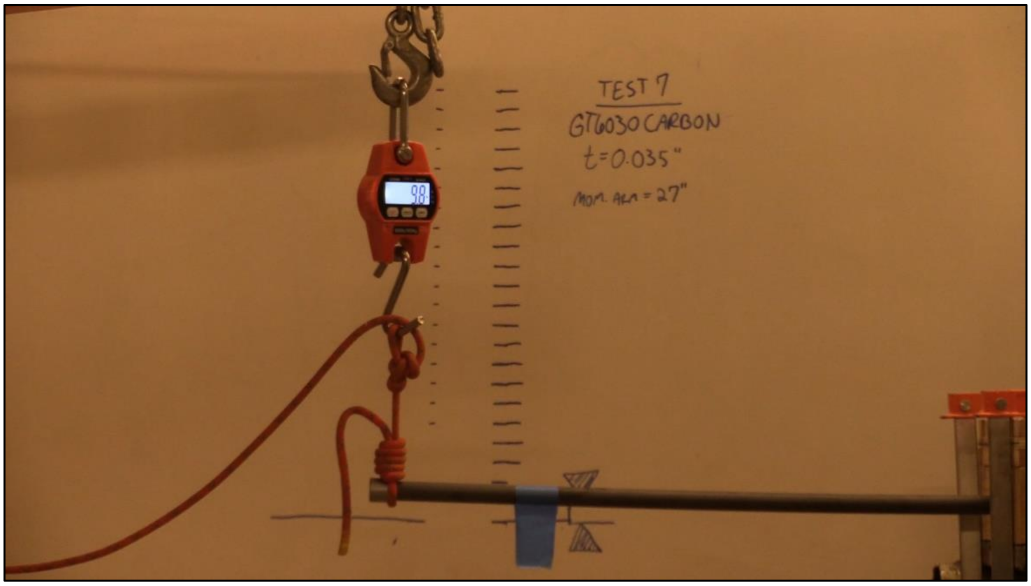

Figure 2.27 Spar Tube Bending Test

The GT6030 carbon fiber spar can support a 4.5 g load by itself. The overall wing is even stronger due to its semi-monocoque design where the skin bears some of the total load. The wing material choices, structural layout, and building methods will be discussed in depth in the manufacturing chapter.

Sample	6061-T6 Aluminum	6061-T6 Aluminum	4130 Steel	4130 Steel	4130 Steel	GT6030 Carbon fiber	GT608 Carbon fiber
Weight/Length [lb/in]	0.013	0.016	0.026	0.036	0.043	0.005	0.005
Force [lb]	35.9	45.1	43.6	58.1	66.7	81.0	74.2
Moment Arm L [in]	27	27	27	27	27	27	23
Moment [in*lb]	970	1217	1177	1570	1800	2187	1670
Yield Strength [psi]	39000	39000	63100	63100	63100	N/A	N/A
Bending Stress [psi]	38990	38995	63097	63099	63096	117249	85368
Max Gs	2.0	2.5	2.4	3.3	3.7	4.5	3.5

Table 2.6 Spar Testing Results

Electrical System

Besides physically flying the aircraft, the electrical system and wiring is the most complicated aspect of the whole design. Due to the wiring diagram being so large and complex, it is broken up into labeled sections in the appendices. The primary flight computer is a Pixhawk II autopilot and its accompanying global positioning system (GPS) unit. All but two signals sent to the aircraft from the pilot pass through the Pixhawk II before being routed to their intended servo or component. The aircraft receives the pilot's command signals through an RMILEC R4047NB20 narrowband telemetry receiver operating on 400 MHz. The two components that get their signals directly from the RMILEC, bypassing the Pixhawk II, are the Eagle Tree Guardian (ETG) and the K-260 engine control unit (ECU). The ETG is an inertial stabilization device used to maintain a wings-level attitude and help the aircraft recover from lost orientation. Conventionally, when in 2D mode, the ETG senses disturbances in the aircraft's attitude and then corrects it by sending correction signals to the aileron and/or elevator servos. However, on Locust, the ETG is used to control the TV unit on the K-260 by sending signals to the TV pitch and roll servos for attitude correction. It should be noted that the ETG is only used for attitude correction during takeoff and landing. Both the ETG's and the ECU's signals bypass the Pixhawk II so that they can be powered off via a Pololu MOSFET power switch during flight. The ECU and K-260 must be shut off during flight to conserve fuel and to allow the exhaust bay doors to be closed (more on the exhaust bay doors later). The ETG must be shut off so that the TV servos are not constantly using battery power.

All the telemetry data, except for K-260 and fuel flow, from the Pixhawk II is sent back to the ground control station (GCS) via an RFD 900 long-range radio modem operating on 900 MHz. The K-260 telemetry data is first read by the onboard Digitech central telemetry unit (CTU) and then sent back to the GCS via the onboard Jeti REX 7 telemetry receiver operating on 2.4 GHz. The CTU is necessary because the Jeti REX 7 cannot interpret the ECU or fuel flow data. The fuel flow is monitored with a Jeti MFlow2 T3000 EX and a Jeti MFlow G800 EX for the K-260 and the DA-120 respectively.

Like most small UAVs, Locust's control surfaces and other moving components are controlled by servos. For simplicity, there are only two types of servos on board: 11 Hitec HS-7245MH and 2

Hitech D930SW. Both types of servos are programmable, which allows for a fully customizable system. The HS-7245MH servos are used for the following components: DA-120 throttle, DA-120 choke, nose gear steering, ailerons, flaps, exhaust bay doors, elevator, and rudder. The D930SW servos have a higher torque output and are only used for the pitch and roll control of the TV unit since they have to deflect 50 lb. of thrust.

The 13 servos are split up into two groups: flight-critical and nonflight-critical. Servos considered flight-critical are those that are required to maintain control of the aircraft during flight, such as throttle, choke, ailerons, elevator, and rudder. These flight-critical servos are powered directly through the Pixhawk II which has a redundant power supply in case of a power failure. The nonflight-critical servos are the flaps, TV control, and exhaust bay doors. While only connected to a single power supply, the exhaust bay door servos and the flap servos are connected through a power distribution board so that they can draw power directly from a battery instead of the Pixhawk II, decreasing the load on the Pixhawk II. As mentioned earlier, the TV servos are controlled by the ETG whose power passes through a MOSFET power switch so that both the ETG and the TV servos can be turned off during flight. Locust also has first-person view (FPV) capabilities with a RunCam Micro Eagle FPV camera in the vertical tail. The FPV camera sends its video feed to the GCS via an FPV transmitter.

Sizing the batteries and power system began with the development of a sophisticated spreadsheet, that contains the required voltage and current draw of each electrical component. The batteries had to be capable of powering the aircraft for at least one hour to meet the one-hour flight time requirement. Also, voltage regulators were not permitted on the aircraft due to their low reliability. After calculating the total current draw and voltage, and isolating ‘sections’ of components in the aircraft, it was decided that 5 batteries were necessary. Each battery and its electronics are shown in Table 2.7.

Battery	3600 mAh 6.6V LiFe	3600 mAh 6.6V LiFe	3300 mAh 11.1 V LiPo	3800 mAh 9.9 V LiFe	3600 mAh 6.6V LiFe
Electronics	Non-flight crit. servos	Flight-crit. servos	DL 500	K-260 starter	DA-120 ignition
	K-260 ECU	RFD 900	TS 4000	K-260 fuel pump	
	Jeti REX 7	RMILEC	FPV transmitter		
	CTU	Pixhawk II backup	FPV camera		
	Pixhawk II				

Table 2.7 Electronics Power Distribution

All but the 3800 mAh 9.9V LiFe batteries are connected directly to double-pole, single-throw toggle switches to simplify operations and to easily power cycle the electronics.

Landing Gear Design

Landing gear is used to provide a means of controllability when the aircraft is on the ground and to absorb some of the impact energy imparted on the airframe during landing. Figure 2.28 shows some of the common landing gear configurations. With the outer mold line (OML) already set, only the taildragger and tricycle configurations, would be possible to implement on Locust. Table 2.8 shows some advantages and disadvantages of both configurations.

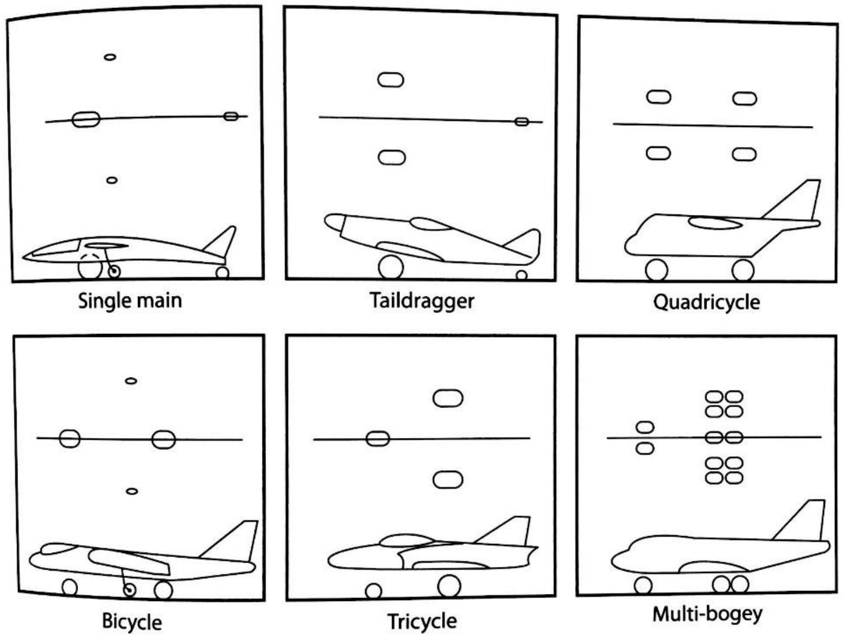

Figure 2.28 Landing Gear Configurations [12]

The taildragger configuration was initially chosen because it allows the wing to sit at a higher angle of attack, which allows the wing to generate more lift for low-speed takeoffs and landings and is better for rough field operations [12].

Tricycle VS Tail Dragger		
Configuration	Advantages	Disadvantages
Tricycle	Difficult to nose over	Nose gear can be easily damaged
	Easy ground handling	Heavier
	Less vulnerable to cross-wind	Not as good for rough landing areas
Tail Dragger	Less complex if tail wheel isn't steerable	Easy to nose over
	Wing sits at higher AoA on takeoff and landing	More vulnerable to cross-wind
	Lighter	Easier to ground loop

Table 2.8 Tricycle VS Tail Dragger

Flight testing showed that this configuration, shown in Figure 2.29, caused the aircraft to bounce during landing which resulted in structural damage. To help reduce the damage caused during landing a new taildragger configuration was designed utilizing gas-spring dampers to help absorb some of the impact energy.

Figure 2.29 Initial Tail Dragger Configuration

This new leading-link configuration, shown in Figure 2.30, allowed the spring-gas dampers to compress upon landing. The compression stroke of the damper dissipated some of the impact energy while slowing expanding which kept the aircraft from bouncing. A leading-link was chosen over the more common trailing-link seen on aircraft due to mounting and wheel location restrictions. For the wheels to be ahead of the CG, the main strut had to be swept forward. The amount of sweep needed to be minimal to reduce the torque imparted on the system during landing and if a trailing link would have been used, the sweep angle would have had to be more extreme to allow the wheels to rest in their correct position. Static drop tests showed that the new leading-link system functioned as expected and stopped the damage caused by impact. However, the initial flight testing of the leading-link system showed that the tail dragger configuration still allowed the plane to ground loop and tip over. The tip-overs resulted in damage to the propeller and wings when they impacted the ground.

Figure 2.30 Leading Link Main Gear

With the taildragger configuration causing damage regardless of the design, it was decided to overhaul the whole landing gear system and switch to a tricycle configuration with a steerable nose wheel to stop the ground loops and nose overs.

One of the main concerns with the tricycle configuration is the integrity and robustness of the nose gear assembly. The tricycle configuration consists of two main wheels aft of the CG and a nose wheel fore of the CG. The design criteria for Locust’s tricycle gear are as follows:

- nose gear had to bear, at most, 20% of the aircraft’s weight
- nose gear had to extend 11.5 in. from the bottom of the firewall
- nose gear had to have an oleo strut or other energy dissipation system
- nose gear had to mount to the firewall
- nose wheel had to be steerable
- tip-back angle had to be between 15^0 and 20^0 with a larger angle being preferred to help mitigate the possibility of an overturn [37]
- mains had to mount behind the jet nozzle
- mains had to be laterally separated by at least 20^0 from the CG to keep the aircraft from overturning [12, p. 356]
- the whole system had to allow vertical clearance for the exhaust bay doors to actuate
- The whole system had to have enough vertical clearance to keep the jet exhaust from damaging the underside of the aircraft

When testing the jet, it was found that the nozzle needed to be at least 3 in. above the ground to prevent backpressure issues and to allow enough room for the jet exhaust to escape. When the exhaust bay doors open, they extend downward by less than 1.0 in. and outward by about 3.5 in, giving them a maximum width of 13 in. when open. With these criteria in mind, it was decided that the aircraft should have 3 in. of ground clearance from the bottom of the lowest part of the aircraft. The necessary 20^0 of lateral separation and 3 in. of ground clearance set the wheelbase to 20 in.

Typically, the mains are mounted to the aircraft directly above where they rest on the ground to prevent adding torque to the system. However, Locust does not have enough space to mount the mains directly above the wheels due to the exhaust bay doors and TV nozzle. To minimize the sweep angle of the main gear strut and allow full actuation of the exhaust bay doors, the mains had to be mounted aft of the aft jet engine bulkhead, beneath the fuel bay. Figure 2.31 shows the CAD model of the mains. Since they had to be able to support 80% of a 50 lb. aircraft and the torque generated by the sweep angle, they needed to be strong while also being lightweight. Instead of calculating exactly how strong they needed to be, a few test samples of various thicknesses were made and drop tested them with a dummy load. These tests showed that a main strut made of 7074 Aluminum at 0.1875 in. thick could handle the weight of the aircraft. The process for making the main gear strut will be discussed in the Landing Gear section.

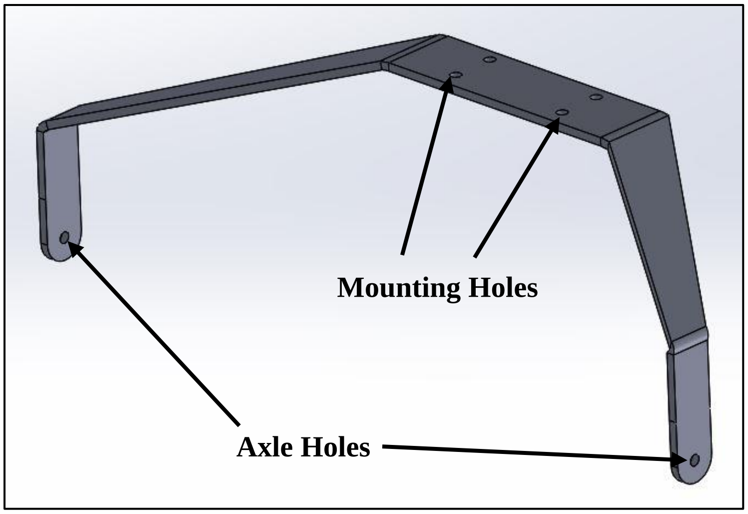

Figure 2.31 Main Landing Gear CAD

The nose gear required little extra design work because Robart, a UAV landing gear manufacturing company, has many different COTS nose gears. A nose gear strut was found that met all the requirements except for the extended length but Robart was able to custom make one with the required length.

To minimize the torque imparted on the nose gear during landing it was mounted on a 15^0 angled block as seen in Figure 2.32. Doing this makes part of the load be transferred axially up the strut as opposed to it being entirely orthogonal, reducing the effective torque. Also, helping dissipate some of the impact energy is an oleo-strut shock absorber. A concern with oleo struts is that, in the compressed state, their effective length is decreased which, for the tricycle configuration, puts the propeller closer to the ground. This particular oleo strut only compresses 1.0 in, which is within tolerance since the 26 in. propeller already has more than 5 in. of ground clearance. The inner tube of the nose gear can rotate inside the fixed outer tube allowing it to be steerable. The steering is controlled by a servo connected to the rocker arm on top of the strut.

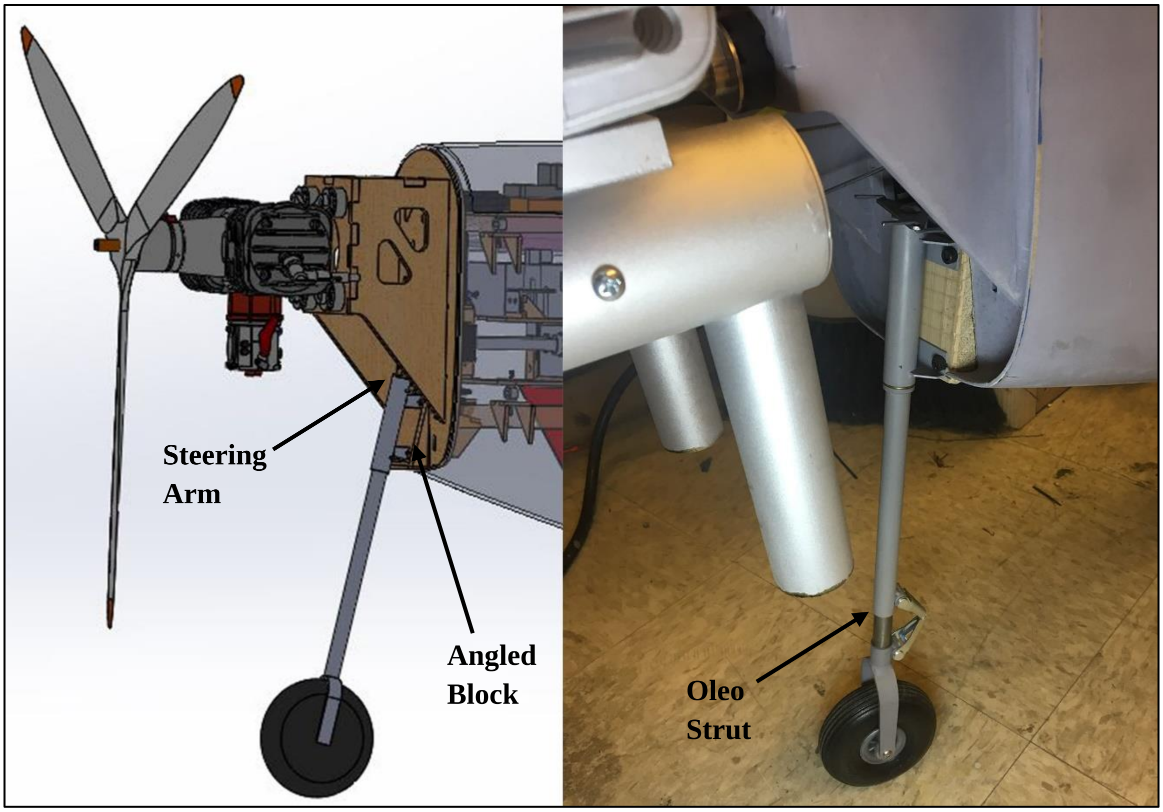

Figure 2.32 Nose Gear

Jet Exhaust Bay Hatch System

Normally, if not wing-mounted, jet engines are mounted in the fuselage with their exit nozzles open to the air at the aft end of the aircraft. Also, jet engines normally operate throughout the duration of the flight at an optimal efficiency point. Since the jet in Locust is mounted vertically, with the nozzle near the bottom of the aircraft, there needed to be a way to shield it against the free stream airflow to reduce drag. On the other hand, the nozzle had to be open to the air to let the exhaust gas escape. After many different configurations, tests, and failures, a system similar to a bomber's bomb bay doors was chosen where the doors open outward to the port and starboard. Figure 2.33 shows the doors both open and closed.

Figure 2.33 Locust Exhaust Bay Doors

The exhaust bay doors (EBD) are actuated by two HS-7245MH servos, one for each door. Since the doors are curved around three different axes, they cannot hinge about one point, so they must move outward as well as rotate. This motion is controlled by a specially designed, 3D printed hinge system. Each of the four hinges has a pivot point mounted to the aircraft's bottom bulkhead, a hinge arm mounted to the EBD structure and pinned to the pivot point, and a pin and e clip that holds the hinge arm in the pivot. The servo control rods are attached to built-in control horns on the front two hinge arms. Figure 2.34 shows the CAD drawing of the hinge system (in orange) both open and closed.

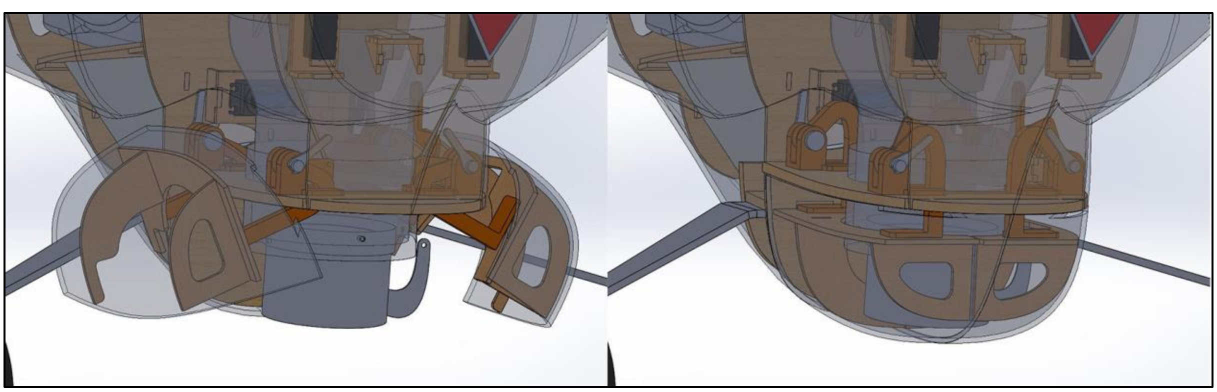

Figure 2.34 Locust Exhaust Bay Doors CAD

Initial testing of the system showed that the servos could not keep the EBD perfectly closed. At the servo's endpoint, there was a small amount of gear slop that allowed the doors to hang slightly open. This was a two-fold problem because it created more drag, and it also caused the servos to be fighting the wind to keep the doors closed. A simple fix using magnets was implemented where the magnets were mounted in the EBD structure about 1/8 in apart. They were close enough to hold the doors closed but not so close that the servos couldn't force them apart.

Allowing the hot gas to escape only took care of one end of the jet engine. At the cold end, the engine needed an air-intake to allow airflow while also blocking FOD. Since the middle, top section of the aircraft was already a removable hatch, the center of it was cut out and replaced with a lightweight aluminum screen. Figure 2.35 shows the screen impeded in the hatch and the Hatches section explains how this screened hatch was made.

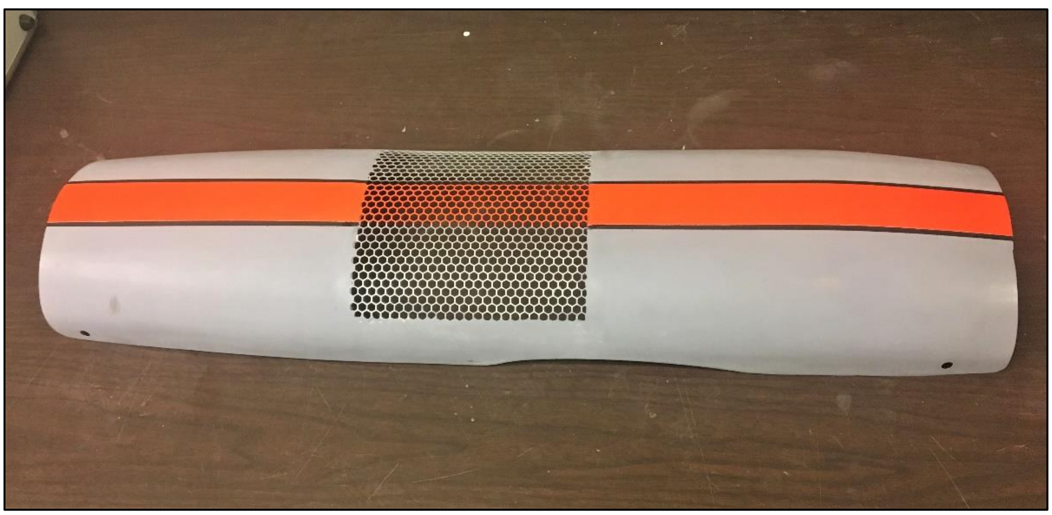

Figure 2.35 Top Hatch with Embedded Screen

Structural Configuration

Four major considerations were kept in mind when designing Locust's airframe: longevity, assembly, maintainability, and future growth. Keeping these in mind ensured that the aircraft was strong, robust, and easy to repair if damaged.

The main structural design choice for the aircraft was to make a monocoque fuselage, wing, and empennage. In monocoque structures, the outer skins take a large portion of the overall load and provides most of the torsional and bending stiffness. This design choice was only feasible since OSU has an industry type composites manufacturing lab with the capability to make composite skins. A schematic of the differences between monocoque and semi-monocoque can be seen in Figure 2.36.

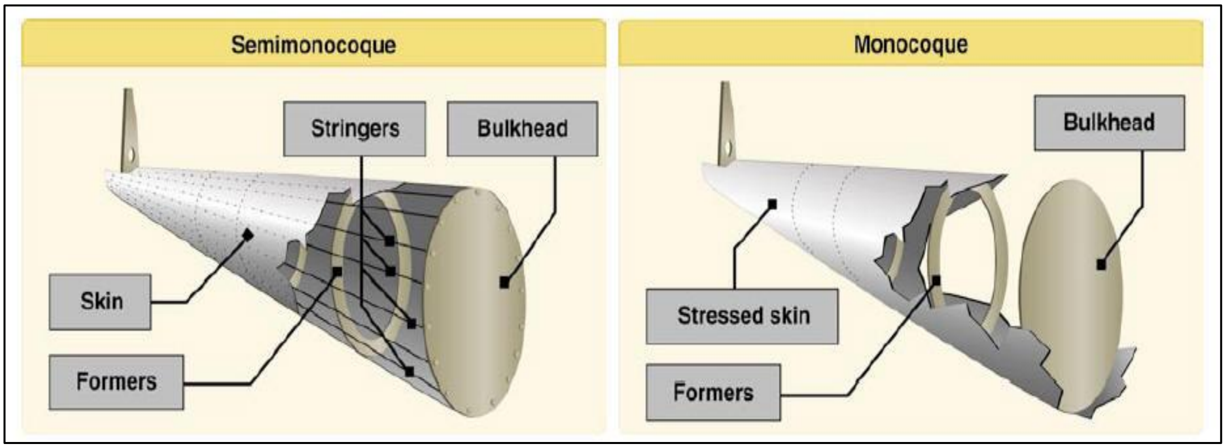

Figure 2.36 Semi-Monocoque VS Monocoque [38]

For all parts of the aircraft, wings, fuselage, and tail, the fiberglass skin halves were joined by bulkheads, or ribs and shear-webs for the wing and tail, made of 1/8 or 1/4 in. aircraft plywood (aeroply). These bulkheads also served as mounting surfaces to support other aircraft components.

All but two of the fuselage bulkheads were 1/8 in. thick. The firewall was made from 1/4 in. aeroply for increased strength and rigidity to support the DA-120 mount and nose gear. The bottom bulkhead was also made of 1/4 in. aeroply to support the main landing gear, which supports about 80% of the aircraft’s 50 lb. GTOW. Figure 2.37 shows the structural layout of the fuselage.

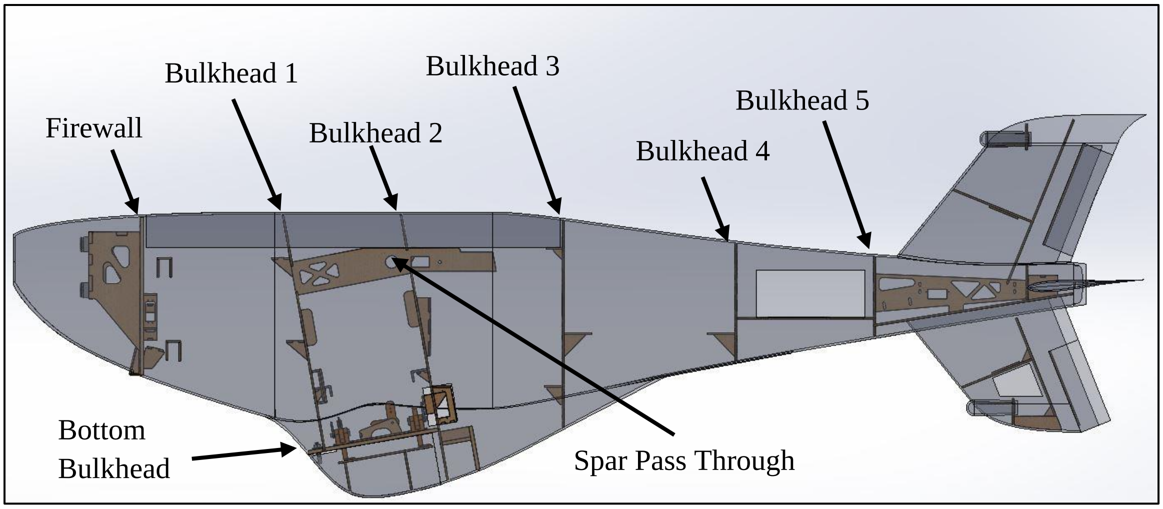

Figure 2.37 Fuselage Structural Layout

The wing structure, seen in figure 2.38, was similar to the fuselage except in place of bulkheads, it had ribs. The ribs joined the wing skins together, supported the spar, and served as a mounting surface for servos and other electronics. Connecting the ribs, on their aft end, was a shear web made of the same 1/8 in. aeroply. The front end of the ribs were connected, just fore of the spar, via a large composite shear web made of high-density foam and unidirectional carbon tow. Supporting the wings was the carbon fiber spar that was discussed in the Spar Sizing section. The spar passed through the fuselage where the load would be transferred to the main fuselage bulkheads by the wing support structure as seen in Figure 2.37.

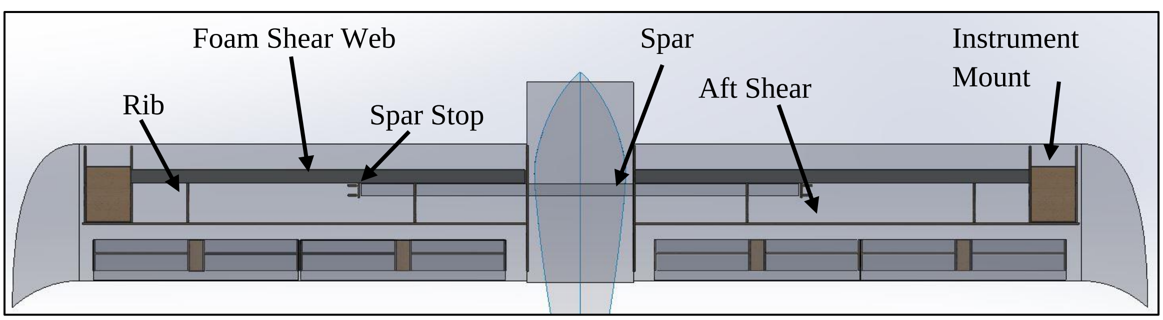

Figure 2.38 Wing Structural Layout

The horizontal tail was made almost identically to wing except it did not have a composite shear web and its ribs did not support servos. The fuselage supported the horizontal tail by 2 guides that matched the tail's cross-sectional shape. The exact construction methods will be discussed in the Manufacturing section.

Mass Properties

Developing the aircraft's weight and balance was an iterative process where the aircraft's weight, CG location, and CG travel were evaluated as the others were changed. While most aircraft designers want to minimize CG travel, Locust's CG travel had to be specifically designed to keep the CG travel isolated directly above the TV nozzle. The weight and CG estimations were done by a component build-up method where each readily available component was weighed and the weights of the missing components were found online. The fuselage, wing, and tail skin weights were estimated based on the surface area of the CAD model and the weight of a 2 in. x 2 in. square of the aircraft's composite skin layup. These weights were then placed into a spreadsheet with a reference distance from the firewall, which was the datum. With the weight and balance spreadsheet, the internal components were easily 'moved' around until the CG was right above the nozzle and had, at most, 1 in. of travel. The total weight breakdown can be seen in the appendices while a system weight fractions chart can be seen in Figure 2.39. From the pie chart, the CWL system is only 14% of the total weight, which is much less than the typical jet VTOL weight fraction of 30% seen in the literature. The components included in the CWL system weight were the: K-260, fuel pump, fuel flow meter, ECU, ECU battery TV unit, TV servos, and the jet pipe.

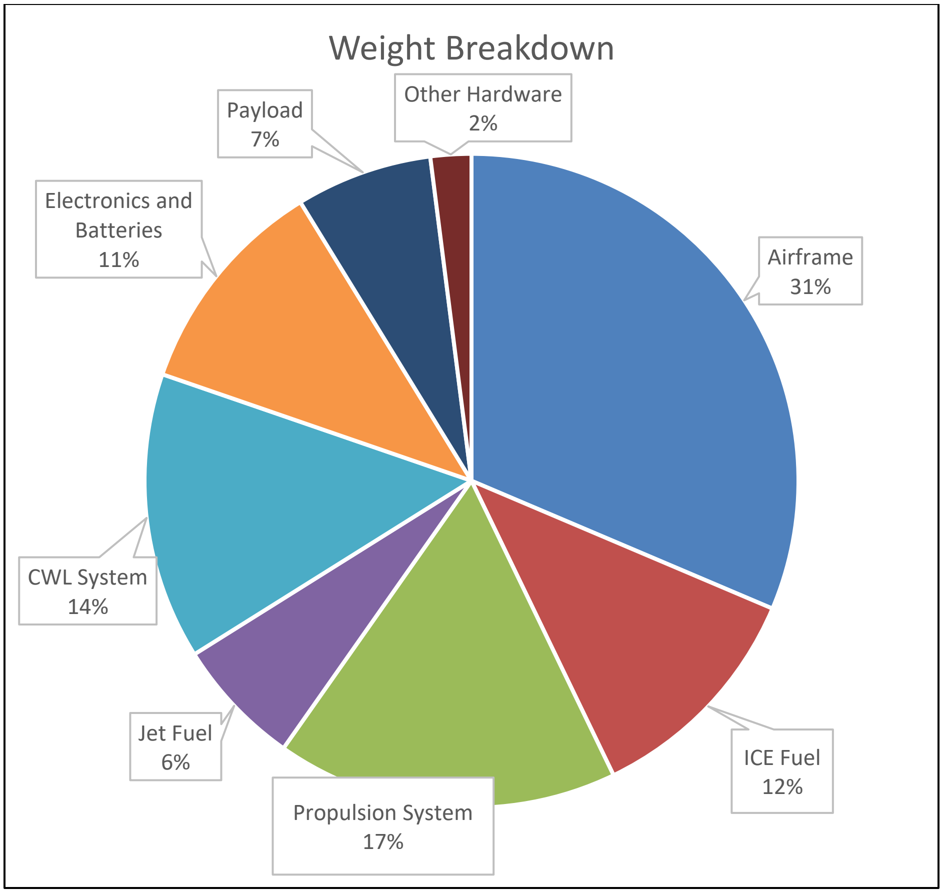

Figure 2.39 Locust's Weight Breakdown

The fuel fraction is the total onboard fuel for both engines. If the aircraft were needed for longer endurance, and the CWL system could be removed, the jet fuel could be replaced with gasoline for the DA-120. Also, with the CWL system removed, the center jet bay could be used as a carry-bay with the capability to deploy droppable payloads.

CHAPTER III

LAUNCH AND RECOVERY

The Launch Crate

Like many point launch UAS, Locust needed a separate launch system; however, unlike most point launch systems, Locust's was simple and did not require a recovery system. The whole launch system was comprised of a launch crate that had a quick-release mechanism that could be attached to a hard-point on the aircraft. On the pilot's command, a cord could be pulled to release the quick release, allowing the aircraft to take off.

The launch crate itself also doubles as the transportation crate. Figure 3.1 and Figure 3.2 show the launch crate in its transport and launch configurations respectively. Most of the box was made of plywood and 2x4s to reduce cost, manufacturing difficulty, and lead time. The base of the box was made of a sheet of plywood with 2x4s running along its length and a 1/16 in steel sheet spanning its width. The plate was used as a deflector plate and heat shield to prevent the problems seen from ground erosion which were discussed in the Problems with V/STOL section. Level with the top of the 2x4s and the metal sheet was another sheet of plywood that served as the main launch platform. This part had to be raised to give the main wheels a flat and unobstructed exit path. Underneath the raised platform and above the steel sheet was the tethering system.

This system was comprised of a chain bolted to the two main support 2x4s, a turnbuckle, and a quick-release mechanism. The turnbuckle was used to keep the chain at a constant tension and the quick-release mechanism was used to clip to a simple U-bolt mounted to the bottom bulkhead of the aircraft as seen in Figure 3.3. The aircraft had to be tethered to prevent movement while the IC engine was started, and the jet engine was brought up to full power.

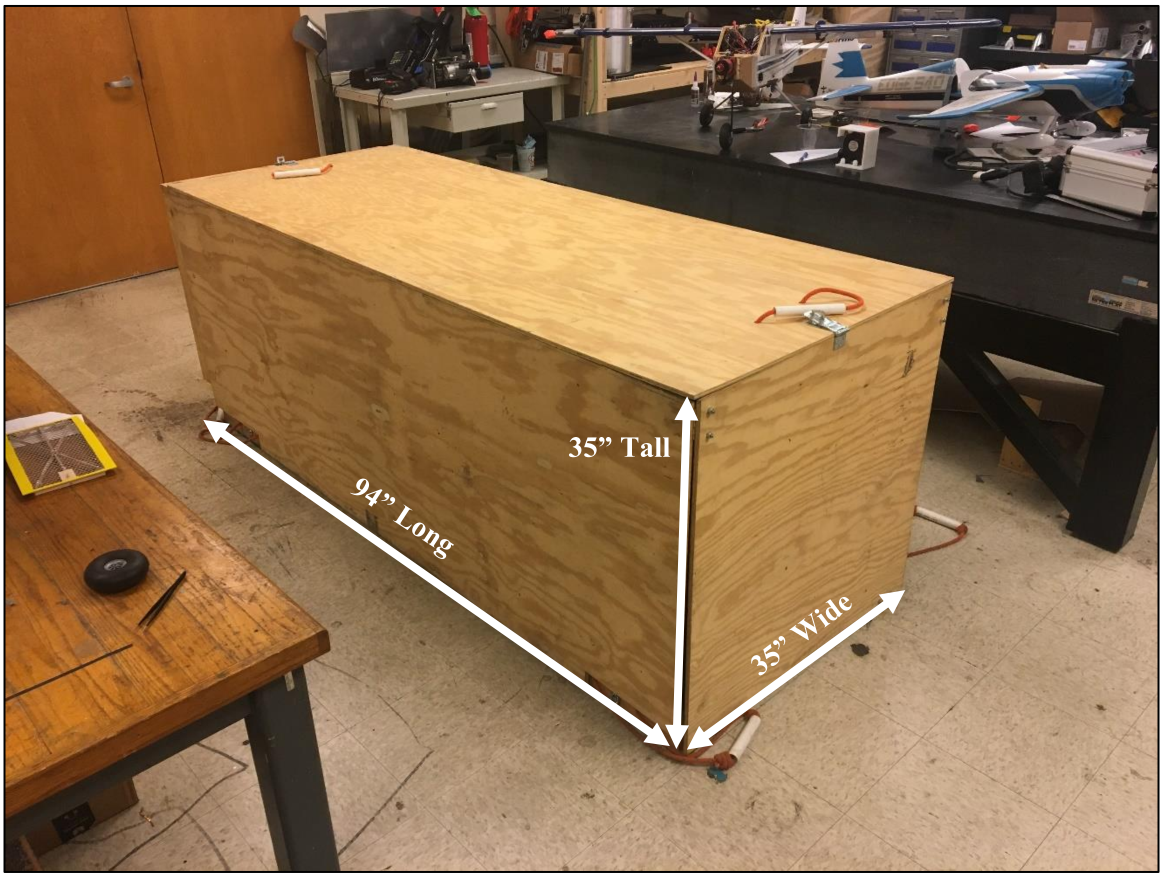

Figure 3.1 Launch Crate (Transportation)

The outer dimensions of the box can be seen in Figure 3.1. Its width was set by the aircraft's horizontal tail span, its height by the distance from the ground to the top of the vertical tail, and its length by the distance from the vertical tail tip to the propeller spinner. Conveniently, it was just short enough that it could fit in the back of a full-size SUV with the rear seats folded down. It could also fit in the bed of a pick-up truck per the initial design requirements. The 'lid' of the box was held in place during transport by a hasp latch at each end. Each wall of the box was connected to the base via simple hinges that allowed all four walls to lay flat on the ground, making up the launch configuration. When in the transit configuration, the walls were held shut by a set of hinges with the main hinge pin replaced by a removable cotter pin. The box was also equipped with 2 nylon straps with quick-release buckles to secure the aircraft during transit. Also, there was a rope handle at each corner for loading/unloading and moving the box.

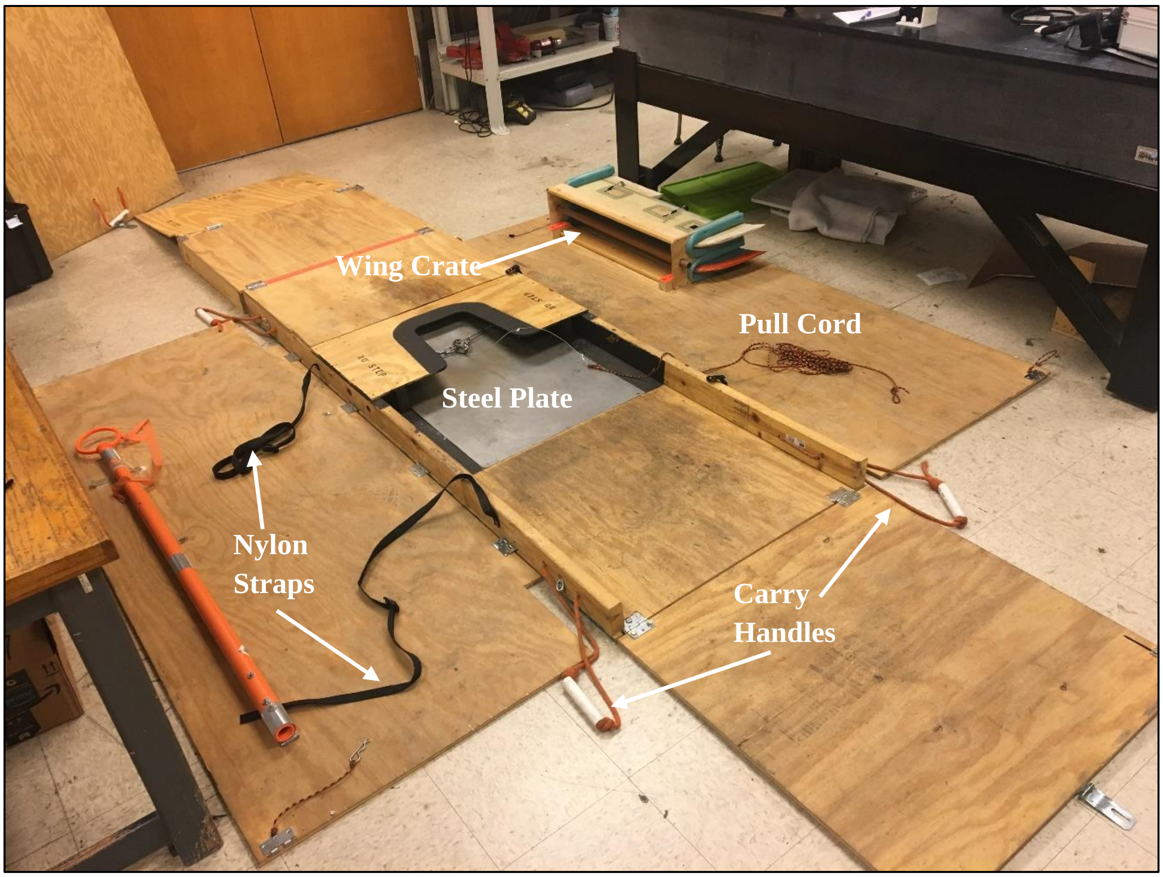

Figure 3.2 Launch Crate (Launch)

With a wingspan of more than 7 ft. the wings and spar had to be carried separately. The solution was a removable rack that could store both wings and the spar which can also be seen in Figure 3.2. For transportation, the wing rack was secured to the inside of the starboard wall of the box and then removed and set aside as the aircraft was being prepared for launch. The wing slots were slightly larger than the wing to allow the foam liner to provide a tight compression fit while the spar was held in place by the phenolic tube beneath the wings.

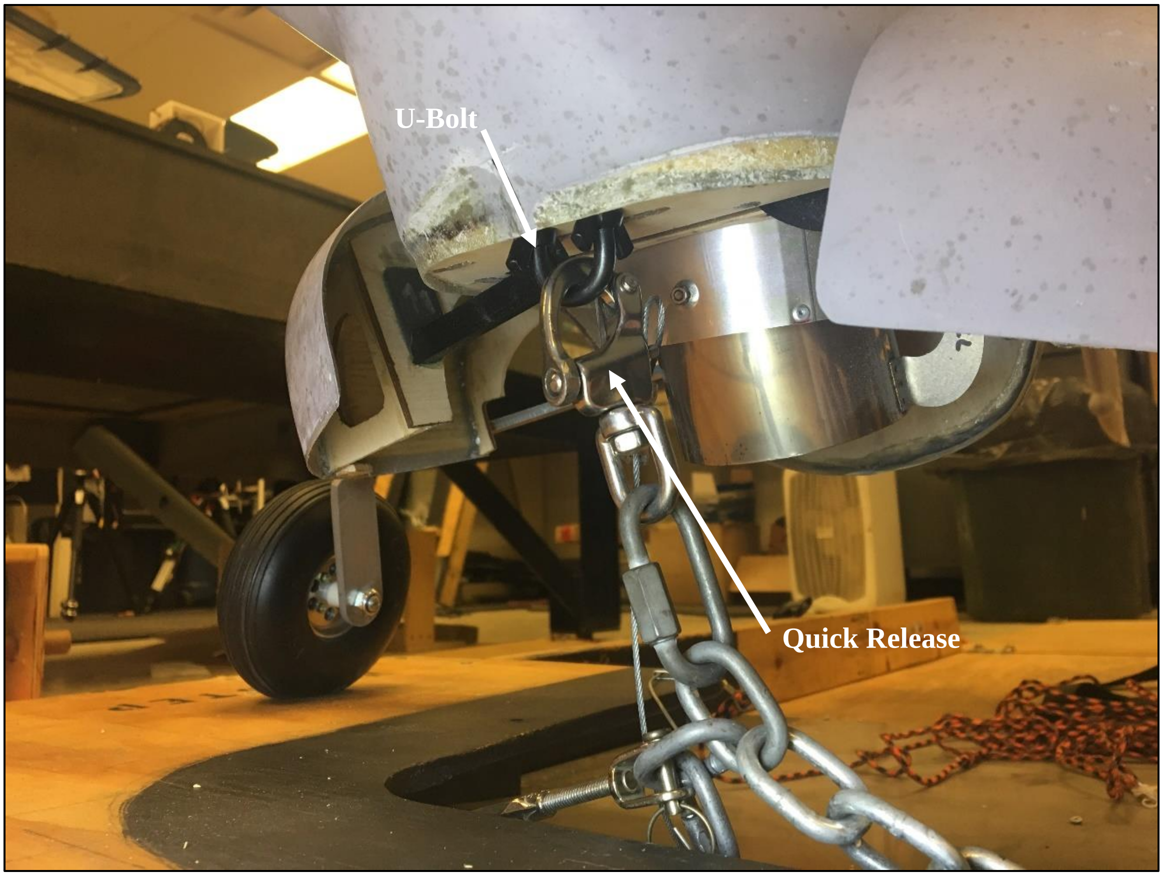

Figure 3.3 Locust Tether System

Ground Control Station

The ground control station (GCS) for Locust was comprised of 7 major components:

- Futaba transmitter
- Jeti transmitter
- Toughbook laptop
- RMILEC repeater
- RFD 900
- Omnidirectional antenna
- Pepperbox antenna

The Futaba was the pilot's flight control transmitter that was the primary method of sending control commands to the aircraft and its signal was sent to the Futaba ground receiver where it was then transmitted to the aircraft's onboard RMILEC receiver via the RMILEC repeater. The Jeti transmitter was used as an onboard-systems monitor that received the K-260 telemetry from the onboard Jeti Receiver. The RFD 900 ground unit communicated with the Pixhawk II by sending mission planner commands and sending/receiving telemetry to and from the onboard RFD 900. The Toughbook laptop was used to view Mission Planner, send mission commands, and view the Pixhawk II telemetry. In the future, as the aircraft's systems are refined, the goal is to have all of the ground station components be able to fit in a pelican carry case. A graphical representation of the aircraft's GCS communication network can be seen in Figure 3.4.

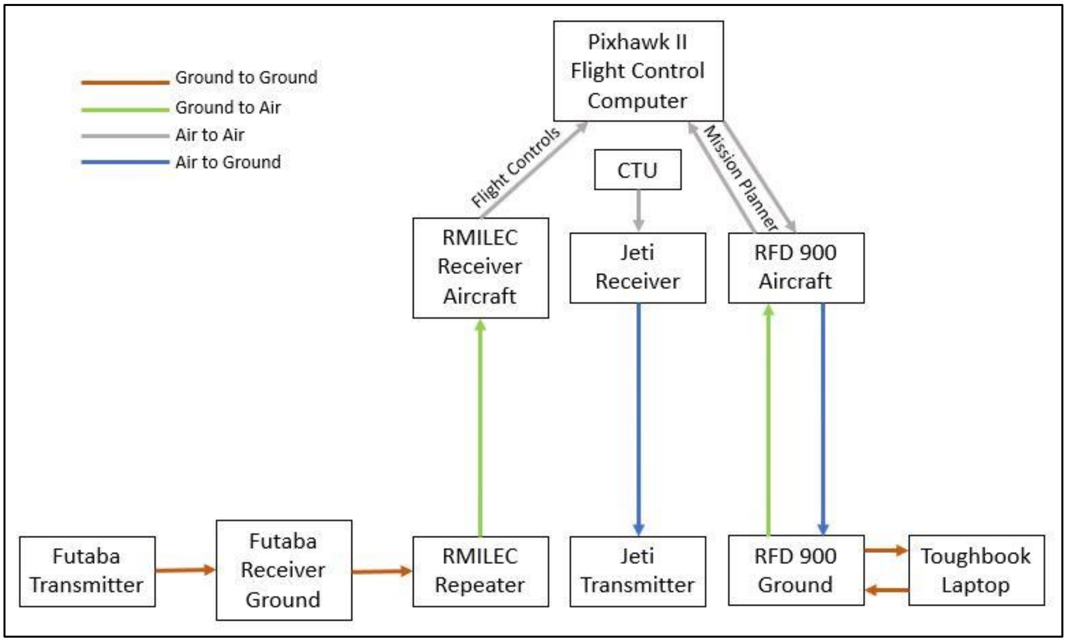

Figure 3.4 GCS Communication Network

Also, at the ground station, although not necessarily part of the GCS, was a CO2 fire extinguisher, battery-charger, fuel, field tool kit, field repair kit, and other necessary equipment.

Takeoff

After the box is unloaded from the transportation vehicle, the top is removed, and the side walls are let down. The five batteries, that were charged and installed before or during transit, are then plugged in and the fuel tanks are filled. Next, the wings are attached, and the wing electronics are connected and secured inside the aircraft. After fueling and connecting the electronics, all three power switches are thrown, giving power to the aircraft's systems and the telemetry is armed by the push of the arming button on the GPS puck. At this point, the aircraft is live, and the ground crew can begin their preflight checks. After all of the pre-flight checks have been completed and the aircraft is deemed flight-ready, the ground crew carries the box to the launch site and places it such that the aircraft will take off into the wind. With the launch box properly positioned, the aircraft is tethered to the quick release mechanism. For launch, a ground crew member holds the aircraft while another ground crew member starts the IC engine by using a torque starter or hand throwing the propeller. Once the IC engine is at idle, the pilot commands the jet to start. As the jet is starting, the internal pilot watches the jet telemetry readout to make sure it is operating nominally. The pilot then commands full power from the jet and 50% from the IC engine. Once the jet telemetry reads full power, the pilot commands a ground technician to pull the release cord. From there, the pilot has command of the aircraft.

Landing

Locust's landing profile follows a very specific set of checkpoints at specific airspeeds, altitudes, and engine power levels. The jet, providing vertical thrust, acts as a CWL device by effectively changing the weight of the aircraft. When the jet is on, the wing loading is less, which lowers the aircraft's stall speed as seen in Figure 3.5. The decrease in wing loading also lowers the amount of induced drag which makes it more difficult to reach slower landing speeds. To compensate for the lost induced drag and to generate more lift, the aircraft utilizes flaps with large deflections for landing.

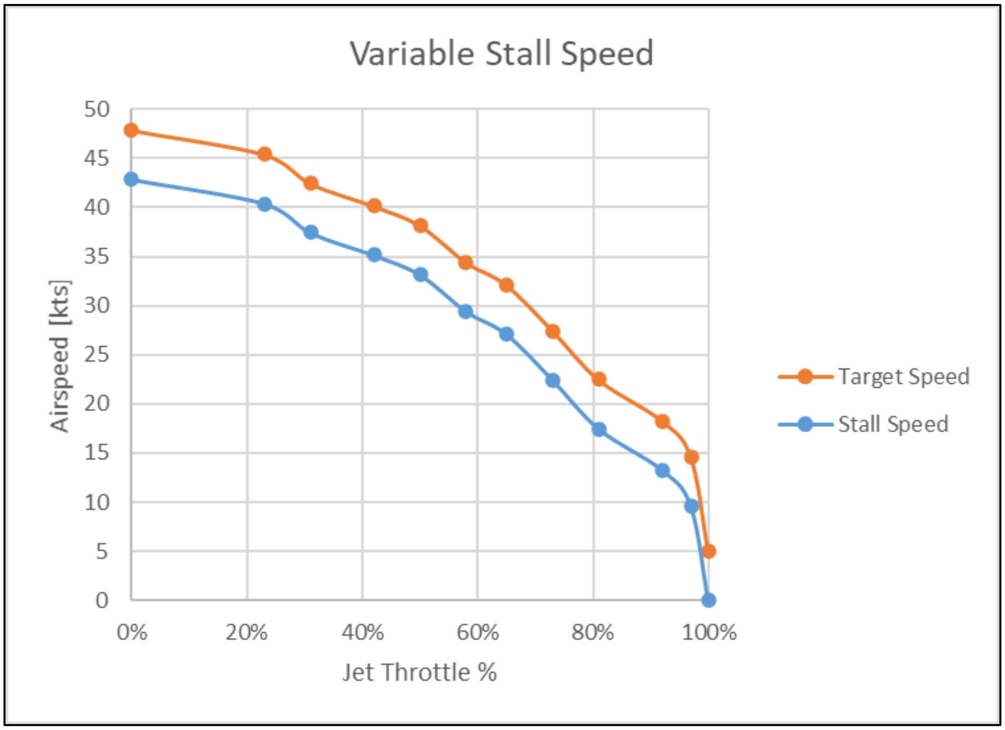

Figure 3.5 Locust's Variable Wing Loading

The pilot must fly a fine line to keep their aircraft in the air while also slowing down for a point landing. Figure 3.6 shows the list of designated airspeeds and jet power levels that the internal pilot reads off to the pilot as he sets up to land. An ideal landing would look like the aircraft coming in at a slight descent rate and then slowing down so much that, as the pilot flares, the aircraft slows to almost zero airspeed and sets down on the ground with little to no rollout.

Pre-Takeoff		**Landing**	
Flight Mode	FBWA	Midfield downwind	
Flaps	Mid Position	Target Speed	45 kts
		Turbine	50%
Takeoff		Slow to	35 kts
Turbine	Start		
Prop Power	40 %	Final Approach	
Turbine Power	100 %	Flaps	Full
Launch System	Release	Turbine	75%
		Slow to	25 kts
		Turbine	As needed
After Takeoff		**Aircraft Limits**	
Airspeed > 45 kts		Vst T0%	48 kts
Turbine	Idle	Vst T50%	35 kts
Airspeed > 50 kts	Flaps up	Vst T75%	27 kts
		Vapp T0%	50 kts
Before Landing		Vapp T50%	35 kts
Begin pattern	200-300 ft	Vapp T75%	25 kts
Turbine	Start		
Airspeed	45 kts	Turbine time ON	9 min MAX
Flaps	Mid	Begin landing	5 min
		WARNING	7 min

Figure 3.6 Landing Procedure

In the Research Rationale and Proposal section, there was a discussion about a headwind being beneficial for Locust's flights. The headwind helps by making the aircraft's airspeed higher than its ground speed which effectively lowers the required speed for takeoff and landing. Also, a headwind decreases the landing distance because the aircraft can land at a lower ground speed which reduces the ground roll-out. An approximation of landing distance with increasing wind speed is shown in Figure 3.7. The landing distance approximations were made by integrating velocity divided by acceleration.

$$D = \int_{V_i}^{V_f} \frac{V}{a} dV \tag{7}$$

Where,

$$a = \frac{g}{W}[T - D - \mu(W - L)] \tag{8}$$

Assuming a rolling resistance coefficient of 0.3 as suggested in Raymer's *Aircraft Design* book for military aircraft with brakes [12, pp. 689-695], negligible lift being generated by the wing during landing, no thrust being provided by the main engine, and a landing weight equivalent to the takeoff weight, equation 7 simplifies to:

$$D = \frac{1}{g}\int_{Landing\ Speed}^{0}\left(\frac{WV_g}{-\frac{1}{2}\rho V_g^{2} S C_D - \mu W}\right) dV \tag{9}$$

where $W = MTOW$ and $V_g = ground\ speed$, and $\mu = rolling\ resistance\ coefficient.$

Assuming a rolling resistance coefficient with brakes allows a conservative estimation to where the actual rollout would be longer than predicted.

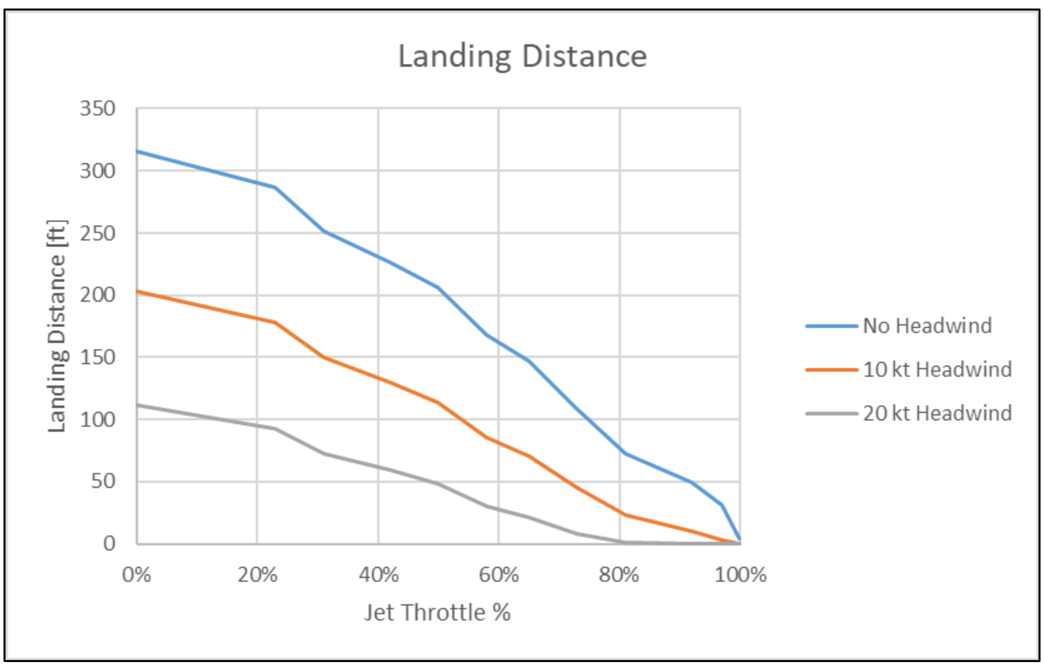

Figure 3.7 Landing Distance

Optional Configurations

Another benefit of using the direct thrust configuration in conjunction with traditional landing gear is that the aircraft is capable of operating in different configurations. First, the CWL system could be entirely removed allowing for additional fuel/payload making it a CTOL aircraft. The CTOL configuration would be useful if extended missions were desired with access to a developed runway. Additionally, keeping the CWL system, the aircraft could be overloaded giving it a GTOW > 50 lb. Being heavier than the MTOW for point launches would prevent the point launch capability but would still allow it to operate as a STOVL or STOL aircraft. Similar to the CTOL configuration, the STOVL and/or STOL configurations could be used if the mission required more fuel/payload but still needed relatively short takeoffs and landings using the lift jet. These configurations would not necessarily need a full runway, but they would need a short ‘quasi-runway’.

The estimated takeoff distances shown in Figure 3.8 were approximated by solving equation 7 for takeoff at different MTOWs.

$$D = \frac{1}{g}\int_0^{TO\ Speed}\left(\frac{WV_g}{T - \frac{1}{2}\rho V_g^2 SC_D - \mu\left(W - \frac{1}{2}\rho V_g^2 SC_{Lmax}\right)}\right)dV \qquad (10)$$

Where $T = thrust$ at takeoff and $C_{Lmax} = Max\ lift\ coefficient$

From Figure 2.14, it can be seen that the maximum, full-power takeoff thrust is about 35 lb. The maximum lift coefficient (C_{Lmax}) used was 1.3 and the rolling resistance coefficient (μ) was 0.05, which is the average rolling resistance value for concrete and asphalt [12, p. 690].

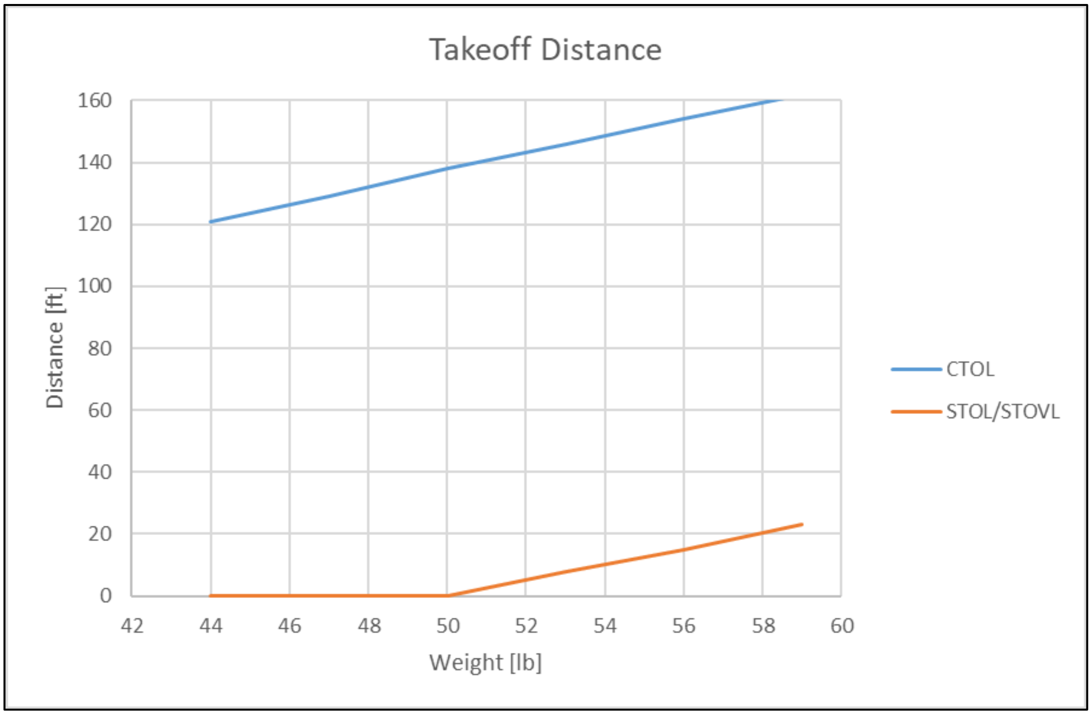

Figure 3.8 Alternate Configuration Takeoff Distances

CHAPTER IV

MANUFACTURING

Methods

There are many ways to build an airplane, the methods used to build Locust were chosen based on the aircraft's mission, cost, and available equipment capability. OSU's Design and Manufacturing Lab (DML) has a composites lab with the capability to manufacture fully composite, monocoque airframes made of materials such as carbon fiber, fiberglass, and aramid (commonly known as Kevlar). Equipment like computer numerical control (CNC) machines, 3D printers, welders, and other equipment likely to be found in an engineering research and design lab were also available.

Locust's mission of taking off and landing from anywhere, on nearly any type of terrain, pushed the airframe design to be strong, robust, and able to survive harsh landing conditions and hard landings. Also, to maximize the thrust to weight ratio, it needed to be as light as possible. To meet the lightweight and robustness requirements, it was designed to be a composite monocoque airframe with lightweight aircraft grade plywood internal structure.

Meeting the low cost and rapid production requirements meant developing accurate, strong, and reusable tooling that could be used to make as many as 50 airframes. Since the DML composites lab has the necessary equipment to manufacture industrial-grade tooling, Locust's molds were made extremely accurate and robust by using a CNC machine and high strength tooling fiberglass.

A basic overview of the manufacturing process of Locust and its tooling can be seen in Figure 4.1. The CAD model's g-code was uploaded to a CNC machine, which cut out the plug halves for the wing, horizontal tail, and fuselage. A plug is a 3D model of the part that is made of special machining foam. The molds were made by draping epoxy-soaked pieces of special tooling fiberglass over the plugs. After the molds cured, they were pried from the plug and used to make composite skins. A special laser cutting CNC machine was used to cut the internal bulkheads and structural parts, which were bonded to the skins using thickened epoxy. After the epoxy cured, the aircraft went through post-processing, basically making it sealed and smooth to minimize parasite drag. While bonding the airframe together, the main landing gear was made by cutting a 2D version of it from an aluminum sheet with a water-jet CNC machine and bent to shape with an oxy-acetylene torch. The finished airframe was then integrated with all of its electronics, engines, fuel systems, and landing gear. Once fully integrated, the aircraft went through a series of rigorous ground tests before finally being tested in the air. Each of these steps, methods, and materials will be explained in-depth in the coming sections.

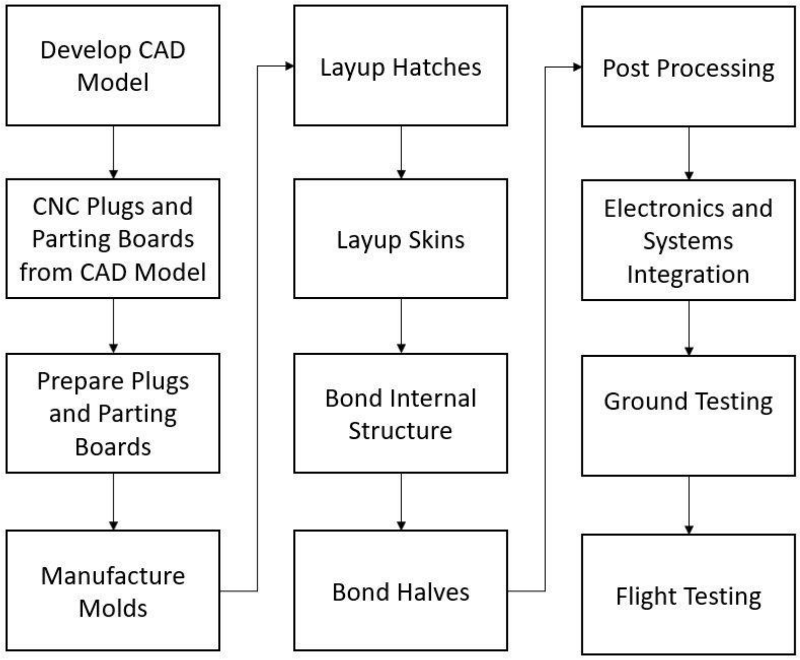

Figure 4.1 Basic Manufacturing Flowchart

Materials and Equipment

Manufacturing a high-strength low-weight composite aircraft required many different materials, tools, and industrial manufacturing equipment. Table 4.1 shows the fabrics, materials, and bonding agents used with descriptions of what they were used for during the build process. The industrial equipment consisted of the following:

- 3-axis rotary CNC machine
- laser cutting CNC machine
- water cutting CNC machine
- vacuum pumps
- band saw
- drill press
- belt sander
- oxy-acetylene system

and other machines/equipment likely to be found in an engineering manufacturing and design research laboratory. The rotary CNC machine was used to carve the plug out of machining foam, the laser cutting CNC machine was used to cut the internal structure, the water cutting CNC machine was used to cut out the main landing gear blanks, and the vacuum pump was used in making the aircraft's skins.

Material	Purpose
Tooling Glass	Mold Backing
Fiberglass	Aircraft Skins
Balsa Wood	Aircraft Skins Core
Aero-Ply	Bulkheads and Structure
Kevlar	Control Surface Hinges
Carbon Tow	Local Skin Stiffener
Tool Coat	Mold Tooling Surface
Epoxy	Aircraft Skins
Shower Drain	Bonding Bulkheads and Structure
Sandable Epoxy	Fillings Divots and Covering Seams
7071 Aluminum	Main Landing Gear

Table 4.1 Manufacturing Materials

Composite Laminates

Before beginning an in-depth explanation of the manufacturing process, it is necessary to have a generalized discussion on composite laminates and the terminology used. Composites can be defined as "materials consist[ing] of strong fibers, such as glass or carbon, set in a matrix of plastic or epoxy resin [39]." For manufacturing monocoque airframes, there are many possible choices of both the fiber-reinforced materials and the resins. Also, these materials and resins can be combined in different ways and layers depending on the desired strength, stiffness, and weight. Sheets of fiber-reinforced materials, like fiberglass, carbon fiber, and aramid, are anisotropic, which is why composite laminates are laid-up with their fiber directions aligned with the major load directions. When strength and stiffness are required in multiple directions, the sheets of fabric can be laid-up in layers with alternating or offset fabric weave biases. Figure 4.2 shows a close up of 2 pieces fiberglass where one weave is at a 0-90 degree bias and the other is at a 45-45 degree bias. Layups using alternating layers of 0-90 and 45-45 have bending strength in both the x and y directions while also having torsional rigidity due to the 45-45 layers. While composite laminates exhibit high tensile and bending strength, they have a relatively low compressive strength due do their typically small area moment of inertia.

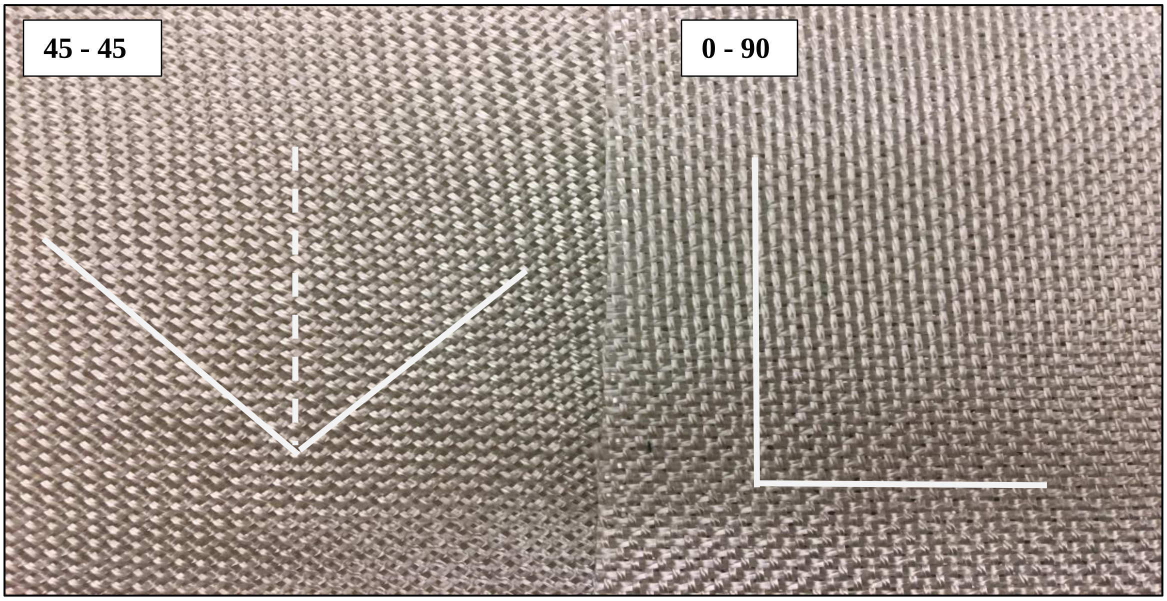

Figure 4.2 Fiberglass Weave Bias

Composite laminates' stiffness can be greatly increased by adding a core material between the layers of fabric. Like the materials and resins, there are many types of cores with various engineering properties; some typical core materials are balsa wood, foam, and honeycomb. Using core materials is preferred over adding more layers of fabric because they offer a large increase in stiffness by increasing the area moment of inertia while adding minimal weight. Also, using core materials is generally cheaper than adding more layers of fabric sheets, especially with carbon fiber.

Sheets of fiber-reinforced materials also come in different weights and weave types. The different weights are area densities that define the fabric's weight per square yard; so, '10-oz fiberglass' refers to a sheet of fabric that is one square yard and weighs 10 oz. The weave types can vary the material's strength and stiffness slightly but are generally selected based on cost and the aesthetics of the finished product [40].

Locust's monocoque airframe was designed for minimal weight with a lay-up schedule of one layer of 1/16 in. balsa wood, sandwiched between two layers of fiberglass. From the outer skin working inward, the layup schedule can be written in shorthand by 3FG x 3FG45 x 1/16BW x 3FG. Table 4.2 defines the shorthand notations listed here and others that will be used later.

The outer skin consists of two layers because, in composite laminates, the outer layer is the primary load-bearer.

Composite Layup Shorthand Notation	
3FG	3-oz. Fiberglass
3FG45	3-oz. Fiberglass @ 45-deg. Bias
1/16BW	1/16 in. Balsa Wood
MAG	Magnets
KEV	Kevlar
CT	Carbon Tow

Table 4.2 Composite Layup Shorthand Notation

The following paragraph explains the general layup process developed for Locust's skins but will be explained in-depth in the skins and hatches sections. The layup process started with applying wax and release to the mold (molds will be discussed in the tooling section). The wax, Partall Paste #2, was used to fill near-microscopic scratches and holes while also helping remove dust and debris that might have been missed during cleaning. It was applied and removed three times using shop cloths with the traditional wax on and wax off method. The release, Partall Film #10, was used to provide a micro-thin, non-permeable membrane to prevent the epoxy from bonding to the mold. Three layers of release were applied to the mold with foam brushes and allowed to dry between each layer. A composites technique known as pre-impregnation was used (pre-preg) to prepare the fiberglass. Pre-pregging is where the fabric is impregnated with epoxy resin on a flat table and then transferred to the molds. The benefit of pre-pregging instead of impregnating the fabric in the mold is that the pre-preg method allows the epoxy resin to be scraped exceptionally thin which helped to reduce overall weight while also ensuring that the fabric was

100% impregnated. The pre-pregged sheets of fiberglass were laid in the mold and worked around until completely smooth against the surface of the mold, free of wrinkles and air bubbles. After the outer layers of fabric were laid, the core layer was added and then covered with another layer of pre-pregged fabric. Depending on the part being made, there could be an additional layer following the last layer of fabric. The final layer was generally either strips carbon tow and/or Kevlar. Carbon tow was used to add localized strength and Kevlar was used to provide an internal hinge for the control surfaces.

After all the layers have been placed in the mold, a series of materials were added to allow the whole layup to be put under a vacuum. The first added layer was peel ply, a permeable plastic sheet used to increase the surface roughness of the inside of the part. This was done to increase the effectiveness of the bond between the structure and the skin. After peel ply came the perforate (perf) followed by the breather. The perf is a non-permeable plastic sheet that is perforated with tiny holes. These tiny holes allow excess epoxy to seep into the breather material when under vacuum. The breather was used for absorbing the excess epoxy and allowing a uniform vacuum over the whole part. A vacuum medallion was then placed on a stack of folded breather on the flange of the mold to allow a connection point for the vacuum pump. Lastly, a sheet of non-permeable bagging material was added to the mold to provide an airtight seal. The edges of the vacuum bag were sealed using chromate tape. Once the vacuum pressure reached at least 20 in. Hg, the whole part was rolled with wooden rollers to help press the layers together by removing air pockets and voids to form a stiffer, more cohesive part. Figure 4.3 shows a schematic of the vacuum sealing method.

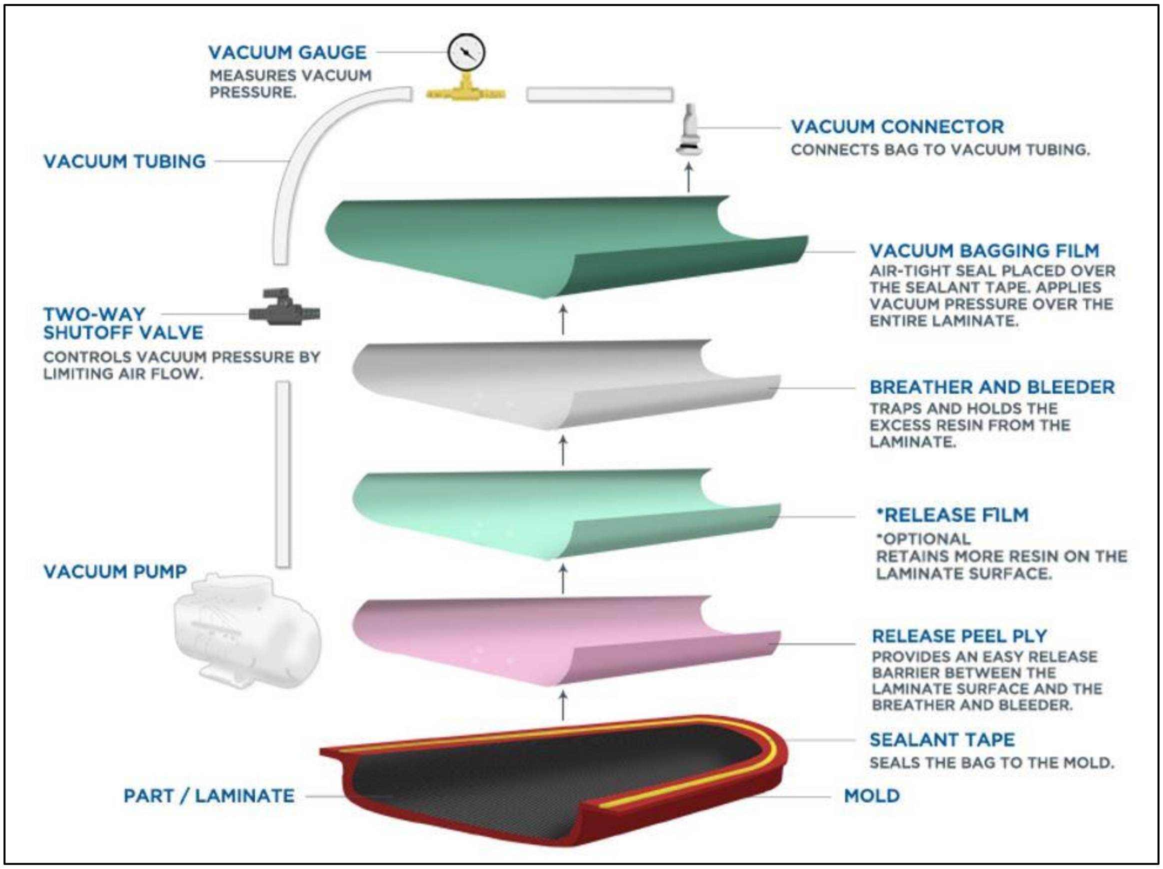

Figure 4.3 Composite Layup Vacuum Sealing [41]

Tooling

As mentioned before, there are many ways to manufacture aircraft and their tooling. The methods used here reflect the methods that have been developed at OSU and refined over the last 10 years from various aircraft design and manufacturing projects. A full manufacturing instruction manual that details how to make an airframe from the CAD model to a finished airframe can be found in the appendices. The following discussion will touch on the steps, methods, and materials used during the manufacturing process, but the detail will be left with the instruction manual.

The first step in the development of the tooling used to create Locust was making a CAD model with the exact shape and dimensions as the actual airframe. As far as molds are concerned, the only necessary part of the CAD is the outer skin shape. To create the plug, G-codes were made from the SolidWorks CAD model and then uploaded to the CNC machine which carved the shape of half of the plug. Plugs have to be made in parts because the CNC machine cannot cut at negative draft angles which are depicted in Figure 4.4.

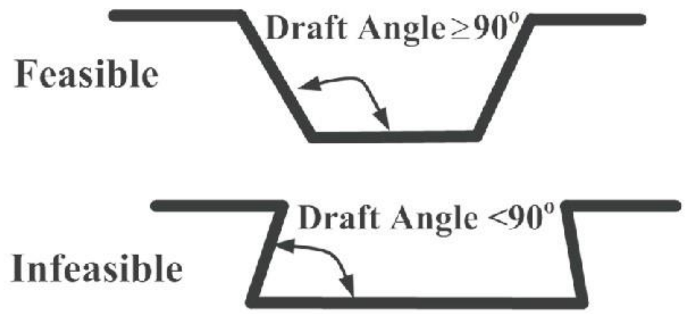

Figure 4.4 Draft Angles [42]

Before the plug halves could be bonded together, the parting board, a type of jig, had to be made to support the plug for both bonding halves and making molds. The medium-density fiberboard (MDF) parting board was made by the CNC machine cutting out a negative shape that would support the plug exactly at the parting line, like in Figure 4.5.

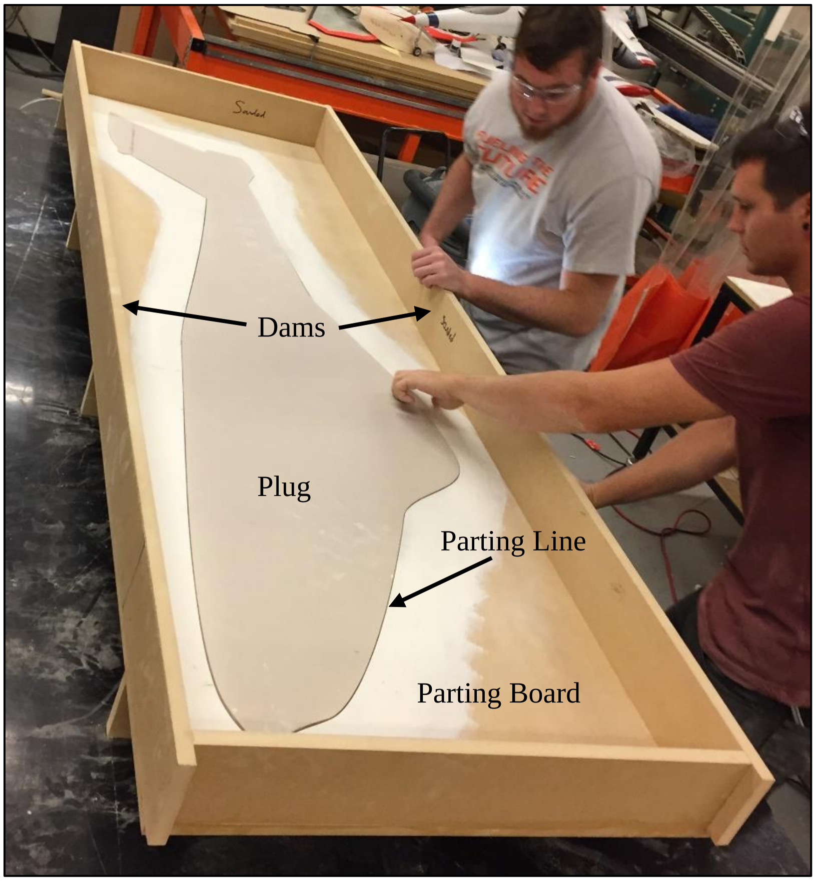

Figure 4.5 Locust Parting Board

Also, dams were added to the parting board to give it and the molds support to sit flat on a table. The dams were simple MDF boards nailed to the sides of the parting board. The dams' height was slightly greater than the maximum height of the plug from the parting line. With the parting board made, the plug halves were then bonded together using 5-minute epoxy. Once in place, sandbag weights were placed on the plug to ensure a complete and solid bond.

Preparing the plug for molding meant transforming a jagged, rough foam finish to an aerodynamically smooth tooling finish. This was accomplished by alternating between sanding, applying coats of primer, and sanding again. In places where the CNC machine's bit gouged or broke parts of the plug, drywall putty was added to fill the void. Once dry, it could be sanded flush with its surroundings. After many iterations of priming and sanding and moving all the way up to 400-grit sandpaper, the plug had a solid and glassy finish. The parting board was treated similarly to ensure a flawless fit with the plug. It should be noted that the plugs, parting boards, and molds for the different aircraft components were made very similarly with no noteworthy differences.

The first step in making the mold was picking a time where all the design team members could work at least 10 hours straight. From experience, it was known that making molds can take anywhere from 2 - 8 hours, depending on the size. The pre-mold processing of the plug began with a thorough cleaning with denatured alcohol and putting clay in the seam between the plug and the parting board. The excess clay was then scraped away with plastic razor blades to reveal a seamless fit. After the clay was flush with the parting line, the parting board, dams, and the plug were waxed and released in the same way as done for doing composite layups.

Tool-coat, a mixture of RSC-301-X Gel-Coat and SC-150-Blue hardener, used in composite mold making to give a smooth, tooling finish, was then mixed in buckets and applied very carefully to the plug, parting board, and dams with foam brushes as seen in Figure 4.6. Once all the surfaces were covered in a thin layer, the tool coat was allowed to kick, a rapid increase in temperature and viscosity that begins curing, before another layer of tool coat was applied.

The next step in the mold making process was to create the structural backing of the mold because the tool coat itself is brittle. Following the second layer of tool coat kicking, the plug, parting board, and dams were covered with 13 layers of tooling fiberglass. Each layer was precut to size and alternated between 0-90 degree and 45-45 degree fabric biases. Each piece of fiberglass, for one layer, was laid on the mold and then covered in epoxy before the next layer was added. The epoxy was a 24-hour cure mixture of WB-400 resin and SC-150 hardener and was applied via epoxy spreading tools. Once finished with laying all 13 layers of the fiberglass backing, the mold was left for 48 hours to cure.

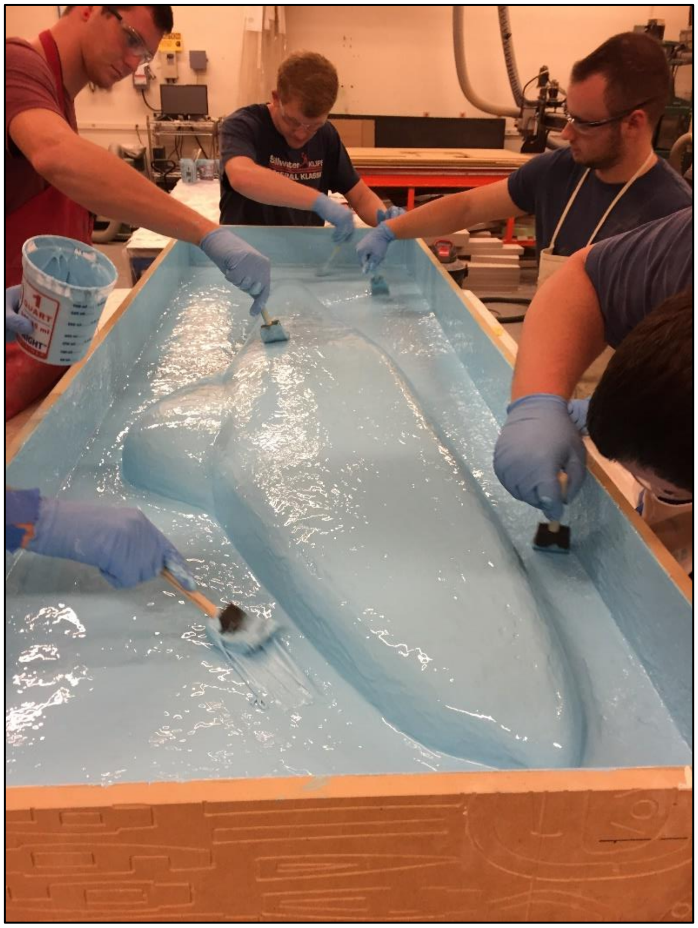

Figure 4.6 Applying Tool-Coat to Locust's Plug

After the mold had cured, a router was used to remove the excess fiberglass to make the bottom of the mold planar so that it could rest flat on a table. Figure 4.7 shows the bottom of a mold after it has been cut and finished. Figure 4.7 also shows the orange rope handles. The handles were added after the molds were finished to allow them to be easily carried since they each weighed nearly 45 lb.

Figure 4.7 Mold Bottom

The second half of the mold was made in almost the same way with the same process and a few minor changes. First, the parting board had to be removed from the mold and discarded while the plug was left undisturbed in the mold as in Figure 4.8. After cleaning off the old release and clay, depressions were drilled into the surface of the mold flange. The depressions were drilled to allow the other mold’s tool coat to fill them which insured that the mold halves could be perfectly aligned later when bonding skin halves together. New dams were bolted to the existing mold to give the opposite mold its own support dams. Like making the first mold, the new mold was made by the same method of waxing, releasing, applying tool coat, and adding the fiberglass backing.

Figure 4.8 Finished Half of Locust's Fuselage

Separating the molds was done by gently pressing plastic wedges between the molds at the parting line. Once apart, the plug was removed from the first mold by inserting thin strips of Mylar between the mold and the plug. Using an air compressor, air was forced into the tiny gap created by the Mylar until the plug popped loose and could be easily removed. If done perfectly, the plug would be undamaged and could be used to create more molds. The scope of this project was small enough that there was no need for duplicate molds.

Hatches

All aircraft, manned and unmanned, must have access hatches for various internal components. The methods developed at OSU utilize flush-mounted hatches because of their simplicity to manufacture, their smooth, flush fit with the outer skin, and their tried and true reliability. The size of the hatches varied widely based on which component they allowed access to and what tools would need to fit in for installation and maintenance. For instance, a servo hatch cannot just be the size of the servo; because to put the servo in, somebody has to fit their hand in there with a screwdriver. When the hatches were designed and sized, great care was taken to consider assembly, maintenance, and future modifications.

Every hatch for Locust was made with the same method. The first step was cutting the balsa core to the correct size and beveling the edges to a fine edge. Beveling the edges ensured that the core was completely sealed off between the layers of fiberglass for maximum strength and rigidity. Before laying up the hatches, the mold had to be waxed and released like how the plug and parting board were when making the molds. The layup schedule for the hatches was 3FG x 3FG45 x 1/16BW & MAG x 3FG45 x 3FG. Originally the hatches were only made with three layers of fiberglass, but they were found to be too flimsy and susceptible to tearing. The raw fabric was cut large enough to allow the hatches to have a ½ in flange around the core. The flange was necessary to allow room for the magnets. Each layer of fiberglass was pre-impregnated and then laid in the mold according to the layup schedule. Before adding the next layer, the previous layer was smoothed out using squeegees to prevent wrinkles and air bubbles which could compromise the hatch's structural integrity. Before laying the third layer of fiberglass, the magnets were placed at the corners of the core and then surrounded by thickened epoxy, epoxy mixed with 406 colloidal silica, to act as a bevel since they themselves could not be beveled. After the subsequent layers of fiberglass were added, the peel-ply and breather were added before it was bagged and put under vacuum. Once finished curing, the hatches were removed from the mold, cleaned, and trimmed to have a ½ in flange around the core. A finished hatch can be seen in Figure 4.9.

Figure 4.9 Finished Hatch

The top hatch required additional post-processing because it was made in two molds. After bonding the fuselage skins together, which will be discussed later, thin painter's plastic was laid over the top of the fuselage to prevent the epoxy from bonding to the airframe. The top hatch halves were set in place on the plastic and automatically aligned with their embedded magnets. Then, a strip of pre-pregged fiberglass tape was laid over the slight gap between the two hatch halves. Once cured, the hatch was removed, and the same process was repeated on the bottom side of the hatch seam to completely seal it.

Once the top hatch was completed, a lightweight aluminum screen was embedded in it to allow air to the lift jet while keeping FOD out. This was done by first cutting out a square hole in the hatch that was slightly smaller than the piece of aluminum screen. Then, the exact shape of the screen was cut out of the outer layer of fiberglass and the balsa core. The inside layer of fiberglass was left slightly smaller so that the screen would have a surface to bond to. The aluminum screen was bonded to the hatch with sandable epoxy, epoxy mixed with 410 microlight fairing filler. Once cured, the excess epoxy was sanded flush with the outer skin and painted to leave an aerodynamically smooth and aesthetically appealing finish. The process can be seen in Figure 4.10.

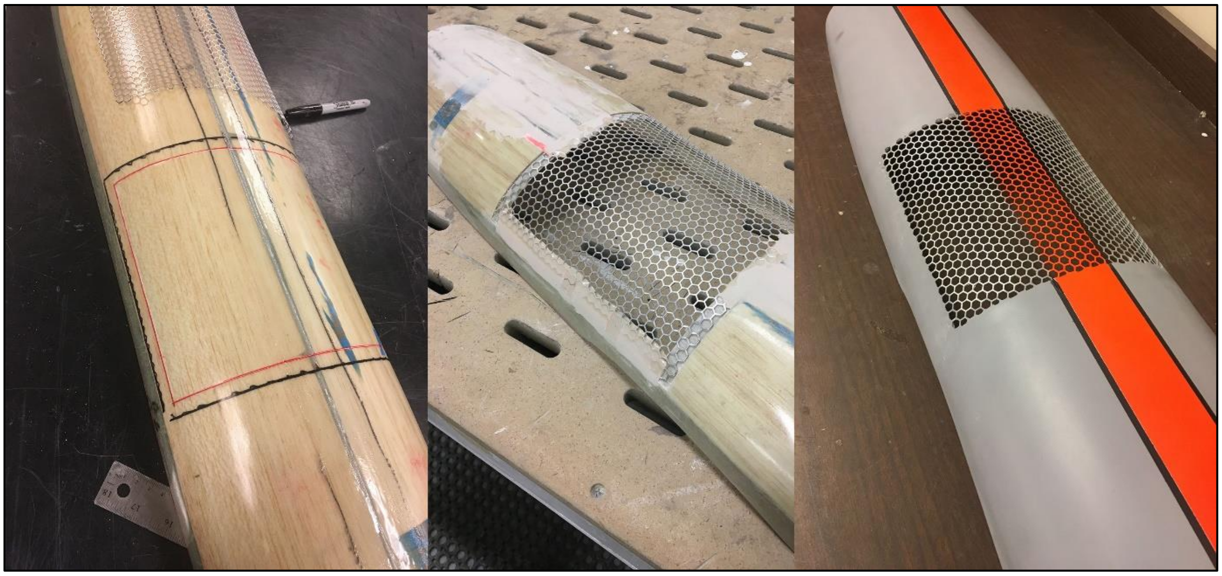

Figure 4.10 Making the Top Hatch

Skins

Every skin of the aircraft was made following the same process as the hatches. The core for each was made by gluing strips of balsa wood together to form sheets and then cutting them to fit specific sections. The fitted pieces of core were then sprayed with water and weighted in the mold. Once the water evaporated, the pieces of core held their formed shape. Holes were then cut in the core for the hatches, magnets, and control surfaces. The edges of the core and hatch holes were beveled to seal the core between layers of fiberglass. After the core was finished, sheets of fiberglass were cut and labeled according to the following layup schedules: 3FG x 3FG45 x 1/16BW & MAG x 3FG x KEV for the fuselage and horizontal tail, and 3FG x 3FG45 x 1/16BW & MAG x 3FG45 x 3FG x KEV & CT for the wing. A visualization of a layup can be seen in Figure 4.11.

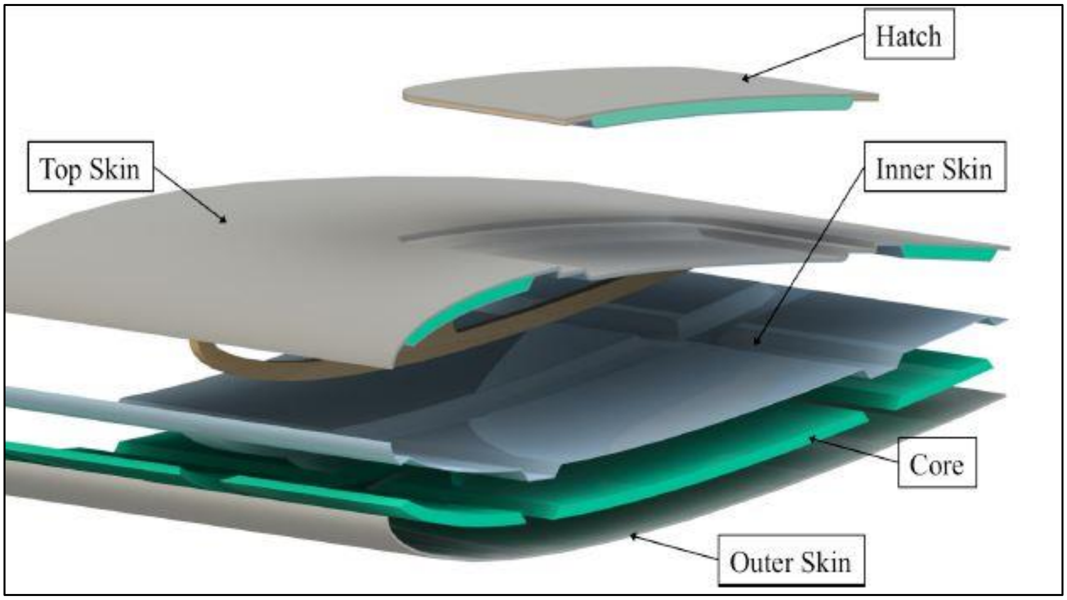

Figure 4.11 Composite Layup [43]

To make flush-mounted hatches, the skins had to be laid up over the hatches like in Figure 4.11. To do this, the hatches were taped, with double-sided tape, to their respective locations in the molds and the edges were sealed with a thin layer of clay. After everything had been cut, formed, and otherwise prepared, the molds were prepared for layups by cleaning, waxing, and releasing.

The skin layups were done by pre-pregging the first two layers of fiberglass and forming them to the mold. After the outer two layers were in place, the core and magnets were placed. Since the hatches already had magnets in them, the airframe side magnets were simply dropped near the hatch magnets and allowed to automatically align via their magnetic interaction. Again, thickened epoxy was placed around the magnets since they could not be beveled. The last layer of fiberglass was pre-pregged and formed over the core and magnets. The Kevlar was pre-pregged and then put over the aerodynamic control surface gaps to act as hinges and the carbon tow was likewise pre-pregged, and then folded in half and laid span-wise across the wing at the quarter-chord, where the majority of the aerodynamic load acts during flight. After the final layer was laid, the whole layup was covered with peel ply, perf, breather, and vacuum bag material and then put under vacuum. The finished skins were post-processed by removing the fiberglass flange and cleaning off the release. The finished fuselage skins can be seen in Figure 4.12 and the wing skins can be seen in Figure 4.13.

Figure 4.12 Locust Fuselage Skins

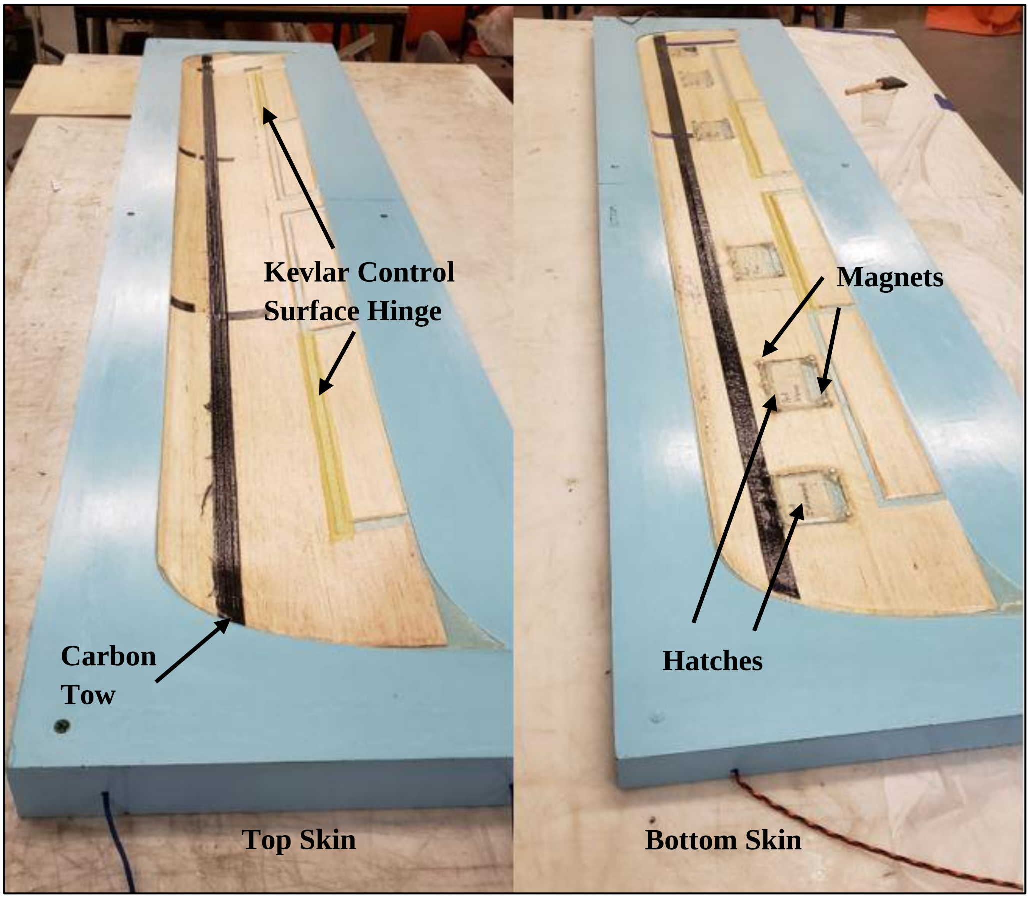

Figure 4.13 Locust Wing Skins

Internal Structure

In monocoque airframes, the skin is the primary load bearer, which means that the airframe does not need longerons or stringers like in a semi-monocoque or truss airframe. But like the other types of airframes, it still needs internal bulkheads to hold the skins together and to support the electronics, avionics, propulsion systems, etc.

The internal structure parts were cut from stock sheets using a laser CNC machine. The CAD files for the parts were converted to DXF files and then uploaded to the laser CNC machine which cut them very quickly and accurately. One of the drawbacks of using the laser was the charred edges caused by the extreme heat of the laser. The charred edges make poor bonding surfaces so any edge that would be bonded had to be thoroughly sanded and cleaned before bonding. Although sanding the edges increased the manufacturing time, it was still faster, cheaper, and more accurate than using the router CNC machine.

Within the fuselage, the primary structure consisted of seven fixed bulkheads with one being the front firewall. Figure 4.14 shows the labeled bulkheads. All of the structure in the fuselage, wings, and empennage, was made 3-ply 1/8 in. aeroply except for the firewall, front engine mount, and the bottom bulkhead. These three structures were made from 3-ply 1/4 in. aeroply due do the increased loading from the DA-120, nose gear, and main landing gear. Initial testing showed that the 1/8 in. aircraft plywood was too flimsy to support the engine and landing gear. The secondary structure consisted of five removable trays that support the avionics and other systems. The removable trays are held in place by mounts that were glued to the primary bulkheads.

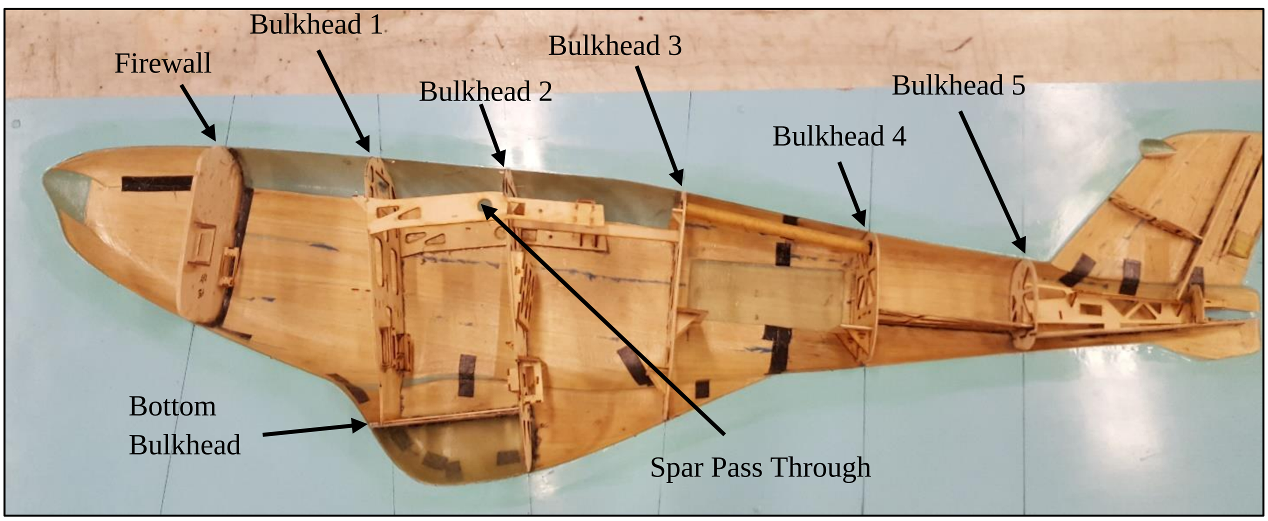

Figure 4.14 Locust Fuselage Primary Structure

The structure of the wing consisted of a foam spar sandwiched between two pieces of carbon tow that were embedded in the wing skins, an aeroply shear web, four ribs in each wing to hold the servos and electronics mounts, and shear webs and endcaps for the control surfaces. The wing also had a spar-tube sleeve that extended from root to mid-wing. The spar-tube sleeve passed through the first inboard rib and butted up against a stop to keep the carbon spar from going too far into the wing. It also served as a means of supporting and aligning the carry carbon spar. Figure 4.15 shows the wing with some of the components labeled. The wing's endcap had three cutouts for the carry-through spar, electrical wires, and a bolt that fixes the wing to the fuselage and doubles as an anti-rotation pin.

The structure for the horizontal stabilizer only had a shear web at the quarter chord and a shear web with end caps for the elevator. The vertical tail had a similar configuration to the horizontal tail but with two added ribs to support the rudder servo and the FPV camera.

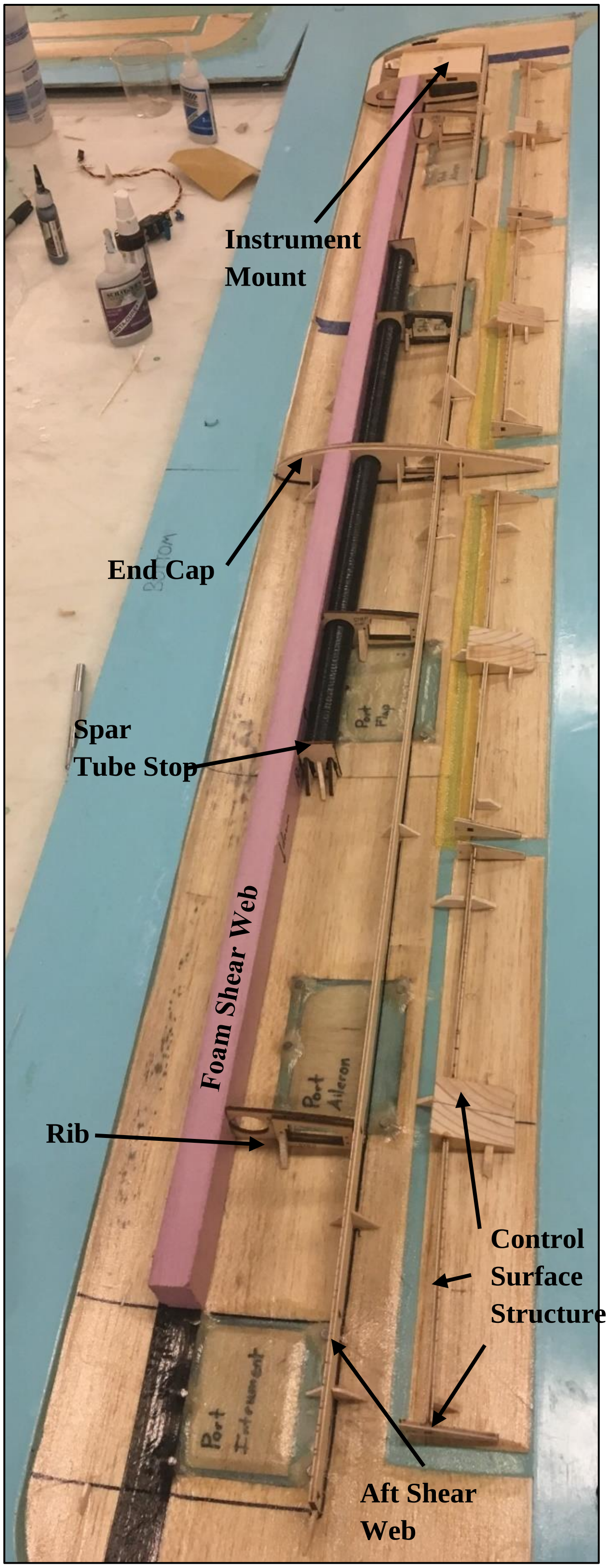

Figure 4.15 Locust Wing Structure

Landing Gear

Due to the complexity and abnormality of the main landing gear design, it had to be manufactured in-house to reduce cost and lead time. The 3-D landing gear CAD model was converted into a 2-D shape that could be cut from a stock sheet of 7071 Aluminum with the water-jet CNC. Once the shape was cut out, the gear was marked and scribed at the bend line. Since 7071 Aluminum is already heat-treated, and the bend angles were so extreme, the gear could not be cold bent. It was tried during initial development which led to snapping the gear in half. Following this, a method was developed using a small, welding tip on an oxy-acetylene torch and a benchtop vice. The gear blank was placed in the vice with the bend line approximately one inch above the vice's jaw. One person would locally heat the gear blank right on the bend line while the other person gently applied force to it. As soon as the gear blank began to fold, the torch operator would remove the flame and the bender would bend the gear blank to the desired angle. This process was repeated four times, one for each bend. The heating and bending process can be seen in Figure 4.16.

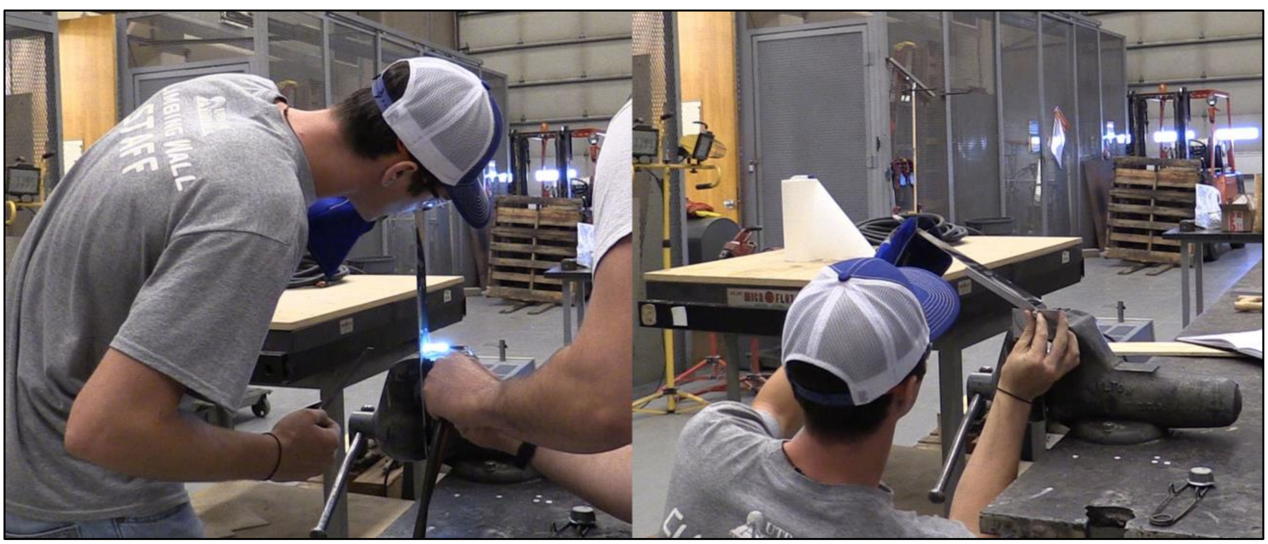

Figure 4.16 Heating (left) and Bending (right) the Main Gear

Applying such high heat to a piece of heat-treated metal destroys its temper. To re-temper it, the gear was put into the oven at $950^0\ F$ for one hour, quenched, put into the oven at $400^0\ F$ for one hour, and then quenched again [44]. The finished landing gear is shown in Figure 4.17

Figure 4.17 Main Landing Gear

Assembly

Assembly is one of the most critical tasks in ensuring a strong, robust airframe. Small mistakes here can lead to catastrophic failures later, which is why great care must be taken when bonding the structure and skins. The assembly process was done in three main steps: bonding the primary structure to one skin, bonding the secondary structures to the primary structures, and bonding the other skin to the primary structure. During these steps, the skins remained in their respective molds as long as they could to prevent warping.

The first task in the assembly process was dry fitting the primary structures into their respective skins. For the fuselage, this meant dry fitting the bulkheads and formers to the fuselage skins. Dry fitting had to be done because the bonding surfaces on the inside of the skins are never perfect due to wrinkles in the fiberglass, misaligned balsa core, excessive glue on the balsa wood core, and magnets. These imperfections prevented the bulkheads and formers from sitting completely flush with the skin which would result in a poor bond. For maximum strength of the airframe, each bulkhead had to be flush with the skin along its entire perimeter. The bulkheads were fitted by setting them in their appropriate locations and marking the spots were the skin imperfections prevented them from sitting flush. The spots were sanded down with Dremels and files and then re-fit. The process of fitting and sanding was repeated until each bulkhead had complete contact with the skin. Once dry fit, the bulkhead guides were hot glued in place to the bulkheads. The guides, which can be seen in Figure 4.18, were specifically sized pieces of aeroply used to hold the bulkheads in place for bonding. Hot glue was used so that the guides could easily be removed later with a heat gun. Following dry fitting, the bottom of the structure, the top of the structure was dry fit. This was accomplished by laying the other skin over the structure and tapping the skin directly over the structure. Tapping the skin allowed the assembler to hear/feel if there was a gap between the skin and the structure. If there was a gap, the assembler searched for the high spot causing the gap and then sanded it down. This was done iteratively until the top skin sat flush with the top of the structure.

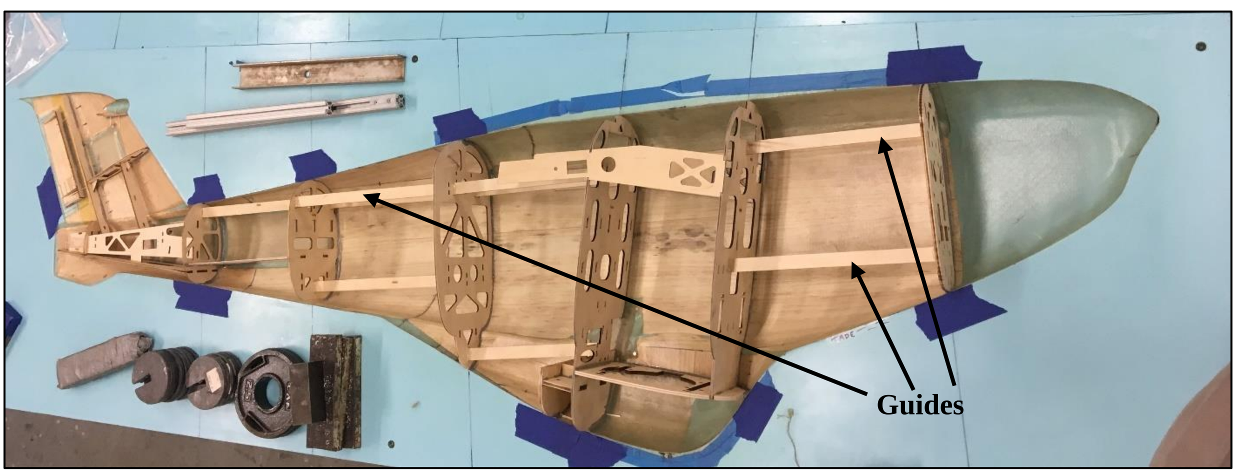

Figure 4.18 Locust's Bulkhead Guides

Once the primary structures were fitted and the secondary structures assembled, the primary structures were ready to be bonded to the skin. The skin and the primary structures were cleaned with denatured alcohol to remove any dust or debris that would inhibit a complete bond. Once clean, the structure was placed back in the skin and traced with a black marker to mark where to apply the bonding agent. The bonding agent was epoxy thickened with 406 colloidal silica and chopped carbon fiber, dubbed shower-drain. The chopped carbon fiber was added for structural reinforcement, similar to rebar in concrete. With the structure removed from the skin, the shower-drain was mixed in a cup until it had the consistency of peanut butter and then put into syringes using wooden tongue depressors. It was then squeezed onto the outline of the structure on the skin. The structure was replaced into the skin and weighted to keep it from moving as the shower drain cured. Once the primary structure was cured in place, the secondary structure was bonded to the primary structure and held in place with various types of clamps.

Bonding the other skin half to the structure began by cleaning the bonding surface of the inside of the skin with denatured alcohol. It was then taped to its mold with double-sided tape to prevent it from falling out when its mold was inverted. The skins were bonded together in their respective molds to help them keep their shape. Without the molds, they would be able to warp under their own weight which could prevent some sections from bonding correctly. Once taped in place, shower-drain was placed on the exposed primary structure and then the other mold was inverted so that its flange guide holes would line up with the opposite molds guide holes. Weights were placed on top to apply an even force over the whole mold to ensure a complete bond.

Assembling the wing and horizontal tail was done almost the same way as the fuselage with one main difference. The structures in the wing and tail were too small to utilize the hot-glue guide method. Instead, the structure was fit together like a puzzle and then set in place. Once in place, small balsa wood triangles were glued with CA to the surface of the skin such that their sides butted up against the structure like in Figure 4.19. This was done all around the structure until it was all held firmly in place. It was then traced with a black marker, removed, and glued in place with shower-drain. Once cured, the top skin was bonded to the structure the same way as the fuselage.

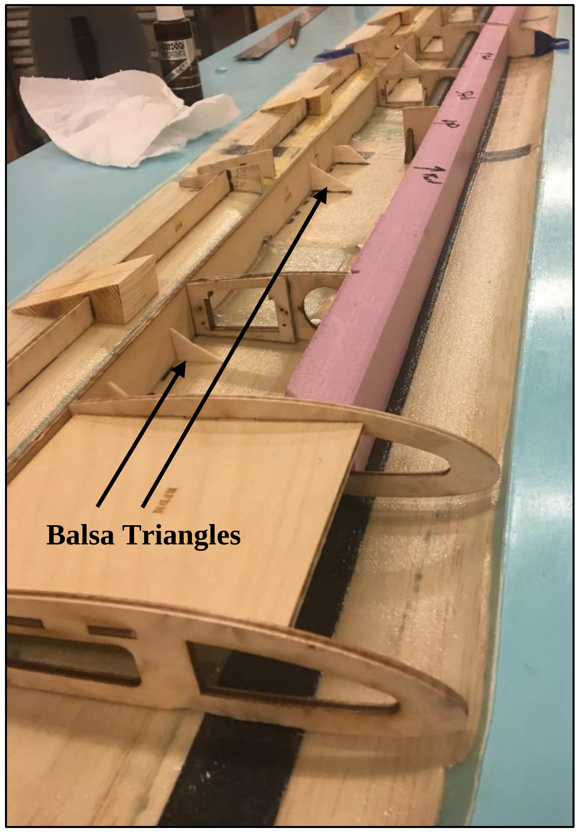

Figure 4.19 Balsa Triangle Structure Support

Since the wing mold makes both wings as one whole wing, the wing had to be cut in half. The cutting was done with a hand saw since it was too large to be cut using the band saw. In order to get the cut as close to perpendicular as possible, a laser level was used to align it and then traced with a black marker. Once cut, the root of the wing was sanded smooth and perfectly flat so that it would sit flush against the fuselage.

Post Processing

The previous section might sound like the end product was a complete airframe; however, there were still many post-processing steps to be completed before the airframe was finished.

The first task following bonding the skin halves was a quality control check. This was done by cutting out the hatch holes and using a snake camera to check each of the bonds. If one of the bonds had an air gap or was otherwise incomplete, more shower drain was injected to fill the void.

After passing the quality control check, the horizontal tail and the ventral tail had to be installed into the fuselage. This was another critical step because, if done incorrectly, it could compromise the aircraft’s stability. The ventral tail was installed first by cutting a hole in the fuselage slightly smaller than the tail itself. This hole was then gradually opened up until the tail would fit with minimal open space around it. Once the tail was fitted, the wings were put on and the whole aircraft was leveled. A laser level, that projects both a horizontal and vertical beam, was set up directly behind the aircraft with the horizontal beam lining up on the trailing edge of the wing and the vertical beam lining up with the trailing edge of the vertical tail. Once properly aligned and leveled, shower drain was applied to the root of the ventral tail and it was bonded to its base plate within the fuselage as seen in Figure 4.20. Sandable epoxy was applied to the junction between the tail and the fuselage to have a seamless fit once the excess was sanded away. The horizontal tail was likewise fit by first cutting its hole in the fuselage and then aligning it with the laser level using the wings and the vertical tail as references. Once in place, measurements were taken from the wingtips to the tips of the horizontal tail to ensure that it was perfectly orthogonal to the direction of flight.

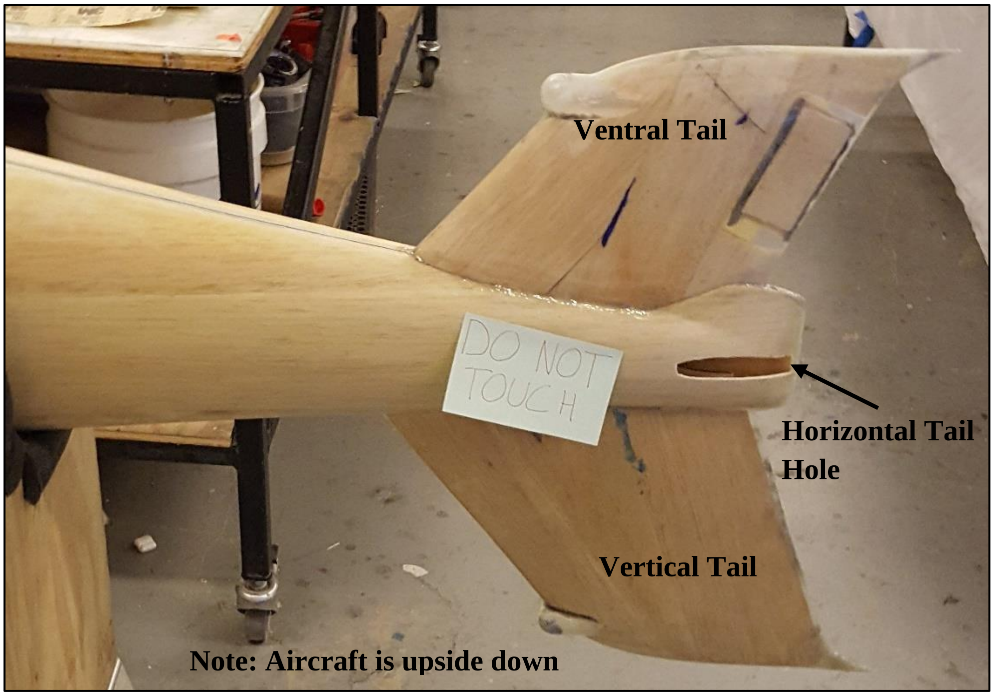

Figure 4.20 Bonding in the Ventral Tail

Next, the parting line seams had to be sealed for two reasons: the gap would allow air in, increasing drag and disrupting the flow over the aerodynamic surfaces, and the open section was a ‘soft’ spot that could easily break or tear. Once any remaining flange and skin inconsistencies were removed, and the skin near the parting line was smooth and flush, a thin, 2 in. piece of fiberglass tape was pre-pregged and placed over the parting line. Thickened epoxy was then brushed over the fiberglass tape to ensure a strong bond to the skin. This process was done for the fuselage, wing, and tail parting line gaps.

At this point, the airframe was structurally finished; however, more post-processing was done to give it a paint-ready finish. During the skin layup process, some small spots of the skin did not get vacuumed against the mold which made small divots. These divots are hard to see when it was just fiberglass and core, but they stick out once painted. Also, the edge of the fiberglass tape on the seams is very visible once painted. So, to hide these blemishes, sandable epoxy was applied to them in a thick layer that could be sanded smooth with the rest of the skin. Once cured, the excess sandable was sanded away and blended flawlessly with the rest of the skin. While sanding, the edges of the hatch holes were sanded round to remove the sharp fiberglass edges. After making the aircraft paint ready, the nose was cut off and sanded flush with the firewall to make room for the front IC engine.

The final step in post-processing was making the control surfaces. First, control horns were bolted and glued to the middle of all the control surfaces. Then, the control surfaces had to be cut free so that they could move. They were cut completely through the fiberglass on each end and the side opposite of the Kevlar hinge. The side with the Kevlar was scored along the hinge line until through the fiberglass but the Kevlar was left intact to act as the hinge. Figure 4.21 shows the cut control surface and the scored hinge line. The structures tutorial in the appendix has the full process of how to accurately cut and score the control surfaces.

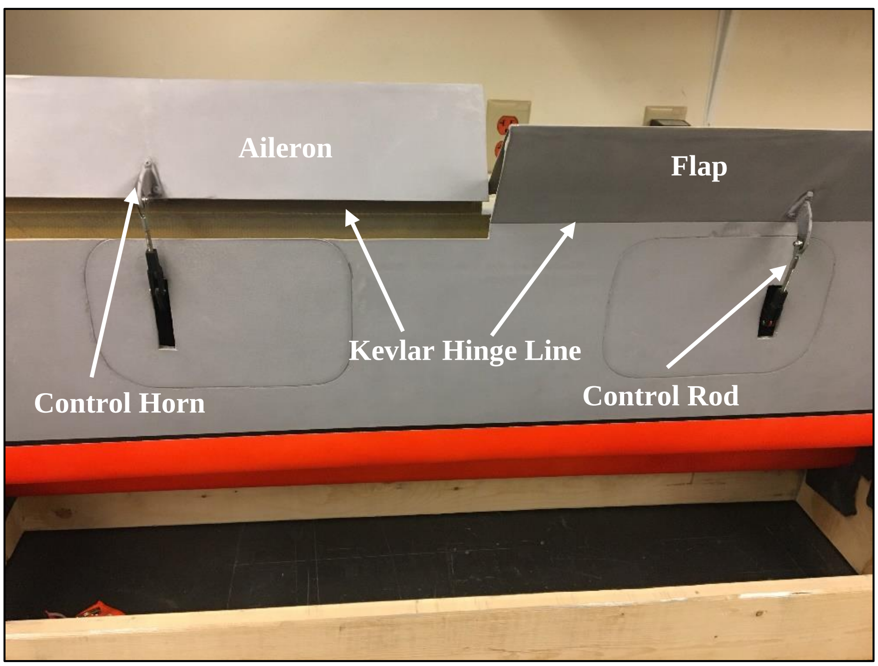

Figure 4.21 Locust Wing Control Surfaces

Integration

Following post-processing was the integration of the electronics, engines, fuel systems, and other on-board systems and hardware. The necessary hardware included blind nuts for bolting on the removable trays, vibration damping mounts for isolating the main avionics flight deck from the DA-120 vibrations, wing bolts to fix the wing to the fuselage, and control rods for actuating control surfaces and the DA-120 throttle and choke. The wiring harness was custom made in house to have the exact lengths and connections required for minimal weight and maximum operational efficiency. Each wire and connection were custom soldered, quality control checked by at least two other people, and checked for continuity using a voltmeter. The wiring diagram can be seen in the appendices. Like the wiring harness, the fuel system was custom made so that each of the lines would have the correct length with minimal connections to reduce the weight and number of places for potential leaks. The propulsion system schematics can be seen in the appendices. Any component that could not be bolted in place, like fuel tanks, batteries, fuel filters, etc., was mounted with either zip-ties or Velcro to prevent unwanted movement during flight.

Once the internal systems were installed, the servos were individually programmed to have overload protection and minimum and maximum allowable movements. Also, the Pixhawk II autopilot was likewise programmed to make sure that all onboard systems were communicating and functioning properly. With everything installed, programmed, and more or less ready, it was time to begin ground testing. A fully assembled Locust can be seen in Figure 4.22.

Figure 4.22 Fully Assembled Locust

CHAPTER V

TESTING AND EVALUATION

Component Ground Testing

The development of a new aircraft is a very complicated process that involves extensive amounts of testing on both the individual component level and the fully assembled aircraft level. Testing individual components helped to quickly troubleshoot and isolate problems. Also, the individual component testing provided a way to learn how each of the components function, how they should be installed, and what types of issues may arise and how to correct them. Knowing how each component works within its sub-system and the aircraft as a whole is of paramount importance to developing a successful and reliable aircraft.

Main Engine

The DA-120 has a manufacturer recommended break-in procedure and once properly broken in, the engine was tuned by adjusting the needle valves that control the amount of fuel allowed into the carburetor. Testing the engine included the following points:

- engine start procedure
- maximum engine speed with the 3-blade Beila propeller
- fuel flow at full throttle
- response speed to a throttle change command

All the DA-120 engine tests were carried out at the DML using the custom IC engine test stand shown in Figure 5.1. The test stand has a built-in rack to store a fuel tank and a fixed servo to actuate the throttle arm. Also, it was designed to be able to quickly swap out different engines to allow testing for different projects. After completing the break-in, tuning, and tests, the DA-120 was cleared for installation and installed testing.

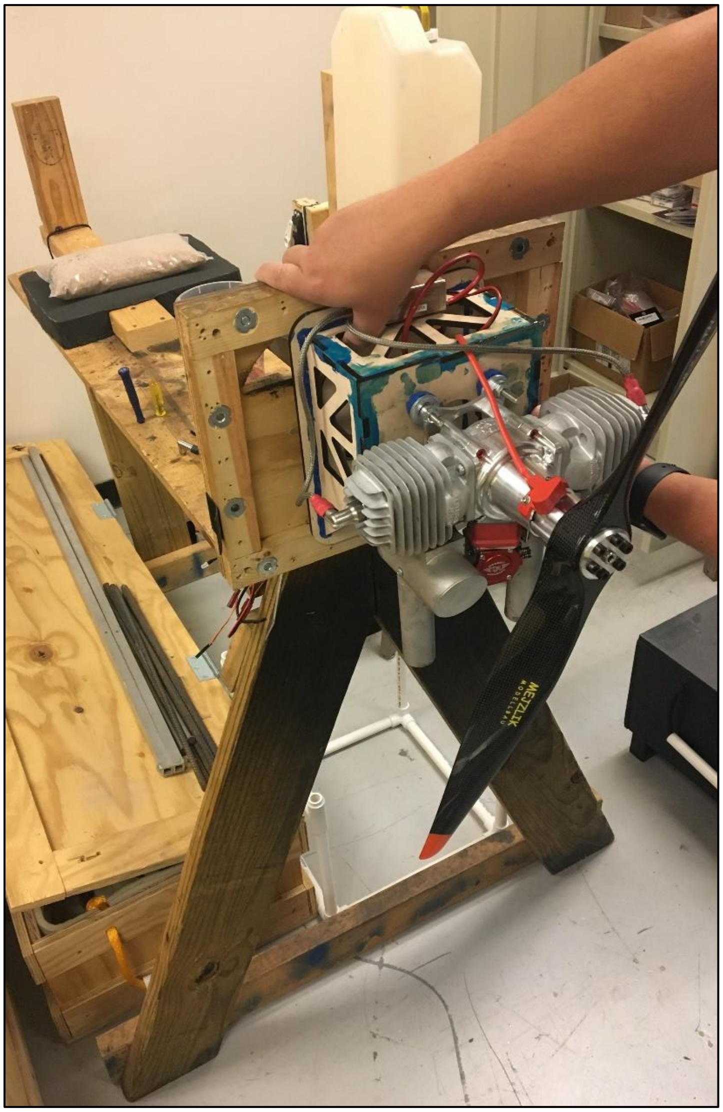

Figure 5.1 IC Engine Test Stand

Lift Jet

The K-260 also underwent thorough ground testing. Its testing was done in two parts. The first part was done on a custom-built thrust test stand, shown in Figure 5.2, used to measure thrust and fuel flow at different throttle settings. Like the main engine test stand, the jet test stand was designed to quickly swap out different size engines for the various projects. The results of the jet testing are shown in Table 5.1.

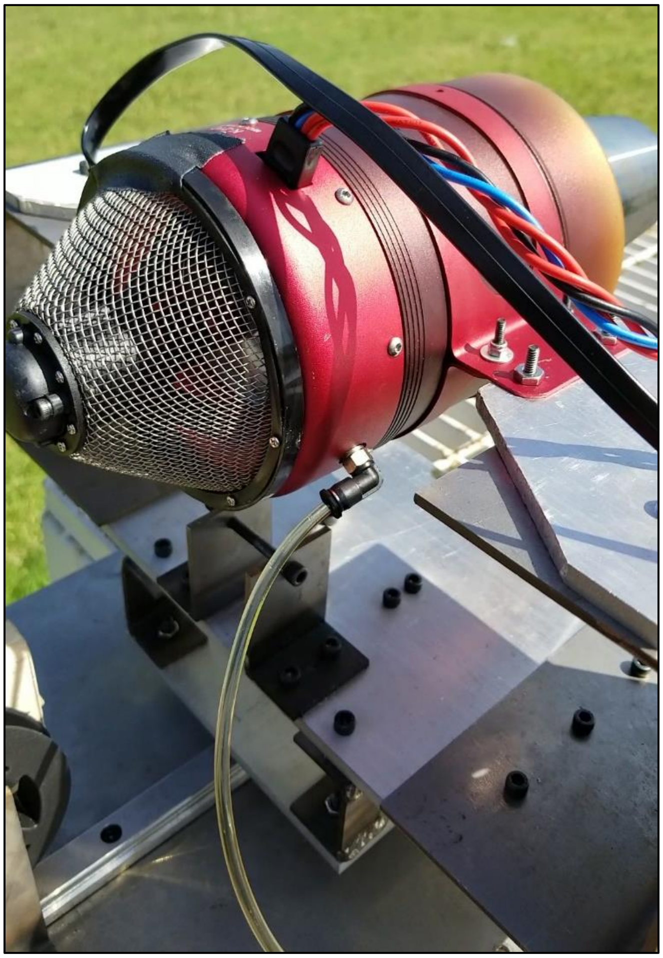

Figure 5.2 Jet Engine Thrust Stand

Jet Testing Results											
Throttle %	0	23	31	42	50	58	65	73	81	92	100
Thrust [lb]	2.4	7.7	13.7	18.0	21.5	27.5	30.9	36.9	42.1	45.4	51.2
Fuel burn [fl oz/min]	4.9	8.4	13.0	13.0	14.3	16.7	18.5	19.3	22.7	24.6	28.1

Table 5.1 Jet Testing Results

After taking engine performance data, the engine was tested vertically to determine if it would behave differently. The vertical tests were carried out on a custom-built stand, shown in Figure 5.3, that allowed the engine to be operated in a vertical or horizontal attitude. The stand needed to be easily moved from horizontal to vertical and vice versa because when the engine failed to light vertically, the burner would have too much excess fuel that needed to be burned out. Rotating the engine to its horizontal position allowed it to 'hot start', shooting a flame out the exhaust nozzle as the excess fuel was burned off. Once clear, the engine could be returned to its vertical position and tested again. These initial tests showed that the engine would not light vertically which was a huge problem because this entire project hinged on the jet's ability to be able to provide vertical thrust.

Figure 5.3 Jet Test Stand

KingTech recommends using Diesel, Jet-A, or kerosene as the primary fuel for the K-260. Due to its accessibility and relatively low cost, Diesel was initially chosen. The immediate problem that arose was that the burner would not light with the engine in a vertical attitude. This forced weeks to be spent altering different ECU parameters to get the engine to light with little success. After seeing marginal results with adjusting the ECU parameters, a mix of a small amount of gasoline with Diesel was tried to lower the fuel's flashpoint. This test also proved inconsequential. Next, since Jet-A is one of the allowable fuels, Jet-A was purchased from the local airport and tried.

During the first test using Jet-A, the burner lit precisely when commanded to by the ECU. Many more vertical ignition tests were carried out to ensure that the Jet-A solved the problem. In these tests, the engine lit vertically almost every time. The times it did not light was due to other issues. Finally, after much trial and error, the K-260 was cleared for installation and ready to undergo installed testing.

Servos

Testing the servos was a much simpler process than testing the engines. The primary purpose of testing the servos was to evaluate the functionality of the built-in overload protection (OLP). The tests were carried out by attaching a 2.2 lb. weight to the servo's 0.75 in. arm and monitoring its temperature. Each test was performed with the servo receiving power from a fully charged, 2S LiFe battery outputting 6.6V. Figure 5.4 shows the results of the test. Both the HS-5245MG and HS-7245MH servos failed due to overload but the HS-7245MH with 20% (OLP) never failed. Its test was ended due to the servo melting its hot glue mount.

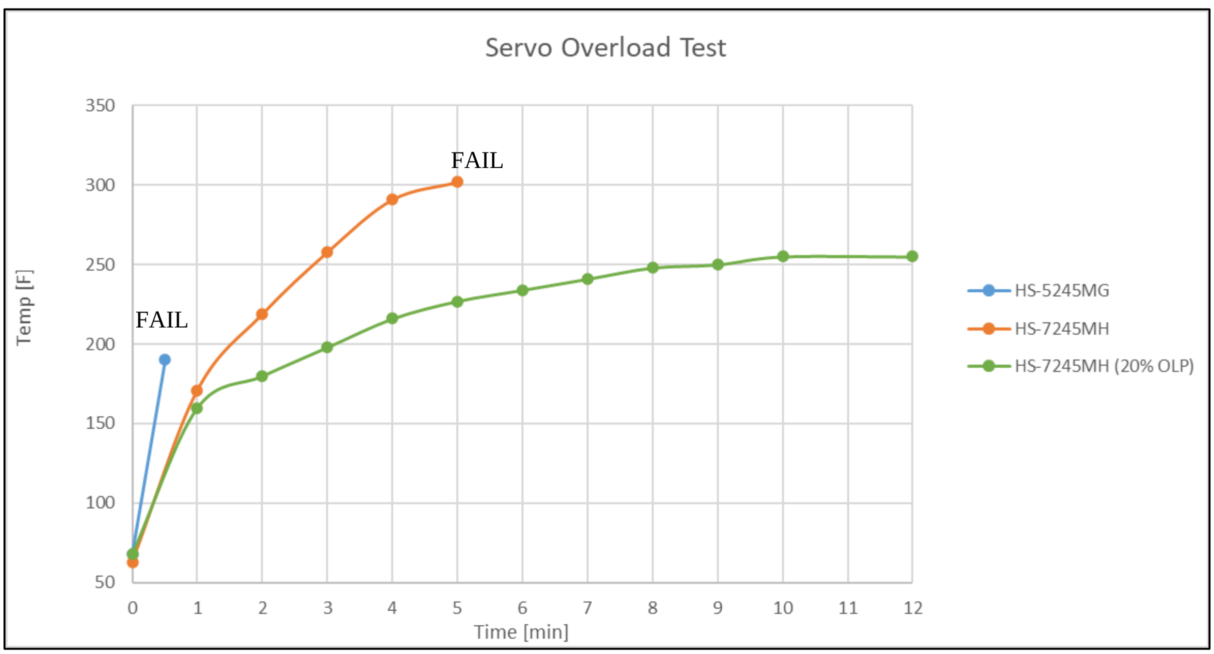

Figure 5.4 Servo Overload Test Results

Flight Control System

The last system tested independently was the flight control system (FCS). Thorough ground testing of the FCS was critical to minimizing the risks to both the airframe and personnel. The overall FCS tests were centered around the following 4 key points:

- Pixhawk II properly relaying pilot commands to the correct servo
- Pixhawk II functioning properly in each flight mode (manual, fly-by-wire, and auto)
- auto-level feature working properly
- ground station receiving telemetry from the aircraft (airspeed, fuel-flow, engine data, etc.)

This stage of testing was done in parallel with the installation of components to make removal and modification of components easier and faster. Figure 5.5 shows the FCS test set-up. The main flight deck was sitting outside the aircraft with extensions connecting the installed components like servos, Jeti receiver, CTU, etc. Ensuring proper communication between the pilot's transmitter and the Pixhawk II was done by first binding them (establishing a remote connection) and then commanding control deflections and/or throttle commands while monitoring the movements on the aircraft. If any behaved incorrectly, a correction was implemented and then it was retested until all servos responded correctly to all commands.

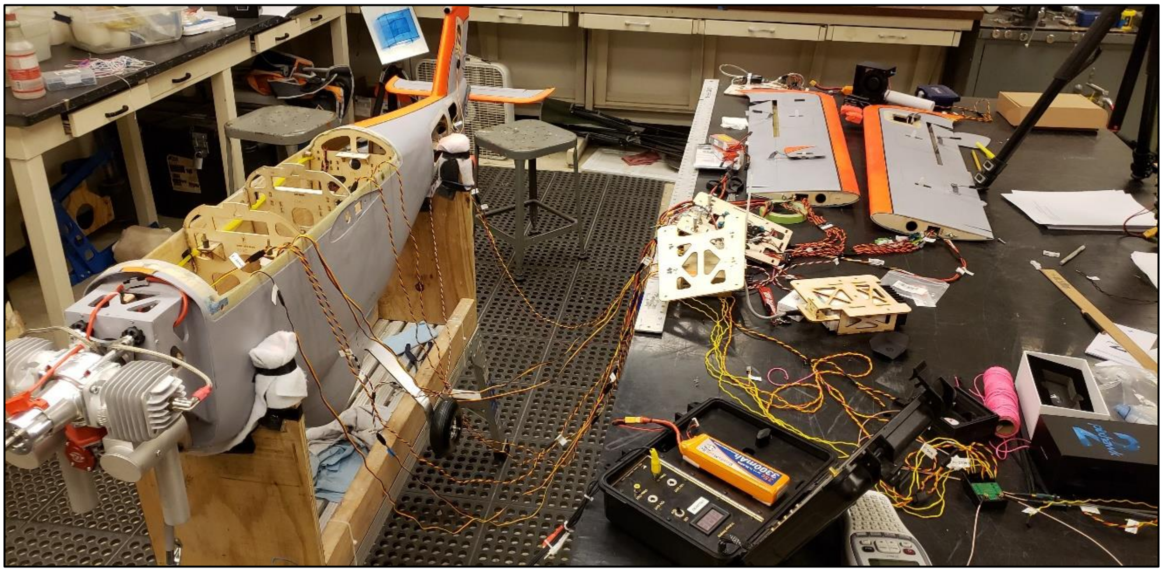

Figure 5.5 Electronics Testing

Testing the Pixhawk's flight modes consisted of repeating the first communication test in each flight mode. The auto-level feature was tested by holding the aircraft and then simulating roll and pitch movements while the control surfaces and TV nozzle were monitored to ensure they had the proper deflection magnitudes and direction.

To test the sending/receiving of airspeed telemetry data, the aircraft was powered on and then an airspeed calibration blower was used to simulate airspeed by blowing into the pitot-static tube. The blower had a known airflow velocity of 30 kts. which was then used to cross-check the airspeed sensor's telemetry readout. This was done for both the Jeti and Pixhawk II airspeed sensors.

The fuel flow meter was tested by powering the K-260 fuel pump and having it push fuel through the flow meter. From initial trials, it was found that the fuel-flow meter had to be placed downstream (positive pressure) of the pump. Having it upstream (negative pressure) introduced air bubbles into the fuel line which caused incorrect fuel flow readouts. The initial amount of fuel and flow rate were known and then cross-checked against the flow meter's telemetry data. Once the FCS was thoroughly checked for proper functionality, it was cleared for installation.

Complete Aircraft Ground Testing

With all the major components tested and cleared individually, it was time to completely assemble the aircraft and begin full systems checks and tests. The competed aircraft ground testing was done for 2 reasons: checking the functionality of the launch crate and tether system and checking to make sure that the individual components functioned properly when working together. The testing followed a sort of buildup type protocol; single components were tested individually and then more and more were tested together until all components were fully operational and the whole system was tested at once.

Launch Crate

The launch crate was tested by simply tethering the aircraft and running up the engines. The ground crew was positioned such that they could ‘catch’ the aircraft if the tether system failed but they did not touch the aircraft so that the tether system took the full load of the engines. Initial tests showed that the tether system, both on the aircraft side and crate side, was strong enough to handle both engines at full throttle; however, the wooden crate caught fire due to the excessive heat from the jet exhaust. During ground testing, there was plenty of personal protective equipment (PPE) and safety equipment, so the fire was quickly extinguished with no damage to the aircraft. The fire problem was investigated and it was found that the maximum exhaust gas temperature (EGT) of the K-260 is 700^0C (1292^0F) while the average auto-ignition temperature of wood is approximately 300^0C (572^0F) [45]. From Figure 5.6, there is a gap on either side of the steel plate that gives access to the cavity underneath the steel plate. The hot air was getting trapped and circulating underneath the plate, causing the temperature to exceed that of the auto-ignition temperature of wood. To fix this issue, the launch crate was partially disassembled and painted with heat resistant paint. The black painted regions can also be seen in Figure 5.6. The implemented fix was then re-tested and found that the heat resistant paint kept the launch crate from catching fire.

Next, the release system was tested by having two people simultaneously lift and push the aircraft to simulate both the lift jet and the main engine thrust. The release cord was then pulled to make sure it would release smoothly and not catch on any part of the aircraft. With the crate tested and cleared, the focus was shifted to testing the aircraft.

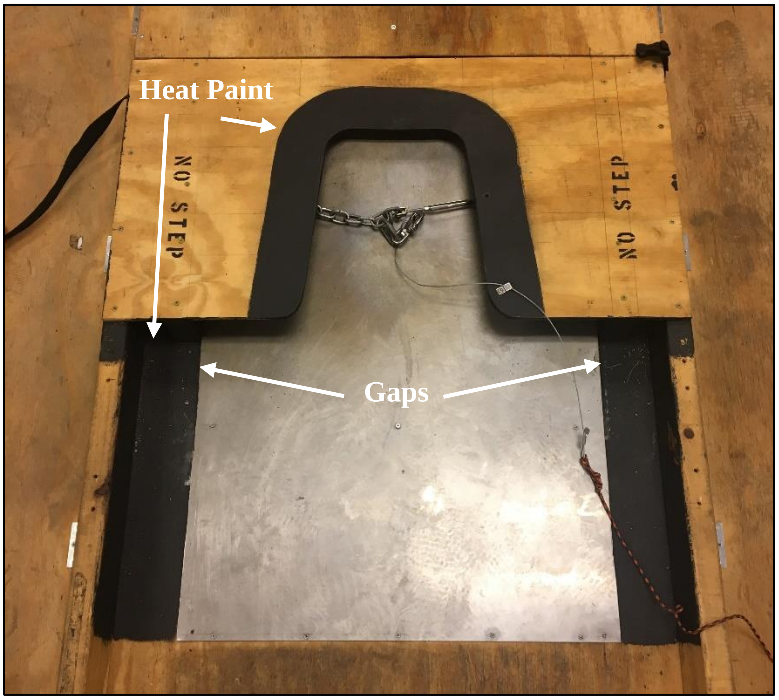

Figure 5.6 Launch Crate Close-Up

Propulsion Systems

The propulsion systems were tested and monitored in parallel with the launch crate testing since both tests required the engines to be running. First, each engine was powered separately and closely monitored. The DA-120 was monitored for abnormalities in the following areas:

- noise
- rapid throttle increase and decrease
- vibration and bolt tightness throughout the aircraft
- throttle response speed
- full throttle and idle
- optical kill
- choke
- fuel lines (kinks, air bubbles, and leaks)
- fuel flow telemetry

After performing multiple tests by both hand starting and starting with a torque starter, the engine was deemed to be functioning nominally across all throttle positions, while having a smooth idle that would keep the engine from dying.

The K-260 was likewise tested and monitored for abnormalities in the following areas:

- start-up sequence
- full throttle and idle
- noise
- throttle response speed
- fuel lines (kinks, air bubbles, and leaks)
- fuel flow telemetry
- engine kill
- engine cooling cycle
- remote control restart

If there was even a slight abnormality from any one of these areas, it was investigated, corrected, and the test was repeated to ensure nominal functionality. Having put both engines through a full range of tests individually, the engines were then tested running simultaneously by monitoring the DA-120, K-260, flow meters, fuel lines, and the telemetry coming from the aircraft. During this test, each engine was tested at each throttle setting with the other engine at each throttle setting. This was done to ensure that nominal engine functionality was independent of the other engine. The start-up sequence was also tested by starting the K-260 first and then the DA-120 and vice versa. Also, the K-260 RC restart was tested by having both engines running, killing the jet, and then restarting it while the DA-120 maintained a cruise throttle setting. For initial testing, only 60 fl. oz. of gasoline was onboard for the DA-120 and 120 fl. oz. of Jet A for the K-260. Since the initial flight testing was mostly focused on learning the short/vertical landing profile, more fuel was allowed for the jet. Once the testing is finished, the actual mission configuration will have 120 fl. oz. of gasoline and 60 fl. oz. of Jet-A.

Avionics

After proving the propulsion system and having a baseline nominal performance, the avionics and FCS were tested with the engines. The FCS was tested by sending various commands, like pitch up, pitch down, roll left, roll right, etc., to the aircraft and monitoring the control surfaces and engines. Once each control surface was deflected in both directions, the engine throttles were changed, and the test was repeated. This was done for all combinations of engine throttle settings.

Next, the entire test was repeated with the flight computer in a different mode. During these tests, the ground crew monitored each control deflection to ensure nominal behavior.

Following the test of the FCS, the flight computer's gain speed scaling and airspeed sensors were tested. This was done by carrying out the previous test while blowing into the pitot tube with a blower. The speed scaling causes decreasing control surface deflection magnitudes with increasing airspeed. The deflections were monitored while under simulated airspeed and confirmed that they were less than with no airspeed. Also, the blower had a known airspeed and was cross-checked with the telemetry readout. Like the previous tests, this test was also performed in each flight mode.

Structure

Lastly, simple structural tests were performed. A tip test was done to test the structural integrity of the wing by picking the aircraft up by its wingtips. This point loading simulated a 2G load. After returning the aircraft to the ground, it was checked for any structural damage and/or fiberglass delamination.

After going through weeks of tests and modifications, all systems were dialed in and functioning nominally across all modes and as many in-flight situations as could be simulated on the ground. From that point, it was time to begin flight testing.

Flight Testing

Aircraft testing is much more high risk than testing ground-based systems, especially fixed-wing aircraft. If an aircraft's whole mission is simply to take off, climb, cruise, descend, and land, 80% of the mission has to be carried out above the stall speed. There is no slowing down to make a minor tweak or if something goes wrong; once the aircraft leaves the ground it has to stay in the air and follow a specific flight plan to land safely.

Performing flight tests started by going through a pre-flight checklist which is shown in the appendices. The purpose of such a specific and rigorous pre-flight was to minimize the possibility of something going wrong in the air. Past aerospace design projects at the DML have seen catastrophic failure due to easily avoidable mistakes such as uncharged batteries, bound control surfaces, and loose hardware. The collective experience of the aerospace research personnel allowed the development of this extensive checklist which has been integrated into the program as a whole to try and prevent any mishaps with future aircraft. Following the pre-flight checklist was a mission briefing with the ground crew and the pilot. This ensured that everybody was on the same page and that there were a specific plan and specific procedures in case of various emergencies.

With the pre-flight checks and briefings complete, the launch crate was positioned into the wind at mid-runway at the OSU UAS airfield and the aircraft was locked in place. The ground crew then started the DA-120 and cleared the area. Once the DA-120 was warm and idling smoothly, the pilot started the K-260 and monitored its startup stages until its ECU telemetry announced 'ready'. The pilot then took the K-260 to full throttle and the DA-120 to 50% throttle. With both engines operating at their pre-determined takeoff power settings, the pilot then signaled to the ground crew to pull the release cord. Upon release, the aircraft began to climb immediately with the aid of the jet. After flying a few patterns to trim the aircraft, the pilot then began to fly the approach pattern to reach the checkpoint configurations and airspeeds shown in Figure 5.7. The approach pattern was flown to smoothly lower the aircraft's stall speed while also losing altitude to set up for landing. Upon final approach, the K-260 was near full throttle and the aircraft weighed virtually nothing. This allowed for the pilot to slow way below the 50 lb. aircraft's normal stall speed.

Pre-Takeoff		**Landing**	
Flight Mode	FBWA	Midfield downwind	
Flaps	Mid Position	Target Speed	45 kts
		Turbine	50%
Takeoff		Slow to	35 kts
Turbine	Start		
Prop Power	40 %	Final Approach	
Turbine Power	10(%	Flaps	Full
Launch System	Release	Turbine	75%
		Slow to	25 kts
		Turbine	As needed

After Takeoff		**Aircraft Limits**	
Airspeed > 45 kts		Vst T0%	48 kts
Turbine	Idle	Vst T50%	35 kts
Airspeed > 50 kts	Flaps up	Vst T75%	27 kts
		Vapp T0%	50 kts
Before Landing		Vapp T50%	35 kts
Begin pattern	200-300 ft	Vapp T75%	25 kts
Turbine	Start		
Airspeed	45 kts	Turbine time ON	9 min MAX
Flaps	Mid	Begin landing	5 min
		WARNING	7 min

Figure 5.7 Target Airspeeds

The testing methods discussed in this chapter reflect the current methods that have been developed along with the aircraft and flight testing. Some of the initial flight tests had serious problems that would have been prevented had it undergone the current testing protocols. Lessons were learned and changes were made to reduce all foreseeable risks.

The first flight test was almost a catastrophic failure, but the pilot was able to save it. During the ground checks, the deflection direction of the TV nozzle was not checked. Had it been checked, the crew would have seen that it was going in the wrong direction.

A subsequent flight test, that resulted in a catastrophic complete loss of aircraft, could have also been avoided during ground checks. During the pre-flight checks, the crew thought that the deflection magnitude of the TV nozzle was too small, so the integral gain (I-gain) in the Pixhawk was increased. This caused a build-up of roll correction in the first turn which caused the aircraft to try and turn the other direction once it leveled out. The I-gain overpowered the pilot's commands and the aircraft dove straight into the ground. The lesson learned here was to not change things in a hurry right before a flight and to not change things without completely knowing how it would affect the aircraft.

Flight Testing Results

The first 10 flight tests and a short summary of their outcome can be seen in Table 5.2. As mentioned previously, the majority of this document reflects the current configuration of the aircraft which has changed considerably from the initial configuration during its development. Most of the flight test results were from previous configurations. The current configuration has only been tested on takeoff because, as seen in Table 5.2, the aircraft had a crash landing. Due to some issues with the customer contracts, the aircraft has been grounded until a UAV testing event later in the year.

.

	Date	Flight Number	Aircraft	Launch	Flight	Landing	Notes
1	5/21/2018	1	CLARC-0	Good	Good	Bad	Maiden flight. Flipped over and broke firewall.
2	7/18/2018	1	CLARC-0	Good	Good	Bad	Flipped over. Still good to fly.
3	7/18/2018	2	CLARC-0	Good	Good	Good	
4	7/20/2018	1	CLARC-0	Good	Good	Good	
5	7/20/2018	2	CLARC-0	Good	Good	Bad	Flipped over. Still good to fly.
6	7/26/2018	1	CLARC-0	Good	Good	Good	
7	9/5/2018	1	CLARC-0	Good	Good	Good	
8	9/5/2018	2	CLARC-0	Good	Bad	Bad	Hit GEO-Fence, autopilot throttle reversed. Aircraft out of commission.
9	11/28/2018	1	CLARC-1	Good	Bad	Bad	Lost telemetry on takeoff. Airspeed not aquired for approach. Broke the fuselage in half. Aircraft set to be repaired.
10	2/20/2019	1	CLARC-1	Good	Bad	Bad	BAD PID Gains. Crashed and burned in field. Aircraft out of commission.
Success Rate				100%	70%	40%	

Table 5.2 Flight Tests

Takeoff

The tethered point launch has been demonstrated many times with both Grasshopper and Locust to be effective and consistent. As soon as the aircraft was released, it began its climb with as little as a few inches of rollout. On one of the initial flight tests, the pilot instinctively held up elevator on launch to help the aircraft begin climb which caused a large pitch up motion. This pitching motion led to a tail strike and then the aircraft rolling out and dragging the tail for about 15 ft. before becoming airborne. After the flight, the pilot was instructed on how the TV nozzle and its stabilization create pitching motions. His instinct was correct for a conventional takeoff, but the pitching moment generated by the lift jet and TV nozzle was much greater than he anticipated. During subsequent flight test takeoffs, he held only a small amount of up elevator which led to smooth takeoffs and climb out like in Figure 5.8.

Figure 5.8 Locust Takeoff

As far as taking off is concerned, the aircraft has performed as expected with only a few, easy to correct issues. Also, both aircraft have proven the launch crate is both simple to used and highly effective. Many UAVs need complicated pneumatic or elastic launching systems that can be expensive and dangerous. The launch crate for the CWL systems is safe, relatively cheap, and easy to use.

Flight

During the first few flight tests, the aircraft exhibited odd flight characteristics such as high pitch oscillations and high roll rates. These abnormalities were due to the control gains not being tuned and control deflections being wrong. It is typical to see these kinds of abnormalities on the first few flights due to the aircraft having unknown handling characteristics. As the pilot learned how the aircraft flew, he was able to communicate its handling issues which were then corrected by implementing control gain and deflection corrections. Later tests demonstrated that the aircraft could be flown smoothly with normal handling characteristics.

One issue the pilot noticed during flight was that he had to keep holding almost full up elevator which limited his pitch up authority. The maximum elevator deflection was increased which slightly increased the pitch up authority, but he was still having to hold too much up elevator. Another problem with little pitch up authority is that, on landing, the pilot could not maintain a high angle of attack which decreased the amount of lift that could be produced, lowering the effective vertical thrust to weight ratio. Also, as mentioned before, a high angle of attack is wanted on landing to create more drag to help slow down.

With the elevator deflection fully maxed out, it was decided that there was a deeper problem than just control deflections and that it might be a stability and control issue. Following that idea, a CFD analysis was performed to study the effect of adding incidence to the horizontal tail. The analysis was performed with the CG at 32% wing chord which is where it would be for landing. The results shown in Figure 5.9 show that the aircraft is untrimmable without any elevator input. The CAD model was modified to have the horizontal tail mounted at four degrees incidence which made the aircraft trimmable at approximately four degrees AOA.

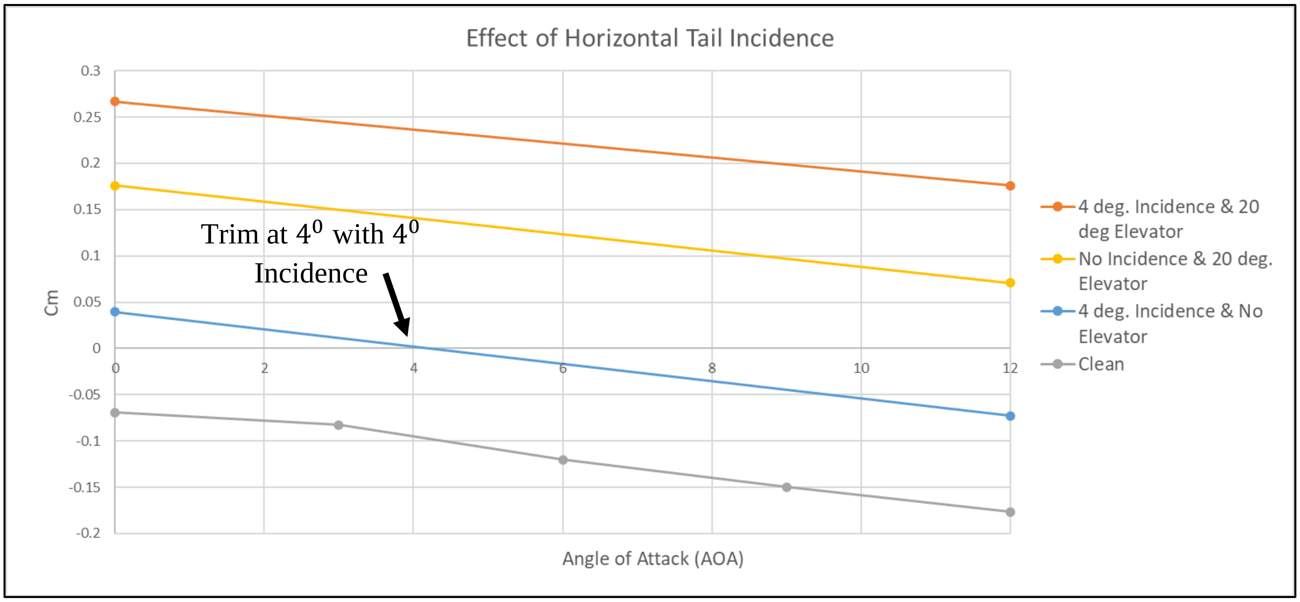

Figure 5.9 Horizontal Tail Incidence

Four degrees AOA was desired because it split the difference for the required AOA for steady level flight at maximum speed and steady level flight at best endurance speed. These speeds and angles were estimated from Figure 5.10 and Figure 5.11 which were also generated from the CFD analysis.

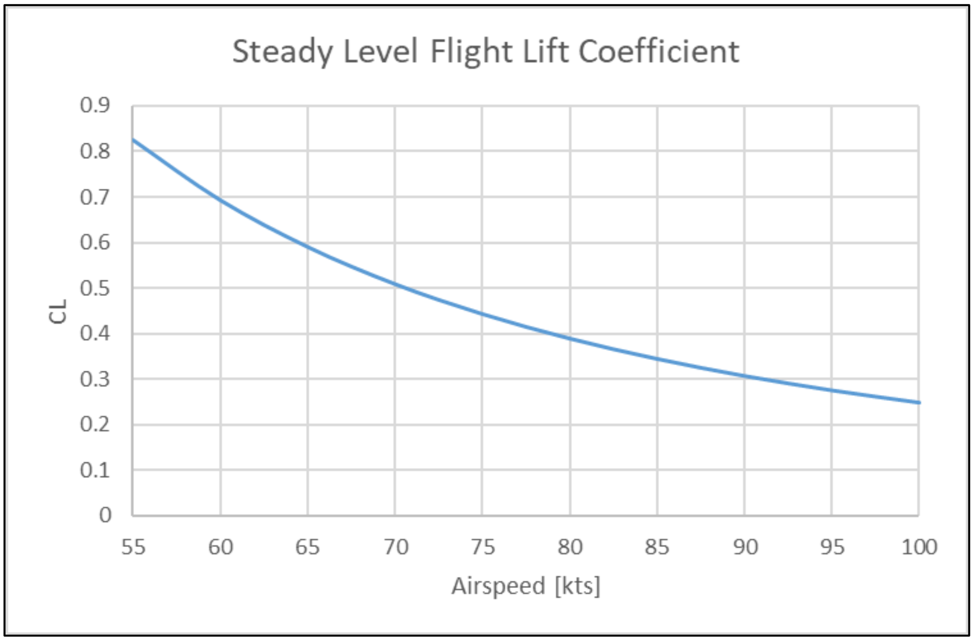

Figure 5.10 Required Lift for Steady Level Flight

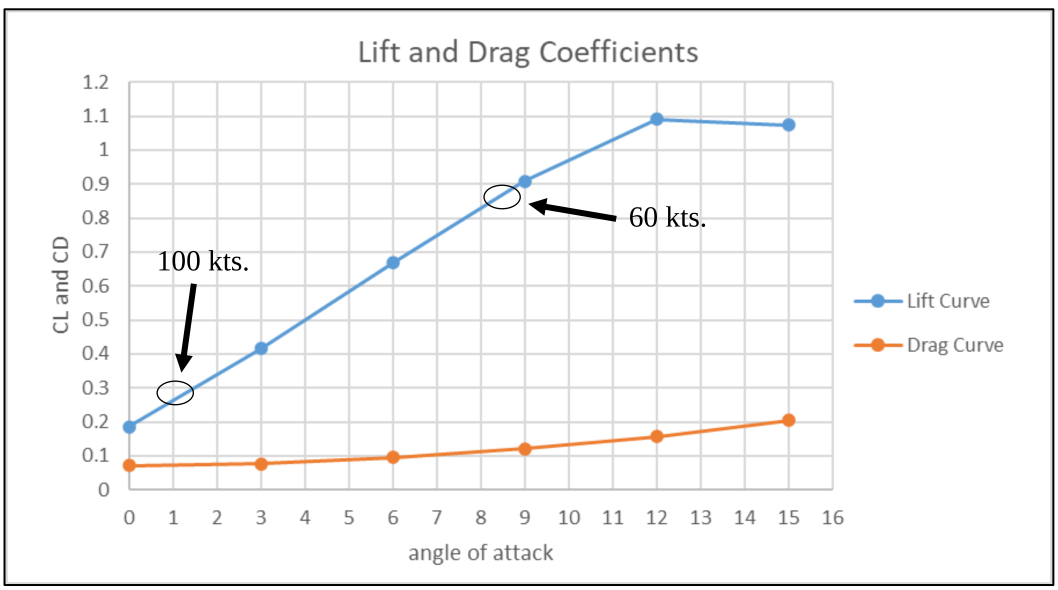

Figure 5.11 Lift and Drag

The new configuration with the horizontal tail mounted with incidence has yet to be tested due to the aircraft being grounded.

Landing

Flight testing has shown landing to be the most difficult part of the whole operation. Table 5.2 shows that Locust has only had a 40% landing success rate. Initially, the bad landings stemmed from the aircraft either tipping over the nose or ground looping and flipping. These failed landings led to the landing gear design configuration changes discussed in the Landing Gear Design section. Like the new horizontal tail configuration, the new, tricycle landing gear configuration has yet to be tested due to the aircraft being grounded. However, the tricycle gear has been tested and proven on the configuration testbed aircraft that will be discussed in the next section.

Katydid

The flight tests were conducted prematurely with too many unknowns still unsolved. So, to work out the problems and continue testing since the aircraft was grounded, another CWL UAV, similar to Grasshopper, was created. The new aircraft named Katydid, 'Katy', was a COTS Legacy Aviation 84" Turbo Bushmaster as seen in Figure 5.12.

The Bushmaster was chosen because once modified, it would have a similar wing loading to Locust and it was larger than Grasshopper which allowed for the replication of Locust's CWL and flight control systems. Also, retrofitting the Bushmaster was much faster and cheaper than building a Locust.

Figure 5.12 Turbo Bushmaster

Katy was made by converting the Bushmaster from a tail-dragger configuration to a tricycle configuration, adding a tether hardpoint, installing a vertical K-85 turbojet, and installing Locust's main FCS. It was also outfitted with two pitot-static tubes and airspeed sensors, one for Mission Planner and one for the transmitter telemetry readout. The middle section of the bottom of the bushmaster and the top hatch were initially made of thin balsa wood structure coated in MonoKote. The bottom was replaced by a solid plate of wood to mount the custom main gear and the tether hardpoint. The top hatch was modified to have a mesh screen to provide air for the lift jet. Figure 5.13 shows the modified Bushmaster called Katy.

Figure 5.13 Katy

One of the main discoveries that Katy lead to was that the CG needed to be slightly aft of the TV nozzle as discussed in the Thrust Vectoring Control System section. With the CG aft, the TV nozzle pointed slightly foreword to keep a wings-level attitude which helped to slow the aircraft. Some of Katy's Specifications can be seen in Table 5.3.

Katy Specifications	
Wing Span [ft]	6.83
Chord [ft]	0.85
Wing Area [ft^2]	5.84
Aspect ratio	8.00
Length [ft]	5.25
Height [in]	2.42
Wheel base [in]	1.21
Empty weight [lb]	15.3
GTOW [lb]	17.3
Max K-85 thrust [lb]	18.7
Thrust-to-weight ratio	1.08
Wing Loading [lb/ft^2]	2.96
CG GTOW(%chord)	40%
CG Empty (%chord)	33%
Nozzle center (%chord)	32%
Jet fuel volume [fl oz]	40

Table 5.3 Katy's Specifications

Katy’s flight tests have shown very promising results with only one minor incident. On the second flight, the structure that the nose gear was mounted to broke due to the moment produced from the aircraft rolling through a hole in the mud. Even though it broke, it did not completely fail which prevented further damage. This type of nose gear failure is common with the tricycle configuration so the nose gear mount was strengthened by adding a bulkhead. Also, a new, spring-loaded mounting system was developed to help absorb some of the horizontal load. The spring-loaded mounting system in Figure 5.14 was 3D printed and designed to be able to bolt to the existing nose gear collar. Multiple springs with varying stiffnesses were tested and it was found that a 70 lb./in. spring provided adequate stiffness while still compressing when the aircraft rolled over holes or large bumps during taxi tests.

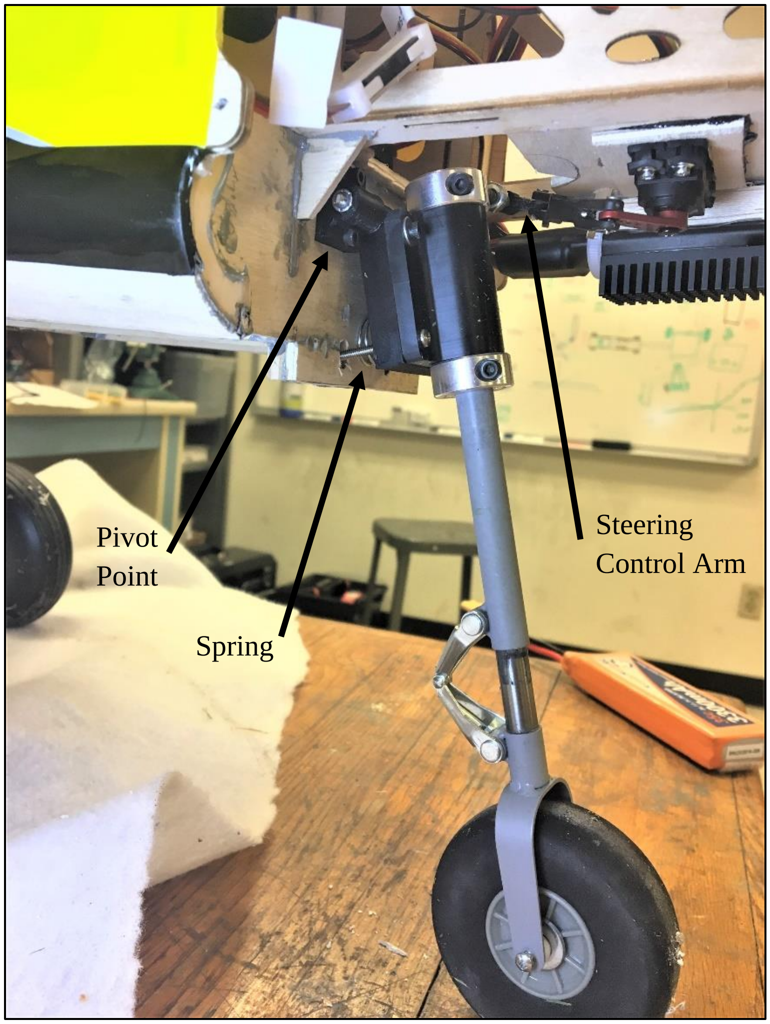

Figure 5.14 Katy's Spring-loaded Nose Gear Mount

With the nose gear fixed, flight tests were resumed and on the third test flight, the pilot was able to take off from the launch pad with no rollout and climb at roughly a 30^0 angle as shown in Figure 5.15.

Figure 5.15 Katy's Point Launch

The launchpad used for Katy was modeled after the launch crate used for Locust. The new launch pad in Figure 5.15 was made because Locust's launch crate is large and requires four people to carry it. The new, lightweight pad takes up much less space making it easier to transport and be carried by one person. Also, this launchpad could be used for Locust with a slight extension of the quick release attachment which would decrease the launch time and complexity. As mentioned before, Locust could be mobiley launched if its launch pad was placed on a raised truck bed or the front of a ship. This smaller launchpad would make the mobile launches much easier and more adaptable.

After takeoff, the pilot flew two laps and began his landing setup. He was able to almost point land the aircraft by following his target speeds and trying to follow a 5^0 glide slope. The landing is shown in Figure 5.16. While difficult to see in the figure, the landing rollout was less than 2 ft.

Figure 5.16 Katy's Point Landing

Using equation 7, the landing distance approximation equation from the Landing section, and assuming the same rolling resistance coefficient and drag coefficient as Locust, Katy's no-lift-jet approximated landing distance was 140 ft. The speed used to estimate the landing distance was 20% greater than the 27 kt. stall speed which was calculated by assuming a maximum lift coefficient of 1.3 (same as Locust) and the wing area and weight listed in Table 5.3. Comparing the 140 ft. prediction to the actual 2 ft. landing distance, Katy's CWL system demonstrated a landing distance reduction of approximately 99%.

CHAPTER VI

CONCLUSIONS AND RECOMMENDATIONS

Conclusions

The results achieved with Grasshopper, Katy, and Locust have proven the viability of the CWL UAS configuration, an effective solution to achieve point launches and landings. The CWL configuration functions by utilizing a turbojet engine mounted vertically in the fuselage to provide vertical thrust. This vertical thrust effectively changes the weight of the aircraft which lowers the wing loading and therefore the stall speed.

This CWL allows the aircraft to bypass the complex and difficult hover and transition phases that many V/STOL aircraft are designed for. Also, it allows the pilot to constantly fly the aircraft like a fixed-wing aircraft. The V/STOL configurations that fly the hover and transition phases have to be flown like helicopters or multi-rotors for takeoff and landing. During the transition phase, they have to be flown like both a fixed-wing aircraft and a rotorcraft simultaneously which is complicated, difficult, and taxing on the pilot.

Additionally, this configuration has proven that it is possible to achieve these point launches and landings using only liquid fuels. Almost all of the current point launch and landing UAVs use battery-powered rotors to provide vertical thrust. While proven to be effective, the battery-powered rotor configuration is generally achieved at the sacrifice of lower top speed from increased drag and lower fuel/payload weight from having to carry relatively low energy density batteries. Also, many of the battery-powered rotor configuration UAVs cannot take off or land in the wind. This restricts them to stationary operations where there are favorable wind conditions. With the lift jet CWL configuration, the wind is a benefit because it effectively gives the aircraft more airspeed; helping it to achieve wing borne flight sooner. So, where the battery-powered rotor configuration has a maximum wind speed tolerance, the CWL configuration exhibits better takeoff and landing performance the higher the wind speed.

The CWL configuration has also shown that it can achieve point launches and landings with minimal ground infrastructure. Unlike many other point launch and landing systems, the CWL system only requires a small, simple launch platform for takeoff. It is also advantageous in that it does not require a recovery system, which minimizes operational complexity and decreases setup and breakdown time.

Furthermore, the Locust aircraft is not limited to point launches and landings. It was designed to be a multi-role aircraft capable of both point and conventional launches and landings. The CWL system was designed to be removable and replaceable with additional fuel and/or payload if extended missions are desired when there is access to a runway. This multi-role capability greatly increases its potential mission utility.

Recommendations

Further Research

Although the CWL configuration has proven effective, it is still in the development stage. Further testing is needed to fully understand this complex dynamic system. Katy is a perfect testbed to continue the research due to its relatively low cost and ease of making modifications. With its skin being MonoKote, it is easy to cut a hole to add a component or piece of hardware and seal it back up with more MonoKote without compromising its structural integrity.

It is recommended that the ongoing auto-landing research being done at the DML be added to Katy's test flights. If the Pixhawk II can be programmed to land the aircraft autonomously, it would greatly unload the pilot's flight duties and reduce the risk of damage to the aircraft.

Further research into the effectiveness of the TV nozzle control system would also be beneficial. If it was found that the jet pipe could be eliminated and that the TV nozzle alone provided sufficient stabilization, Locust's belly pod could be removed which would greatly simplify both the main and nose landing gear system. Also, removing the belly could potentially allow the whole OML to be redesigned to optimize internal volume and reduce the overall airframe weight.

Initial Design Phase

The OML was defined too early in the design phase with too many variables left unknown. Part of the project stemmed from OSU's capability to rapidly develop and test prototypes. Rapid development is great, but more development could have saved trouble later on. The CFD analysis should have been performed before manufacturing the tooling to learn more about the aircraft's stability and controllability. Had the CFD been performed earlier, the directional instability could have been addressed by possibly increasing the vertical tail size, having the ventral be a part of the tooling, and/or rounding out the sides of the fuselage to reduce the fuselage's effect on directional stability.

Along with directional stability issues, the pitching moment issues could have been noticed which would have led to increasing the horizontal tail size or changing its shape and/or location. The whole empennage could have been iterated on until the optimum controllability and stability was achieved with minimal weight.

Also, the initial shape of the fuselage was created under the assumption that a much smaller main engine would be used. With the smaller engine, the front of the fuselage could have been kept to act as a cowling to reduce drag. A more in-depth CFD analysis and main engine sizing could have led to the front of the aircraft having a more aerodynamic shape by internally housing the engine. Although, one of the advantages of having the main engine completely exposed is that it has not had issues with overheating which can be a problem with internally housed IC engines.

REFERENCES

[1] W. P. Nelms and S. B. Anderson, "V/STOL Concepts in the United States Past, Present, and Future," *Advisory Group for Aerospace Research and Development,* vol. Special Courses on V/STOL Aerodynamics, no. 710, pp. 4.1 - 4.44, 1984.

[2] K. R. L. J. C. Branco and N. B. F. da Silva, "A new concept of VTOL as fixed-wing," in *International Conference fo Unmanned Aircraft Systems*, 2013.

[3] J. Gundlach, Designing Unmanned Aircraft Systems A Comprehensive Approach, Reston, Virginia: American Institute of Aeronautics and Astronautics, 2014.

[4] J. Barnes W. McCormick, in *Aerodynamics of V/STOL Flight*, New York, New York, Academic Press Inc., 1967, p. 1.

[5] Unknown, "8 Major Companies Using Drone Technology," Nevada Institute for Autonomous Systems, 27 October 2018. [Online]. Available: https://nias-uas.com/7-major-companies-using-drone-technology/. [Accessed 12 November 2019].

[6] W. Contributors, "Tail-sitter," Wikipedia, The Free Encyclopedia, 15 October 2019. [Online]. Available: https://en.wikipedia.org/w/index.php?title=Tail-sitter&oldid=921317834. [Accessed 26 October 2019].

[7] W. contributors, "Tiltwing," Wikipedia, The Free Encyclopedia, 1 July 2019. [Online]. Available: https://en.wikipedia.org/w/index.php?title=Tiltwing&oldid=904384753. [Accessed 26 October 2019].

[8] W. contributors, "Bell Boeing V-22 Osprey," Wikipedia, The Free Encyclopedia, 20 October 2019. [Online]. Available: https://en.wikipedia.org/w/index.php?title=Bell_Boeing_V-22_Osprey&oldid=922245452. [Accessed 26 October 2019].

[9] Unknown, "Ryan XV-5," Anigrand Craftswork, [Online]. Available: https://www.anigrand.com/AA2007_XV-5.htm. [Accessed 26 October 2019].

[10] C. L. Adcock, "VTOL Designs Turbojet Configurations," *Los Angeles Section Monographs: VTOL Vehicles,* p. 70, 26 October 1965.

[11] Unknown, "Aviation," StackExchange, 30 September 2016. [Online]. Available: https://aviation.stackexchange.com/questions/31925/how-does-the-f-35s-roll-posts-work-and-how-does-its-engine-turn-down-90-degree. [Accessed 26 October 2019].

[12] D. Raymer, Aircraft Design: A Conceptual Approach, Reston, Virginia: American Institute of Aeronautics and Astronautics, 2012.

[13] F. J., "Layout Considerations and Types of VSTOL aircraft," *Advisory Group for Aerospace Research and Development,* vol. Special Courses on V/STOL Aerodynamics, no. 710, pp. 5-1 : 5-36, 1984.

[14] E. C. P. Ransom and J. R. Smy, "Introduction and Review of some Jet Interference Phenomena Relevant to V/STOL Aircraft," *Advisory Group for Aerospace Research and Development,* vol. Special Cources on V/STOL Aerodynamics, no. 710, pp. 2-1 : 2-23, 1984.

[15] E. F. Katzenberger, H. D. Ulisnik and A. Adler, "Some Considerations of Direct-Lift V/STOL Aircraft," *Annals of the New York Academy of Sciences,* vol. 107, no. 1, pp. 380-408, 1963.

[16] J. I. Hope, "Propulsion Turbojet and Turbofan," *Los Angeles Section Monographs: VTOL Vehicles,* p. 159, 2 November 1965.

[17] M. Wong and C. L. Adcock, "Los Angeles Section Monographs: VTOL Vehicles," *The AIAA Los Angeles Section Monographs,* vol. 3, pp. 68-104, 1966.

[18] G. Verver, "Bell X-14 VTOL," Flickr, 10 December 2012. [Online]. Available: https://www.flickr.com/photos/skyhawkpc/8261851995/in/photostream/. [Accessed 26 October 2019].

[19] W. Contributors, "Hawker Siddeley P.1127," Wikipedia, The Free Encyclopedia, [Online]. Available: https://en.wikipedia.org/w/index.php?title=Special:CiteThisPage&page=Hawker_Siddeley_P.1127&id=918060112. [Accessed 26 October 2019].

[20] "McDonnell Douglas AV-8B Harrier II," Wikipedia, 15 Fenruary 2019. [Online]. Available: https://en.wikipedia.org/wiki/McDonnell_Douglas_AV-8B_Harrier_II. [Accessed 4 April 2019].

[21] Unknown, "Youtube," AiirSource Military, 26 February 2014. [Online]. Available: https://www.youtube.com/watch?v=94c3a7NXxVs. [Accessed 26 October 2019].

[22] "F-35 Capabilities," Lockheed Martin, 2019. [Online]. Available: https://www.f35.com/about/capabilities. [Accessed 7 April 2019].

[23] "Lockheed Martin F-35 Lightning II," Wikipedia, 7 April 2019. [Online]. Available: https://en.wikipedia.org/wiki/Lockheed_Martin_F-35_Lightning_II. [Accessed 7 April 2019].

[24] Unknown, "F-35 Lightning II," Lockheed Martin Corporation, 2019. [Online]. Available: https://www.f35.com/about/variants/f35b. [Accessed 26 October 2019].

[25] Unknown, "Alti Gallery," Alti UAS, [Online]. Available: https://www.altiuas.com/gallery/. [Accessed 28 October 2019].

[26] H. Otsuka, D. Sasaki and K. Nagatani, "Reduction of the head-up pitching moment of small quad-rotor unmanned aerial vehicles in uniform flow," *International Journal of Micro Air Vehicles,* vol. 10, no. 1, pp. 85-105, 2017.

[27] A. F. Sciences, "Aurora Excalibur UAS Makes First Flight," AUVSI, [Online]. Available: https://www.auvsi.org/aurora-excalibur-uas-makes-first-flight. [Accessed 9 April 2019].

[28] "VTOL X-Plane," Wikipedia, 2 January 2018. [Online]. Available: https://en.wikipedia.org/wiki/VTOL_X-Plane. [Accessed 4 April 2019].

[29] G. Warwick, "Aurora Flies Hybrid VTOL UCAV Demonstrator," McGraw-Hill , 20 July 2009. [Online]. Available: https://structures.aero/wp-content/uploads/2016/09/Aurora-Flies-Hybrid-VTOL-UCAV-Demonstrator-Aviation-Week-20090720-2-1.pdf. [Accessed 4 April 2019].

[30] Unknown, "Excalibur," Russina Unmanned Vehicle Systems Association, 2011. [Online]. Available: https://en.ruvsa.com/catalog/excalibur/. [Accessed 26 October 2019].

[31] N. S. Drones, "North Sea Drones," North Sea Drones, [Online]. Available: http://www.northseadrones.com/nsd/wp-content/uploads/2018/11/STOVL-Presentation.pdf. [Accessed 9 April 2019].

[32] K. D. Atherton, "This weird wedge could be the jet-powered drone navies want," 13 November 2018. [Online]. Available: https://www.c4isrnet.com/unmanned/2018/11/13/this-vtol-wedge-could-be-the-jet-powered-drone-navies-want/?fbclid=IwAR22HU9XMZY2Tw4gOP08dopq3q141siA8vPfdsnplBwYK3jKxQHzTU0kQWk. [Accessed 4 April 2019].

[33] Unknown, "IndoDefence 2018: NorthSeaDrones unveils jet and prop STOVL drone," Army Recognition, 08 November 2018. [Online]. Available: https://www.armyrecognition.com/indodefence_2018_news_official_show_daily/indodefence_2018_northseadrones_unveils_jet_and_prop_stovl_drone.html. [Accessed 26 October 2019].

[34] E. Johnson, W. Allen and J. Neidhoefer, "Flight-Test Results of Autonomous Airplane Transitions Between Steady-Level and Hovering Flight," *Journal of Guidance, Control, and Dynamics,* vol. 31, no. 2, pp. 358 - 370, 2008.

[35] E. ToolBox, "Flash Point - Fuels," Engineering ToolBox, [Online]. Available: https://www.engineeringtoolbox.com/flash-point-fuels-d_937.html. [Accessed 14 May 2019].

[36] R. C. Nelson, Flight Stability and Automatic Control, United States of America: McGraw-Hill Companies, Inc., 1998.

[37] J. Fletcher, "Layout Considerations and Types of VSTOL Aircraft," *Advisory Group for Aerospace Research & Development,* vol. 710, no. Special Courses on V/STOL Aerodynamics, p. 9, 1984.

[38] Unknown, "Types of Aircraft Construction," Waybuilder, [Online]. Available: https://www.waybuilder.net/free-ed/Resources/15-Transportation/Aviation/AircraftStructure.asp?iNum=3. [Accessed 30 October 2019].

[39] T. H. G. Megson, *Introduction to aircraft structural analysis,* Waltham, MA, Elsevier, 2007, p. 351.

[40] F. G. D. Corp., "The Fundamentals of Fiberglass," Fibre Glast Development Corp., 2019. [Online]. Available: https://www.fibreglast.com/product/the-fundamentals-of-fiberglass/Learning_Center. [Accessed 6 August 2019].

[41] Unknown, "Vacuum Bagging Equipment and Techniques for Room-Temp Applications," Fibreglast, 2019. [Online]. Available: https://www.fibreglast.com/product/vacuum-bagging-equipment-and-techniques-for-room-temp-applications/Learning_Center. [Accessed 30 October 2019].

[42] W. Zuo, "Bi-level optimization for the cross-sectional shape of a thin-walled car body frame with static stiffness and dynamic frequency stiffness constraints," *Journal of Automobile Engineering,* vol. 229, no. 8, pp. 1046-1059, 2015.

[43] J. W. Combs, "Design and Development of a Quiet Unmanned Aircraft System," Oklahoma State University, Stillwater, OK, 2011.

[44] A. H. Committee, "Heat Treating of Aluminum Alloys," *ASTM Handbook,* vol. 4, no. Heat Treating, pp. 841-879, 191.

[45] E. ToolBox, "Fuels and Chemicals - Auto Ignition Temperatures," 2003. [Online]. Available: https://www.engineeringtoolbox.com/fuels-ignition-temperatures-d_171.html. [Accessed 27 August 2019].

APPENDICES

Flight Cards

CLARC Pre-Flight		
☐	Safety Equipmen	Requried equipment on hand. CO2-Fire Extinguisher, *see FR Card*
☐	Attachments Secure	Spars, Mounts, Pins, Bolts, Nuts
☐	Landing System	Main Gear, Nose Gear, Controls
☐	Release Syste	Secure and Armed
☐	Equipment Secur	Trays, Payload, Internal Equipme
☐	Batteries	Secure, Voltage Check
☐	Fuel System	Fuel Level at Spec's, Valves ON
☐	ower Switches O	
☐	Flight Controller Arm	
☐	Comms Check	Flight Controller, Telemetry, Vide
☐	Controls	Quick Look at Response/Deflecti
☐	Hatches Secu	
☐	Remove RBF-Tag	
☐	Remove Pitot Cove	
☐	Area Clea	Non-Essential Personnel Clear
☐	Launch System	Location and Direction Check. Aircraft Secure. System Armed.

CLARC Post-Flight

☐	Lift Jet Cooldown	
☐	Prop Engine OFF	
☐	Fire Check	
☐	Power Switches OFF	ONLY with pilot authorization and jet engine cooldown complete.
☐	Accounted For	ALL components safe, secure and accounted for.
☐	Quick Look	Damage inspection.

Aircraft:	**CLARC**	Location:	Date:

Flight Readiness Inspection

☐	Fuselage Integrety	Check skin and bonds for damage or wear.
☐	Attachments Check	Inspect all attachment points, check for any damage to mount locations.
☐	Landing System Check	Inspect all landing gear and mounting points.
☐	Launch System	Look over launching system. Mounting points on the aircraft or launch stand. Check for fatigue and damage.
☐	Equipment Mounts	Check Trays, Payload, Internal Equipment.
☐	Electrical System	Check for damage or wear: exposed wires, safety clips broken or missing
☐	Fuel System	Inspect connections and fuel lines.
☐	GCS/Pixhawk OPS Check	Run through operational procedures.

Engineer:	Time:	Section: 1 of 5

Aircraft:	CLARC	Location:	Date:

Flight Readiness Inspection

- [ ] Control Systems — Inspect control surfaces, servos, pushrods, hinge lines, quick connects and control horns. Ensure safety connections are installed.
- [ ] TV Check — Gyro gains, I/O and deflections.
- [ ] Controls Check — Gyro gains, I/O and deflections.

Manual Mode Tests

Deflect the control surfaces.

Look for: Correct deflection directions

Correct deflection angles

Assisted Modes (Repeat for All Assisted Modes)

Deflect the control surfaces.

Look for: Correct deflection directions

Correct deflection angles

Roll/Pitch (2D Motion Respectively)

Quick +/- Rotations

Look for: Correct direction of correction response

Slow +/- Rotations

Look for: Correct direction of correction response

Angle Hold Responses

Look for: Holding of errors/bad corrections

Engineer:	Time:	Section:
		2 of 5

Aircraft:	CLARC	Location:	Date:

Flight Readiness Inspection

☐ Pixhawk Calibration

Compass Calibration: Notes:

IMU Calibration: Notes:

Pixhawk Notes:

☐ Range Check (Comms/Telem)

☐ Dry Weight Checks

Dry Weight: ____________

Dry CG Location: ____________

Notes:

Engineer:	Time:	Section:
		3 of 5

Aircraft: CLARC	Location:	Date:

Flight Readiness Inspection

☐ Payload Check

Weight: ________

Description: ______________________________

____

____

____

☐ GTOW Weight Checks

GTOW Weight: ________

GTOW CG Location: ________

Notes:

Engineer:	Time:	Section: 4 of 5

Aircraft: **CLARC**	Location:	Date:

Flight Readiness Inspection

Required Safety Equipment

- [ ] Fire Extinguishers — CO2 and non-CO2 Extinguisher
- [ ] First Aid Kit

Engineer:	Time:	Section: 5 of 5

Aircraft:	CLARC	Location:	Date:

Flight Card - Batteries Pre-Flight

Battery (ID/Position)	**Voltage** (Vtotal/C1/C2/…)

Notes:

Engineer:	Time:	Section: 1 of 6

Aircraft: CLARC	Location:	Date:

Flight Card - Batteries Post-Flight

Battery ID	Before Charge Voltage (Vtotal/C1/C2/...)	After Charge Voltage (Vtotal/C1/C2/...)	After Charge Amp. Charged [mA]

Notes:

Engineer:	Time:	Section: 2 of 6

Aircraft: CLARC	Location:	Date:

Flight Card - Weather

Time	Temperature	Wind	Pressure	Humidity

Comments:

Time	Temperature	Wind	Pressure	Humidity

Comments:

Time	Temperature	Wind	Pressure	Humidity

Comments:

Time	Temperature	Wind	Pressure	Humidity

Comments:

Engineer:	Time:	Section: 3 of 6

Aircraft: CLARC	Location:	Date:

Flight Card - Aicraft Data

TIME			
Max/Warning Time [min]	Take-Off	Landing	Duration

WEIGHTS			
Dry	GTOW	Landing	Comments

CG		
Dry	GTOW	Comments

	Filled	Landing	Burned
Jet Fuel			
Prop Fuel			

Comments:

Engineer:	Time:	Section: 4 of 6

Aircraft: **CLARC**	Location:	Date:

Flight Card - Flight Notes

Flight Notes

Comments on the flight. (Pitch/Roll/Yaw control, Take-off, Landing, etc.)

Engineer:	Time:	Section: 5 of 6

Aircraft: CLARC	Location:	Date:

Flight Card - Specifications and Capacities

Specifications & Capacities	
Max Prop Fuel:	Vpf
Max Turb. Fuel:	Vtf
Max Prop Flight Time:	Calc.: Vpf*0.00
Max Turb. Flight Time:	Calc.: Vtf*0.00
Max Battery Time:	
Max. Payload:	

Note: the above values and calcs. have SF built in and should not be exceeded

Engineer:	Time:	Section:
		6 of 6

Weight and Balance

CWL System				Propulsion				
Component	**Weight [lb]**	**Arm [in]**	**Moment [lb*in]**	**Component**	**Weight [g]**	**Weight [lb]**	**Arm [in]**	**Moment [lb*in]**
K-260 G2	5.1	15.3	77.5	DA-120	2245.0	4.9	-7.2	-35.6
Jet Pipe	0.6	16.8	9.3	DA-120 ignition	145	0.3	0.8	0.3
ECU	0.1	19.5	1.8	DA-120 Mounting Hardware	131	0.3	-3.7	-1.1
Thrust Vector Servo (Hitec 930)	0.1	20.8	3.0	Fuel Flow Meter	40	0.1	32.5	2.9
Thrust Vector Servo (Hitec 930)	0.1	19.4	2.8	fuel tank 60 oz w/clunks and hose (jet)	216.0	0.5	26.2	12.5
Fuel Flow Meter	0.1	32.5	2.9	fuel tank 60 oz w/clunks and hose (jet)	216.0	0.5	22.1	10.5
Fuel Pump w/valve and filter (K-260)	0.3	25.9	7.3	fuel tank 60 oz w/clunks and hose (prop)	216.0	0.5	22.1	10.5
Battery (kingtech LiFe 3800 mAh 9.9V)	0.7	24.0	15.8	Fuel line (5ft @10.5g/ft)	52.5	0.1	16.4	1.9
60 oz fuel (jet A)	3.1	22.1	69.5	prop (Biela 26x12 3 blade)	329.0	0.7	-11.4	-8.2
Total	**7.0**		**120.4**	Prop spinner w/plate	162.0	0.4	-11.7	-4.2
				Prop Bolts (x6)	50.0	0.1	-11.7	-1.3
				120 oz fuel (gasoline)	1288.0	5.7	26.2	148.8
				Total	**3802.5**	**8.4**		**-11.9**
				Fuel	4141.0	5.7		148.8

Airframe				Payload			
Component	**Weight [lb]**	**Arm [in]**	**Moment [lb*in]**	**Component**	**Weight [lb]**	**Arm [in]**	**Moment [lb*in]**
weighed fuselage	7.5	23.3	173.9	DL-500 DGPS	1.3	5.3	6.7
weighed wing (both halves)	4.1	19.5	79.6	TS-4000 Datalink Radio	1.2	7	8.3
weighed horizontal tail	0.4	64.3	23.1	Antenna	0.8	37	28.8
Weighed Ventral	0.3	60.2	19.4	Reflector (fore)	0.1	6.5	0.4
Landing gear (nose)	0.5	-1.9	-0.9	Reflector (aft)	0.1	25.4	1.6
Nose Gear Mouting Hardware	0.0	-0.4	0.0	**Total**	**3.35**		**45.73**
Landing gear (mains)	0.6	19.6	12.5				
Main Gear mounting bolts	0.1	21.8	1.3				
Main wheels (x2)	0.7	18.0	12.4				
Nose wheel	0.2	3.6	0.7				
mains axles and collars	0.1	18.0	1.8				
3D Printed hatch arms	0.1	16.5	2.2				
Shower drain, FG tape, Sandable	1.0	27.8	27.8				
Total	**15.56**		**353.88**				

Electronics and Batteries			
Component	**Weight [lb]**	**Arm [in]**	**Moment [lb*in]**
RMILEC Receiver	0.0	52.0	1.3
Elevator Servo	0.1	54.7	4.1
Rudder Servo	0.1	59.4	4.5
Throttle servo	0.1	0.7	0.1
Choke servo	0.1	0.7	0.1
Nose wheel servo	0.1	0.7	0.1
bombay servo port	0.1	12.2	0.9
bombay servo starboard	0.1	12.2	0.9
Flap servo port	0.1	18.9	1.4
Aileron servo port	0.1	18.9	1.4
Flap servo starboard	0.1	18.9	1.4
Aileron servo starboard	0.1	18.9	1.4
Pitot Assembly	0.0		0.0
pixhawk 2 w/cube	0.2	5.1	0.8
pixhawk GPS	0.1	1.7	0.2
Jeti REX 7	0.0	17.3	0.5
CTU Aero Panda	0.1	19.5	2.0
guardian	0.0	8.8	0.2
wiring	2.0	14.8	29.5
RFD-900 telemetry (w/2 antenna)	0.1	17.1	1.1
RunCam Micro Eagle FPV	0.0	59.0	1.0
FPV antenna	0.0	43.4	0.0
Battery (LiFe 3600 mAh 6.6V)	0.4	25.4	10.5
Battery (LiFe 3600 mAh 6.6V)	0.4	40.7	16.8
Battery (LiFe 3600 mAh 6.6V)	0.4	40	16.5
Battery (LiPo 3300 mAh 11.1V)	0.6	5.1	2.9
Switches (x3)	0.3	8.5	2.2
Total	**5.4**		**101.7**

Wiring Diagram

The wiring diagram is laid out as follows:

Pg. 1	Pg. 2	Pg. 3
Pg. 4	Pg. 5	Pg. 6

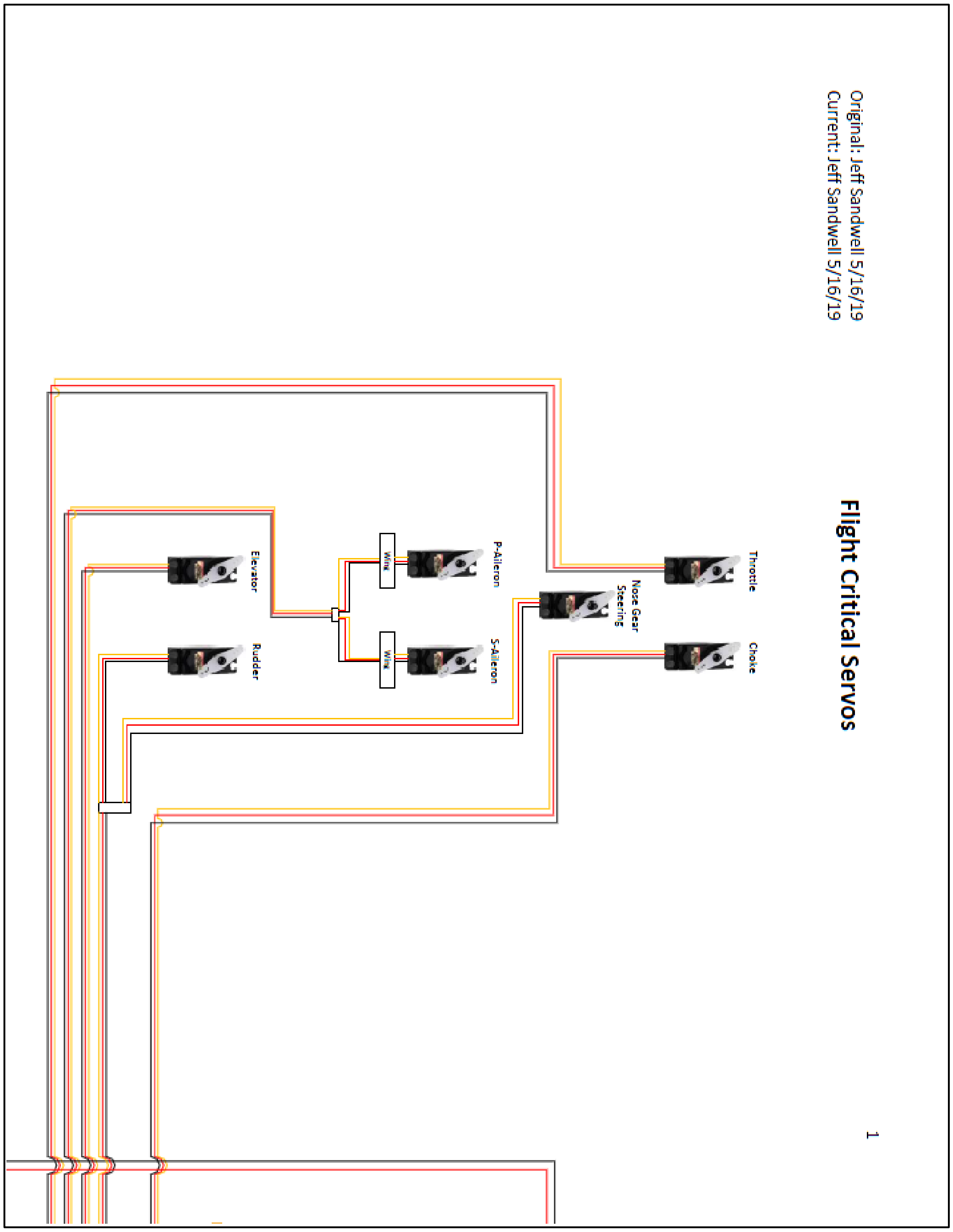

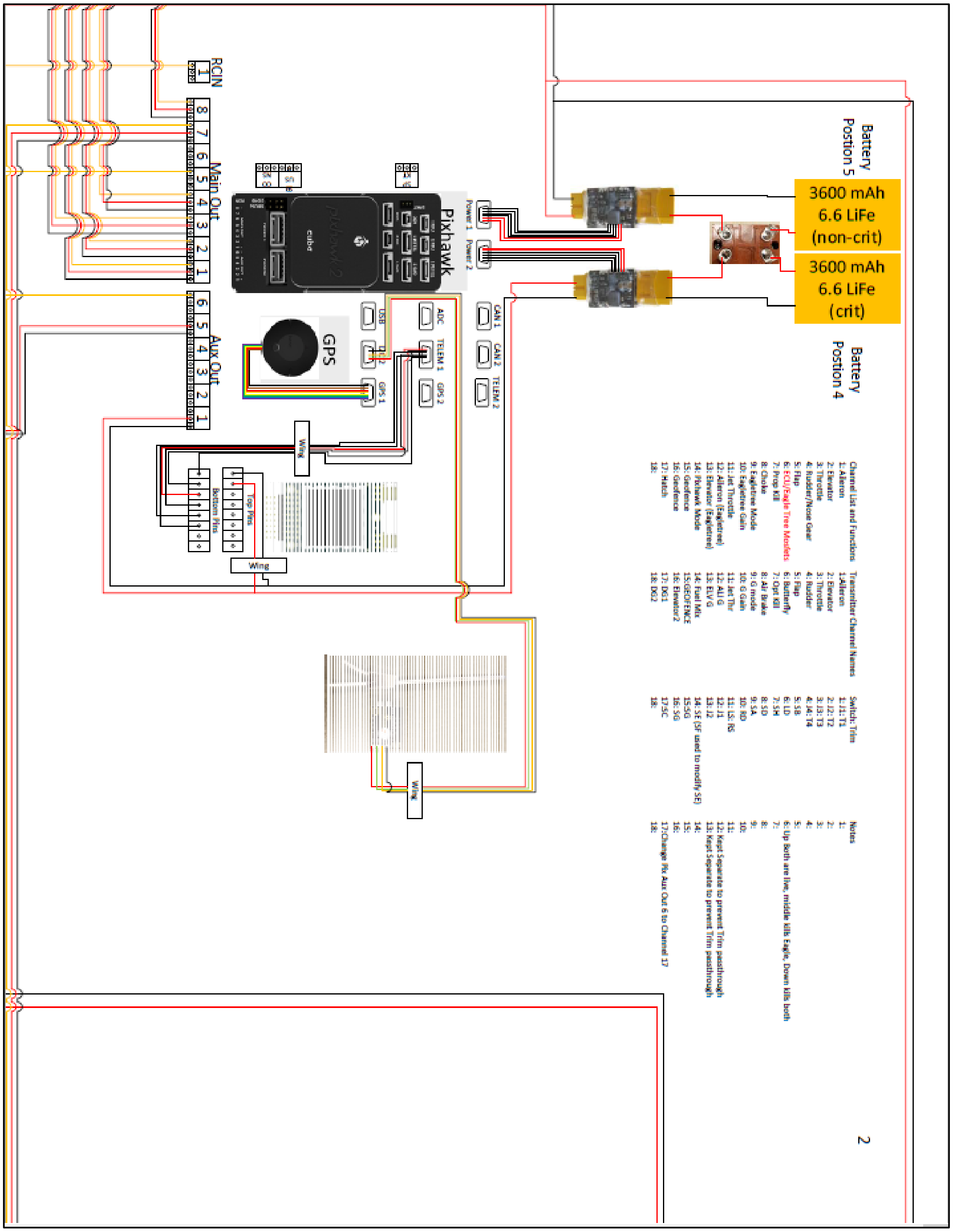
Battery
Postion 5
3600 mAh
6.6 LiFe
(non-crit)
3600 mAh
6.6 LiFe
(crit)
Battery
Postion 4
RCIN
Main Out
Aux Out
Pixhawk
GPS
Power 1
Power 2
CAN 1
CAN 2
TELEM 1
TELEM 2
ADC
USB
GPS 1
GPS 2
Wing
Top Pins
Bottom Pins
Wing
Wing
2

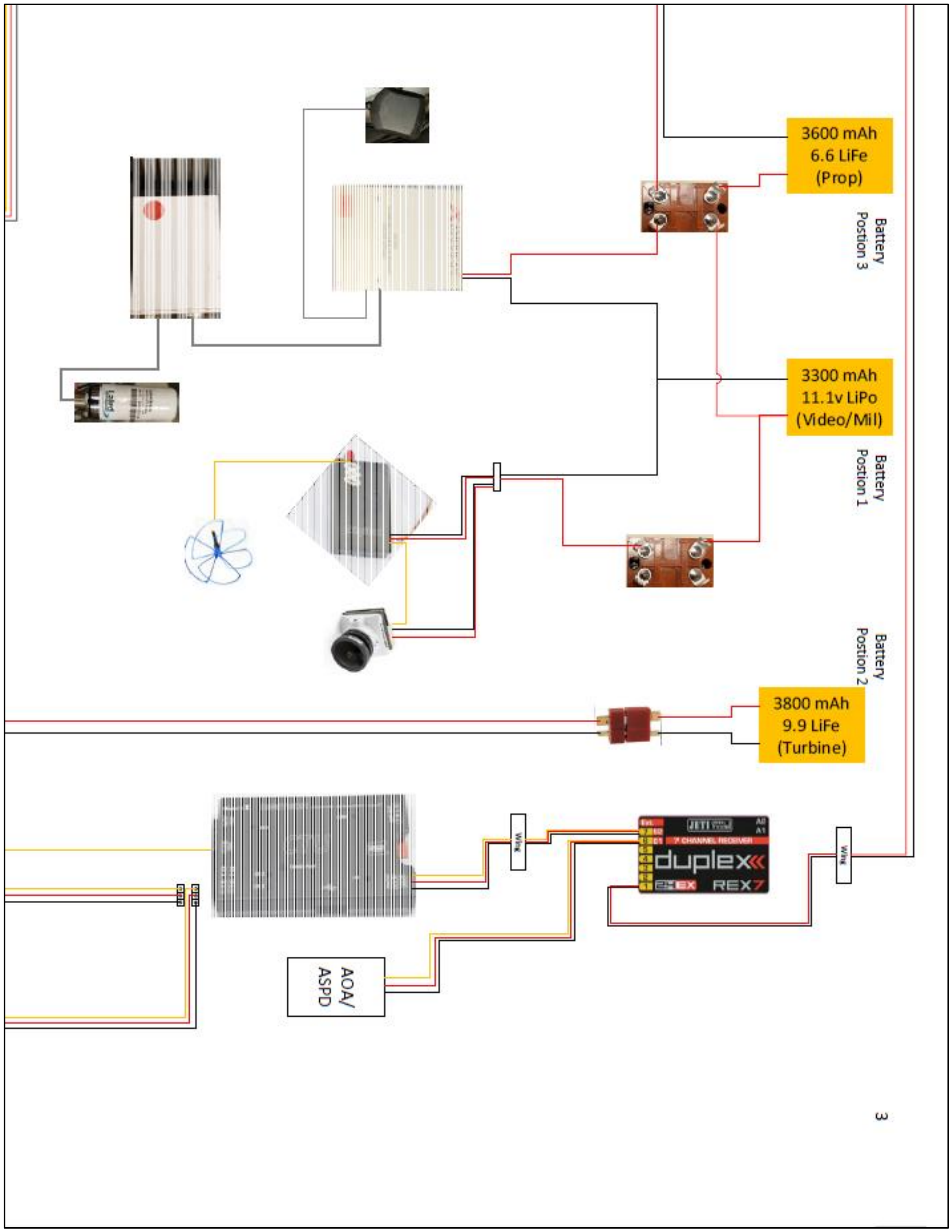
3600 mAh
6.6 LiFe
(Prop)
Battery
Postion 3
3300 mAh
11.1v LiPo
(Video/Mil)
Battery
Postion 1
Battery
Postion 2
3800 mAh
9.9 LiFe
(Turbine)
duplex
REX7
AOA/
ASPD
3

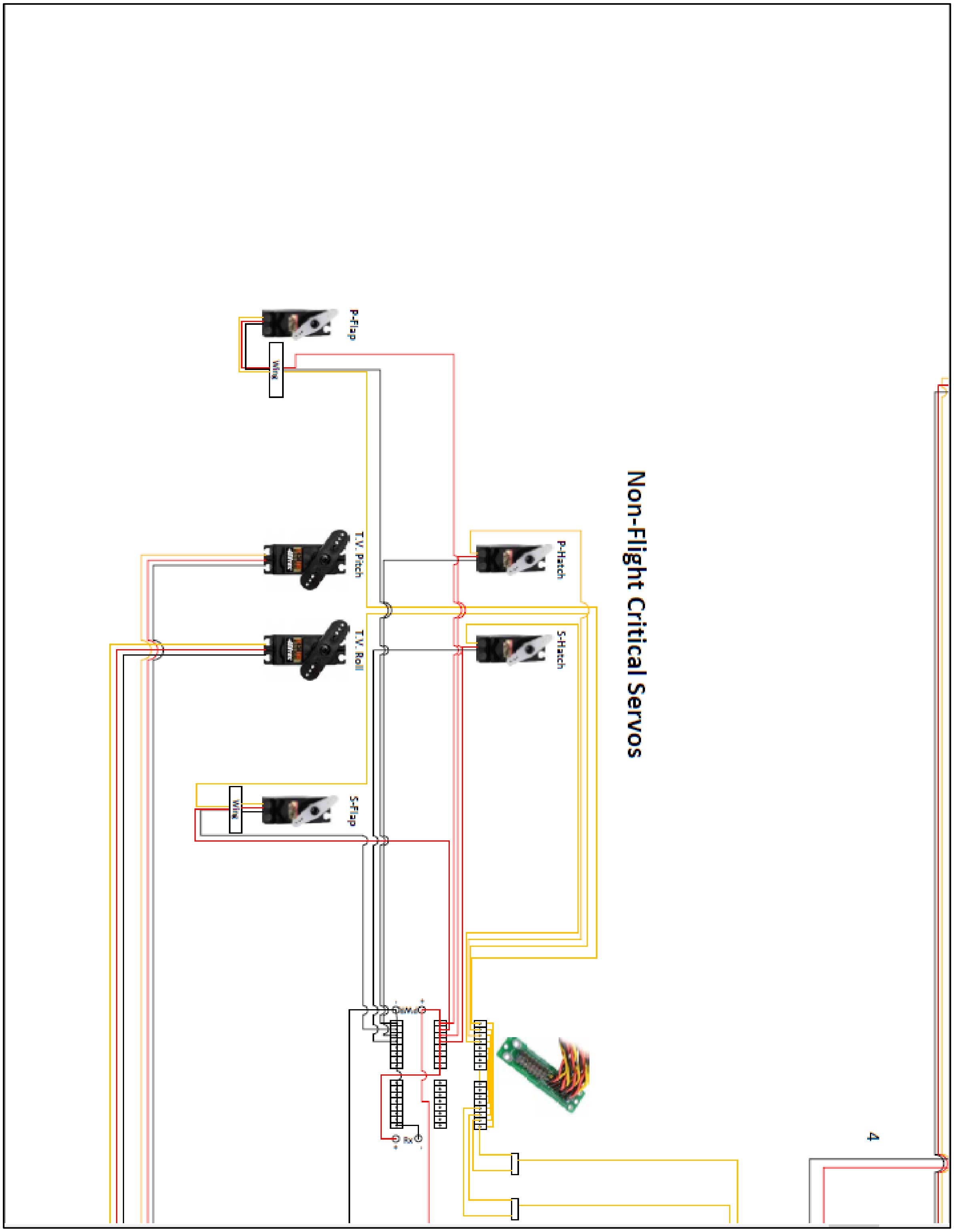

Non-Flight Critical Servos
P-Flap
Wing
T.V. Pitch
T.V. Roll
P-Hatch
S-Hatch
S-Flap
Wing
Rx
4

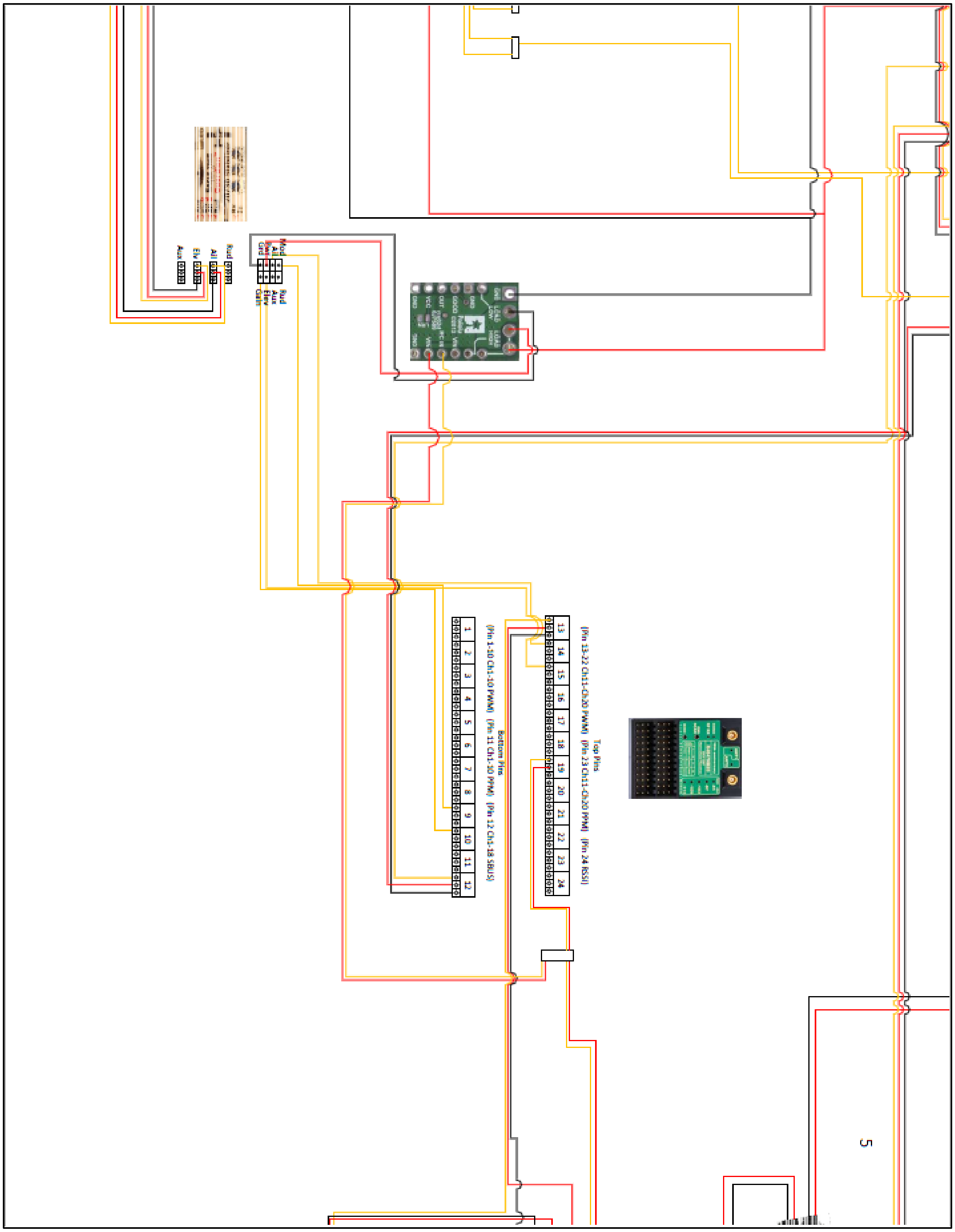

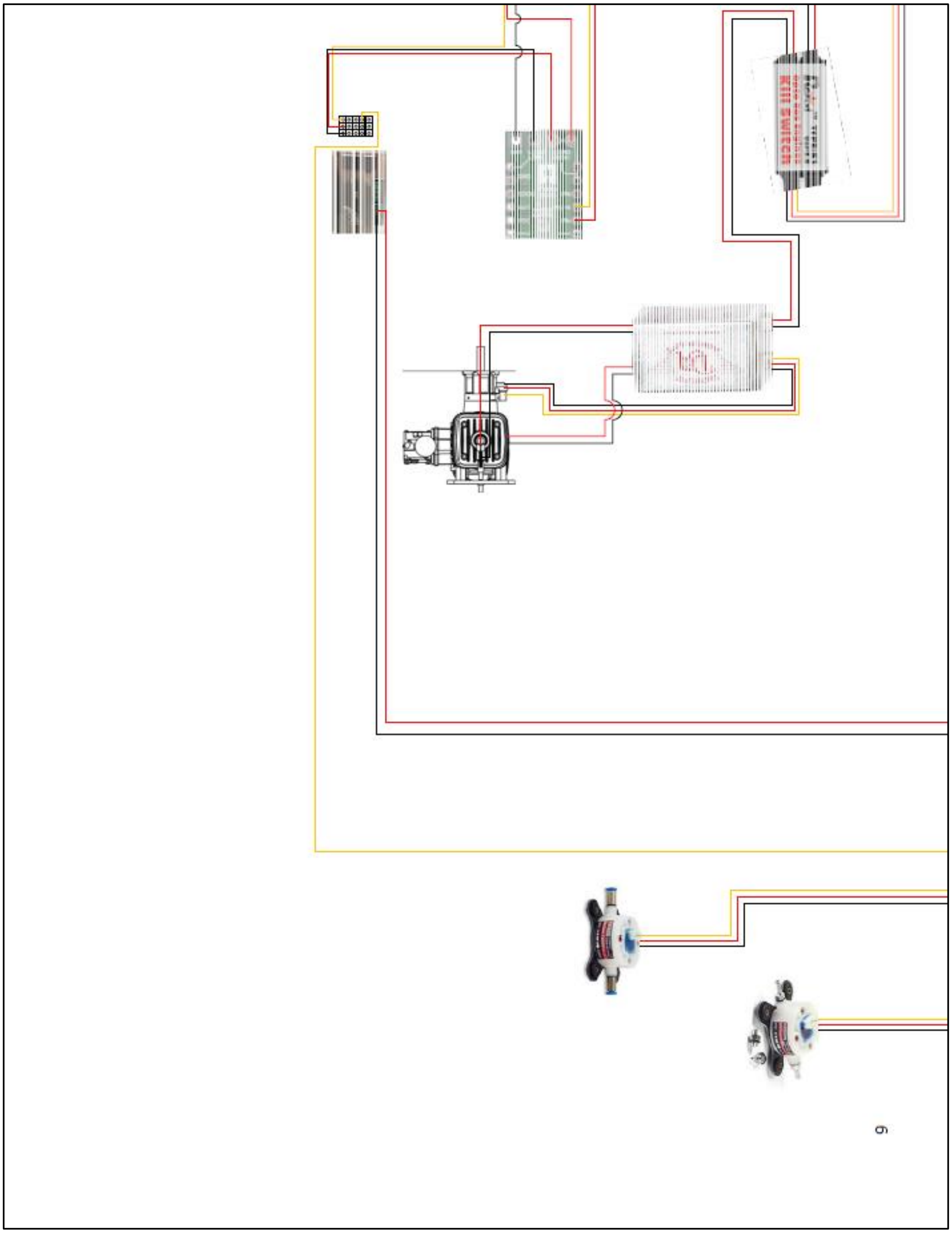

Structures Tutorial

This structures tutorial was created by Rachel Wamsley in 2016 and modified by Garret Castor and Jeff Sandwell on 2/2/2018.

STRUCTURES TUTORIAL

PART 1: MACHINING THE PLUG

1. Model male plug in CAD. The model should be divided into however many sections are required for the mold. For each section, there should be one planar side (this will be the side that is stuck to the table during the CNC process and is also the side that will be bonded to the other sections of the plug).
    a. Allow room for error in the model. <u>Minimum thickness</u> on any part of the section to be cut on the CNC is 0.03 in.
        i. Trailing edges of wing, horizontal stab, and vertical stab are very thin and have a higher chance of breaking upon removal from the table post-machining if thickness is not added to the model to be cut.
        ii. Thickness should only be added to the thin parts of the model. Otherwise, the whole part will be thicker and will stray from the design.
        iii. Extra thicknesses can be sanded away post-machining if necessary.
2. Create g-code from CAD model.
    a. Use a pass of 0.03 in.
    b. Choose tools for each cut. There is a roughing cut, final cut, and a pencil cut. Different bits are used for each cut.

i. The larger end mill should be used for rougher passes and the smaller ball mill should be used for pencil cuts.

c. Run the cutting simulation in Solidworks and make sure the cut is theoretically smooth.

   i. This is an easy step to do before actually cutting into expensive materials the plugs will be made of. Sometimes it may take a while, but it's worth the check.

3. Refer to Operating the CNC Router Table document for CNC operation instructions.

   ***Make sure to put double-sided tape on the bottom of the foam before putting it on the table to machine.

   ***Make sure the bit is hand-tight. No need to over-torque.

   ***DO NOT FORGET to re-zero the z-axis after changing bits.

4. Repeat steps 1-3 for the second half of the plug.
   a. Double check the G-code to make sure you are cutting the correct half!
5. Epoxy raw plug halves together using 400/150 epoxy/hardener with 406 (colloidal) filler to thicken the epoxy.
   a. Set one half of the plug in the parting board before epoxying them together.
   b. For a rough estimate of amount of epoxy, begin with 5g resin per 60 in^2 and add more as necessary.
      i. Using too much epoxy to mate the plug will increase thickness of the total part and result in contour issues along down the road (especially with airfoils).
      ii. Using a wooden tongue depressor, scrape the epoxy as thin as possible. Be sure to not

get epoxy on the sides (outside of the bonding area)

6. Wipe dust and excess epoxy from foam plug and use painters tape to secure the two halves together while the epoxy cures.
7. Allow to cure for 12 hours.

PART 2: PRIMING AND SANDING THE PLUG

1. Begin with a single, thin, even layer of Zinsser BIN shellac-based primer. Apply with a foam brush. Before sanding, three thin layers of paint should be applied. See Figure 1.
    a. The majority of the first layer will soak into the foam.
    b. Thick layers of primer will appear dry on the surface, but will not be completely dry on the inside. Trying to sand the plug with tacky/thick paint will result in paint rolling into little balls (BAD!)
        i. Thicker/more paint at once does not speed up this process.
    c. Use the yellow triangles to hold the part off the table. Sometimes balancing is required.
        i. Make sure to not press down on the part because the triangles could damage it.
2. Allow at least 30 minutes for dry time. Use a hairdryer or fan (within a reasonable distance away from the part, about 6 inches) to accelerate dry time.
3. Starting with 150-grit sandpaper, lightly sand the plug. Sand in long, continuous strokes and also small circles. The long strokes help keep the plug smooth and the circles help to further eliminate brush strokes. Brush strokes should be

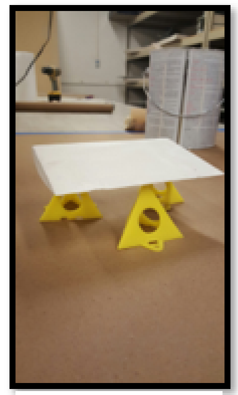

Figure 1: First Coat of Primer

sanded out and the shiny finish of the primer should be dulled out by the sanding.

   a. If sanding goes through the primer and into the plug, use the drywall to repair.
      i. Drywall application should be similar to paint application. Thick/more does not equal faster.

4. Once the brush strokes and shiny finish have been sanded, switch to 220-grit sandpaper and repeat the process.
5. Add another thin layer of primer. Repeat steps 2-4. Do this until the plug is smooth and free of imperfections. The plug should feel like plastic.
   a. See Figure 2. The trailing edge has bumps and brush strokes on it. This still needs to be sanded.
      i. The smoother your plug, the smoother your plane will be!

Figure 2: A Second Coat of Primer

PART 3: MOLDING PROCESS


Figure 3: Example of 3D Parting Board


Figure 4: Example of 2D/3D Parting Board

1. Make a parting board. A hole should be cut in a piece of MDF that is slightly larger than the cross section of the midpoint of the plug. This is typically the mating point of the two machined plug halves. Allow about 3 inches for a flange surrounding the part.
    a. 3D contour of part – Figure 3.
    b. 2D/3D of contour of part – Figure 4.
    c. 2D contour of part with support jigs.
2. Make dams for the parting board. The dams serve as a 'stand' for the mold.
    a. The dams should be taller than the maximum height of the plug as it sits in the parting board.
        i. If the dams are too short, the mold will not sit flush on the table and it will wobble and damage the mold.
        ii. Be sure dams are taller than the plug!
    b. Using a brad nail gun, nail the dams into the side of the parting board.
3. Once dams have been installed, paint dams and parting board with primer. Sand and repeat as necessary to get a perfectly smooth surface. Follow the same method addressed in part 2.
4. Once both plug and parting board have been primed and sanded, dry fit the plug into the parting board. If there are areas that the plug does not sit flush, find the high areas and carefully sand them. Repeat this process until the plug sits flush in the parting board.
5. Put clay in between the cracks of the parting board and plug. Make sure to use a plastic paint scraper or plastic razor blade as to not ruin the plug or scratch the paint off the parting board.

a. Technique: roll the clay like a Tootsie Roll and place it on the crack. Use the plastic razor blade and run it along the edge ensuring the clay is in the crack and not on the plug.
b. It is important to not leave any clay residue on the side of the plug that is to be molded. Excess clay left on that part of the mold will result in bumps in the mold, and bumps in the final part.

If this is the second half of the mold, ensure chamfer holes are drilled into the existing mold on the tool coat side before continuing to Step 3

6. Apply three coats of wax.
   a. The wax theoretically should not add any thickness. Wax on, wax off.
      i. Use either a paper towel or a soft cloth towel.
7. Apply three coats of release.
   a. Use a foam brush.
   b. Release should also be as thin as possible. The thinner, the better. Each layer will dry quicker and you won't add too much thickness to your mold.
   c. Squeeze excess release out of the foam brush into the cup and soak up excess release that puddles up on the part.
8. Cut fiberglass prior to mixing tool coat. There should be 7 layers of 0/90 bias and 6 layers of 45-degree bias. Once fiberglass is cut, label each piece with a sharpie (0/90 layer 1, 45/45 layer 2 etc.).
9. Mix the tool coat. Use gel coat and blue 150 hardener (30 minute).

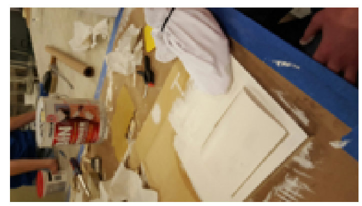

Figure 5: Waxing

Figure 6: Releasing

a. Make sure it is mixed completely (no white is visible). The polymers will not cross-link if it is not mixed properly.

10. Apply first layer of tool coat.
    a. Use a foam brush to apply. Run the foam brush along edges to ensure there are no voids. Do NOT pour tool coat onto plug. Pouring and smoothing the tool coat over could result in the release ripping off the part and removal of the mold from the plug will be damaging to the plug.
    b. See Figure 7.
    c. Keep the same foam brush to use in Step 8.
        i. Tip: Set the foam brush across the top of the tool coat container to keep your work area clean.
        ii. Mark the time the tool coat was applied on the container for documentation.

Figure 7: Tool Coat

11. Wait 45 min – 1 hour before applying 2nd layer of tool coat. About half way through this wait time, check to make sure no bubbles have formed. Remove any bubbles by gently running the SAME foam brush you used to apply the layer over the bubbles.
    a. The amount of pressure applied to run the brush along the bubbles should be minimal. The weight of the brush should suffice. Simply drag the brush along where the bubbles are.
12. Repeat steps 5 - 7 for the second layer of tool coat.
13. Mix some epoxy with colloidal silica (thickener) added.
    a. It should be thick enough that it does not drip.
        i. A little less thick than peanut butter but thicker than yogurt.

b. Add the thickened epoxy to the junction where the dam meets the parting board using your fingers and tongue depressors.
    i. This is done to get rid of the 90 degree angle which will make the molding process much easier and will end in a stronger mold.
    ii. The 'fillet' should extend about half an inch from the junction.

14. Mix 400/250 (70 minute) resin/hardener (make sure to reference the ratios!).
    a. Mixing too much too early can result in decrease cure time for the epoxy and melting containers.
15. Using the little black bristle brushes, paint all of the tool coat with a layer of epoxy. This will keep the fiberglass from sticking to the tool coat so that it can be moved if necessary.
    a. Be sure all of the tool coat has a layer of epoxy on it (don't be afraid to use a generous amount).
16. Place first layer of tooling glass at a 0/90 bias. If there are complex curves, cut small pieces of a 45 degree bias to lay on those curves. The entire first layer shall not be at a 45 degree bias. It'll help you not cut yourself.
    a. Make sure to lay the first few layers of tooling glass by hovering the glass above the mold and laying it down from the CENTER FIRST.
        i. Have a few people hover the glass while one person presses down in the middle and smooths the glass down to the outside edges.
17. Place second layer of tooling glass at a 45 degree bias. Alternate bias of each layer. There should be 7 layers of 0/90 degree bias and 6 layers of 45 degree bias.

    a. Exception is the small pieces cut for complex contours.

18. Allow 48 hours for cure time.
19. Use the heavy duty dremal to cut off excess fiberglass from the top of the dam.
    a. Use the dam as a guide and make the cut as straight as possible.
    b. Sand down the edges until they are no longer sharp.
20. Use a paint scraper/wedge to remove the parting board from the mold. This should be done very gently as to not damage the mold.
    a. Use the paint scraper/wedge in between the parting board and the tool coat.
21. Drill holes (chamfer) into the first half of the mold on the tool coat side (the blue side) for mold alignment.
    a. This shall be done prior to wax and release of the second half.
    b. Do not drill all the way through.
22. For the second half of the mold, repeat step 2-14.
23. Separate the two halves of the mold with a paint scraper.
24. Remove the plug from the mold.
    a. This is difficult to do so be careful to not damage the plug.
    b. This can be done using paint scrapers, mylar sheets, and/or the shop compressed air.

PART 4: LAYUP

1. Clean the mold with water and a paper towel.
2. Cut fabric to use in mold.
3. Weigh each layer and make note of how much each layer weighs.
   a. Tip: Write it on the fabric with a sharpie.
4. Place ½" – 1" painter's tape to the flange of the mold. See Figure 8.
   a. This step is to ensure there is an area near the layup that is without wax or release so the chromate can stick during bagging process.

Figure 8: Tape on edges before wax and release

5. If there are hatches, continue reading. If not, skip to step 8.
6. Use double sided tape and tape in the hatch where it goes.
7. Add clay around the edges of the hatch so that epoxy will not get underneath it.
   a. Try to make the clay as thin as possible while maintaining a seal around the hatch,
      i. It needs to be thin so there isn't a void in the final layup.
8. Apply three layers of wax to mold.
9. Apply three layers of release to mold.
   a. Let each layer dry before adding another layer.
      i. The drying process can be sped up using a fan or hair dryers.
      ii. If using hair dryers, make sure that the heating element is OFF.
10. Measure and mix the resin/hardener required for the first layer (make sure to reference the ratios!).
11. If there is Kevlar and/or carbon tow in the layup, it goes on LAST (on the inside of the part).
12. Apply epoxy mix to first layer by one of the following methods:
    a. Pre-preg.

Figure 9: Pouring Epoxy to Prepreg

i. Tape plastic sheet on table.
    1. Make sure plastic is taut and winkle free.

ii. Lay layer of fabric on plastic sheet.

iii. Spread epoxy (weighed and measured amount) over fabric. Make sure there are no resin-rich or resin-dry areas. See Figure 9.
    1. Use a squeegee (little yellow tool in figure 10) to spread out epoxy.
        a. Make sure to only spread epoxy in the direction of the weave.
    2. Be careful when pulling the fiberglass off the table. Especially with 45 degree bias, the weave will deform, as shown in Figure 10. NOTE: Avoidance of deforming the glass as in Figure 10 is imperative.
        a. Tip: Pick up from an entire edge. If it is a wide piece of fabric, multiple people may be required.

Figure 10: Deformation of fiberglass during prepreg

b. Wet layup
    i. Place dry layer of fabric in the mold.
    ii. Spread epoxy (weighed and measured amount) over fabric. Make sure there are no resin-rich or resin-dry areas. See Figure 11.

Figure 11: Wet Layup

c. NOTE: It is generally easier to pre-preg at least the first layer of fabric. Spreading the epoxy evenly is easier on a planar surface.

13. Repeat steps 6 - 8 for each layer of fabric.
14. Ensure control surfaces and hatches are cut out of the core.

15. Ensure the whole layup team is aware of the layup and which layers go first, last, etc.

PART 5: VACUUM BAGGING

1. Place a layer of peel-ply on the wet part inside the mold.
    a. This is beneficial for bonding later. It is possible to vacuum bag without a layer of peel ply; sanding is required on areas where bonding will occur.
    b. It is light blue in color and not shiny. See Figure 12.
2. Place a layer of perforated ply on top of the peel-ply.
    a. It is blue in color, shiny, and has holes in it. See Figure 13.
3. Place a layer of breather on top of the perforated ply.
    a. It is white in color and is similar to a soft cloth. See Figure 14.
    b. If the layup is not a continuous part, connect the separated areas by strips of breather. This allows for all of it to be vacuumed.
4. Use extra breather for the medallion. This extra piece should be about 5"x5" in size and 2-3 plies in thickness.
    a. Cut a thin strip (about 5"x10" and fold it in half).

Figure 12: Peel Ply

Figure 13: Perforated Ply

Figure 14: Breather

5. Place the medallion in a flat area (on top of the extra breather).
    a. See Figure 15.
    b. NOT ON THE PART, ON A FLANGE.
6. Remove painter's tape from mold – carefully as to not peel up the release. See Figure 15.
    a. Tip: Fold the tape from the corner at a 45 degree angle and peel at an angle. See Figure 16.

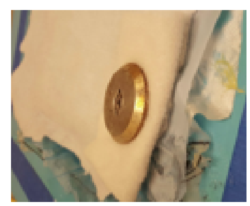

Figure 15: Medallion on Extra breather

Figure 16: Peeling tape without peeling off release

7. Place chromate along lines of where the painter's tape used to be. Make sure there are no bubbles. Especially on the corners. See Figure 17.
    a. For corners, simply cut the chromate at the end of a side and begin laying chromate perpendicular to previously laid chromate.

Figure 17: Chromate Application

8. Place the bagging along the chromate. Be sure there are no bubbles or air pockets.
    a. Bagging is blue. It is also very stretchy. See Figure 18.
    b. Press firmly on bag attached to the chromate. Press firmly especially on corners as corners are more susceptible to air pockets.
    c. BEST PRACTICE: Place the bagging material on the chromate on one side and continue placing the bag along adjacent edges. Placing the bag along chromate on parallel sides at the same time can be tricky (especially with dog ears).
    d. If there are deep contour in the part, dog ears will need to be made for the bag with chromate. See Figure 19.
        i. DOG EARS
            1. The dog ear shall be approximately as tall as the part is deep.
            2. Tip: Place the bagging on the chromate and remove the paper covering from the chromate and you place the bag down. This will help avoid air pockets.

Figure 18: Bagging

9. Cut a small slit where the vacuum will attach to the medallion. See Figure 20.
10. Apply vacuum pressure. Make sure the bagging is air tight. Listen for high-pitched noises (telling of air 'straws').

Figure 19: Dog ears

Vacuum pressure should be at about 24 psi (minimum of 20 psi is required).

11. Using the rollers, firmly roll over the entire part. This will ensure a strong bond between the fiberglass and core.
12. Write information on the bag:
    a. Team.
    b. Time and date the bag was sealed.
    c. Cure time needed.
    d. Circle the medallion so that the vacuum hole will be easier to find for the next layup.
        i. It is fun to draw a picture around it ;)
    e. What the bag is for (wing, tail, starboard wing, port wing, etc.).
13. Allow 12/24 hours vacuum time (depending on which epoxy mix was used).

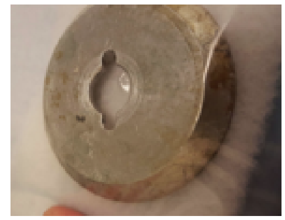

Figure 20: Slit in bag for vacuum

PART 6: CLOSING THE MOLD

1. Lightly sand anywhere a rib, spar, or any other interior part will go.
2. Place any interior parts (i.e. ribs, spars, bulkheads) and keep in place using small triangles of balsa without epoxying them to the part.
    a. Tack the balsa triangle to the part with CA. This will help keep the ribs and spars in place while the epoxy from the next step cures.
    b. Sand down internal parts where they do not sit flush with the fiberglass part.
3. Dry-fit the other half of the fiberglass part.
    a. Lightly press down and see if the seams close completely. If they do not, find the high spots on the internals and sand them down.
    b. Repeat until the top part fits perfectly.
        i. This step is time consuming and annoying but if not done correctly if will result in a poor/weak final product. Take the time and do it right.
4. Once everything is properly positioned, take it all out and clean both the fiberglass part and the internal structures with alcohol.
    a. This helps to ensure a solid bond.
5. Use resin/150 hardener mixed with 406 colloidal and chopped carbon to secure the ribs and spars into place. Do not remove balsa triangles.
    a. The resulting concoction was dubbed 'shower-drain'
    b. It is easiest to use a syringe to apply the epoxy.
    c. Make sure there are no voids in the epoxy line.
6. Allow epoxy to kick (1 – 2 hours).
    a. It should feel hard if it has kicked

    b. After curing, balsa triangles may be removed if desired, but not necessary.
7. Clean the tops of interior parts and the interior of the other fiberglass part with alcohol.
8. Using shower-drain, close out the interior parts by placing the shower-drain on the tops of the interior parts.
9. Use double sided tape to tape the other half of the part into the other mold.
    a. Make sure it is perfectly aligned and all the way in the mold
10. Carefully lower the other half of the mold onto the mold with all the interiors placed inside via Step 6. Make sure to align using chamfered holes/divots from Part 3: Molding Process Step 15.
11. Once the mold has been aligned, use one or more of the methods below to add weight to the mold to ensure the epoxy cures to the part:
    a. Vice grips along flanges.
    b. Sand bags and weights on one side of the mold.
12. Allow 12 hours cure time.

PART 7: SEALING SEAMS

1. Measure and cut fiberglass tape.
2. Weigh the fabric.
3. Mix resin/hardener (make sure to reference the ratios!).
    a. Use epoxy filled with 406 colloidal to fill the seams.
4. Apply fiberglass tape symmetrically to the seam. Use one of the two methods below:
    a. Pre-preg.
        i. Place plastic sheet on table.
        ii. Lay layer of fabric on plastic sheet.
        iii. Spread epoxy (weighed and measured amount) over fabric. Make sure there are no resin-rich or resin-dry areas. See Figure 9.
            1. Be careful when pulling the fiberglass off the table. Especially with 45 degree bias, the weave will deform, as shown in Figure 10. NOTE: Avoidance of deforming the glass as in Figure 10 is imperative.
                a. Tip: Pick up from an entire edge. If it is a wide piece of fabric, multiple people may be required.

Figure 10: Deformation of fiberglass during prepreg

    b. Wet.
        i. Place dry layer of fabric over seam.
        ii. Spread epoxy (weighed and measured amount) over fabric. Make sure there are no resin-rich or resin-dry areas. See Figure 11.

Figure 11: Wet Layup

5. Smooth epoxy over glass tape.
6. Allow 12 hours cure time.

PART 8: FILLING SEAMS – Smoothing the Surface

1. Mix a small amount of sandable epoxy (5/8 ratio of 400/150 resin/hardener combination).
    a. Add 410 filler until the mixture has a peanut butter consistency.
2. Smooth epoxy mixture to smooth out any bumps along where the fiberglass tape ends.
    a. Tip: Use your finger and carefully wipe epoxy up over the fiberglass lip onto the fiberglass seam. Smoother transitions from fiberglass seam to the main part will make the airflow smoother (especially over the wing) and make the paint job look better.
3. Allow cure time.
4. Sand down (starting with 180, 220, then 330) until the seam and transition is completely smooth. This is especially important on leading and trailing edges.
5. Clean off with damp paper towel.

PART 9: CONTROL SURFACES

1. Cut up from the trailing edge to the hinge line to create the control surface.
2. The piece that will be cut from the forward side of the hinge should be measured and cut from the core before the layup.
3. Cut the piece of the control surface out of the part.
4. Score the Kevlar with the scoring knife. Do not cut all the way through the Kevlar. Scoring the Kevlar will make it flexible and able to hinge.

Control Surface Wiper Fabrication Procedure

A.S. Arena

1) Read through this entire procedure *before* beginning.
2) Make sure that control surface can deflect enough in order to be able to work inside the gap (typically close to 90 deg.)
3) Look inside the control surface and wing gap in front of the shear webs. If there are any globs of epoxy, or anything else that would interfere with the wiper, make sure it is Dremmeled out and smooth.
4) See figure 1 for the following three steps
5) Apply masking tape to the wing so that its edge is flush with the edge of the wing cut. This is to eliminate the chance that epoxy will end up on the wing, and have to be sanded and re-painted.
6) Apply a strip of 3M double sided tape along the control surface. Make sure that the edge is flush with the forward edge of the control surface cut. Otherwise epoxy will run on to the outside of the control surface and have to be sanded later.
7) Apply a strip of 4 mil Mylar to the double sided tape and rub it down to make sure it sticks. The Mylar strip needs to be at least wide enough on the control surface side to cover the tape, and also long enough ahead of the control surface so that it is at least as long as the wiper plus a little extra.
8) Use masking tape or some other means to be able to hold the control surface open wide enough to be able to work. Make sure this is secure so the tape does not allow the control surface to slip.
9) Mix epoxy with thickener so that the epoxy will not run.
10) Apply a thin coat of the epoxy to the inside of the Mylar and into the control surface. Cover completely.
11) Apply a strip of fiberglass “tape” on top of the epoxy. Make sure it spans from the Mylar edge back to the shear web of the control surface.
12) Apply another layer of thickened epoxy on top of the fiberglass. Run a tongue depressor along the epoxy and on top of the fiberglass to make sure it is down along the Mylar and to remove any bubbles. It is better to have too much epoxy than too little. Thicker epoxy will not interfere with the operation of the wiper.
13) Make sure there is no epoxy on the outside of the Mylar. If there is, clean with alcohol.
14) Hold the control surface securely and remove the tape that is holding open the control surface.
15) Slowly close the control surface while guiding the Mylar strip into the wing. This is the most difficult part of the process. It may take two people. Use a clean thin sheet of Mylar or other thin tool in order to help carefully guide the entire Mylar strip into the wing.

16) Close the control surface to an angle slightly larger than the maximum angle the control surface will see in operation. For example, if control surface maximum deflection is 35 degrees, set the surface to about 40 degrees. The Mylar will curve into and under the wing skin.

17) Lock the control surface in that position with tape as was done to hold the control surface open earlier. This must be secure since if the tape fails before the epoxy cures, the wiper will have to be cut off and remade, and it will be more difficult since the fiberglass and epoxy will have to be ground out of the control surface under the skin.

18) Flip the wing upside down, and secure the wing in a position so that the Mylar strip is approximately level, or at least angled slightly towards the control surface. This will minimize the amount that the epoxy will sag as it starts to cure, before it enters the green state. Make sure that there is no way that any epoxy can sag back to interfere with the Kevlar hinge.

19) Let the epoxy cure to full hardness.

20) Turn the wing back over

21) Remove the tape securing the control surface open

22) Carefully try to open the control surface. The Mylar will prevent a secure bond, but there still will most likely be a “pop” or two, as the control surface is opened. It is not necessary to open it wide.

23) Carefully remove the Mylar from the tape, and from the wiper by sliding it out.

24) Move the control surface back to the previous position. (eg. 40 degrees if max deflection is 35)

25) Draw a line on the wiper along the edge where it goes under the wing skin and masking tape. That will be the cut line.

26) Open the control surface slightly to allow room to cut off the excess wiper.

27) Lock the control surface in that position using tape, and using a thin cutoff wheel, carefully cut along the line.

28) Remove the cut material, vacuum out the control surface.

29) Close the control surface and check operation. If some sanding needs to be done, slide a thin piece of sandpaper into the slot, close the surface, and sand the wiper or the skin for smooth operation.

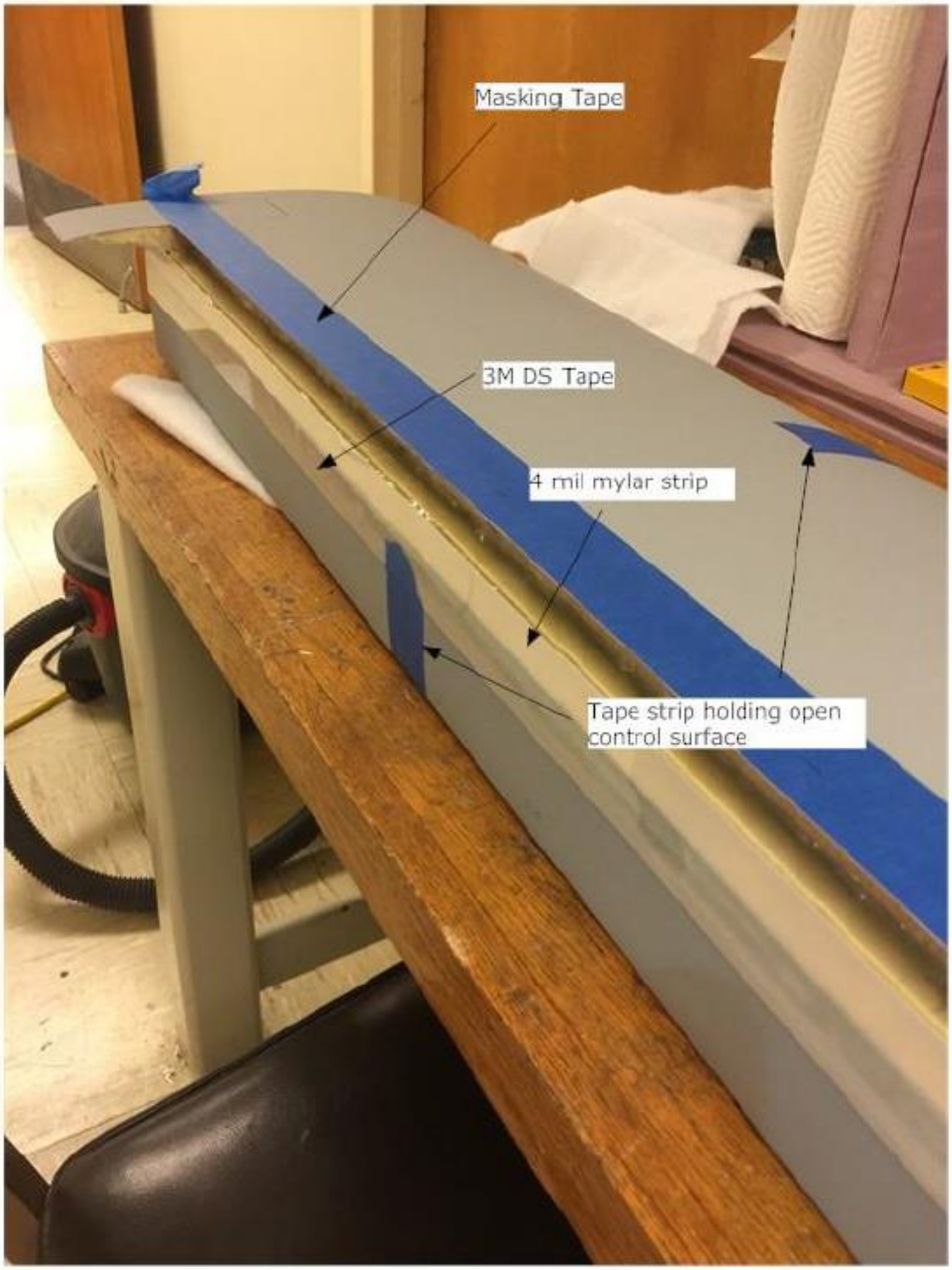
Masking Tape
3M DS Tape
4 mil mylar strip
Tape strip holding open control surface

Shear web spacing and wiper sizing for live control surfaces

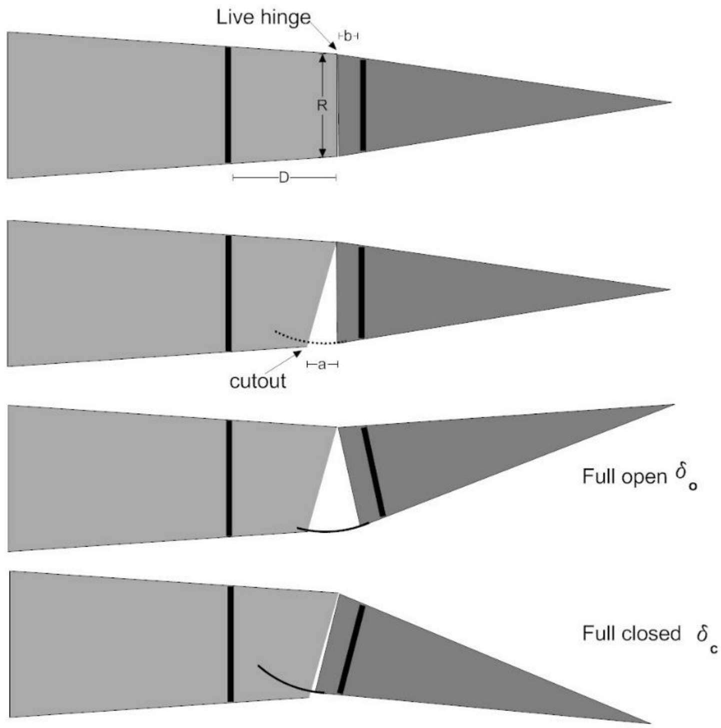

Notes:

- R is outside thickness, measured at thickest part of the entire control surface span.
- All measurements are clearance distances
- Kevlar on *inside* of live hinge surface (last layer in layup on female mold). No core on kevlar or opposite side of hinge. 3/8 to 1/2 wide.
- Bond ribs into kevlar hinge side of wing skin first so excess epoxy can be wiped off
- **D** = 1.6*R or larger. (never less than 0.25 in)
- **b** = R / 2 *or* 0.25 inch. Whichever is *larger*.
- Mark and cutout forward **a** = R * tan(δ_c) (make cut clean and straight. Line will be visible.)
- Wiper made using 4 mil mylar and double stick scotch tape.
- Mylar should extend approximately 1.2*R*(δ_o+δ_c) [rad] forward of the surface LE.
- Wiper length and curvature set by deflecting and holding flap with tape, several degrees larger than δ_o when wiper epoxy cures.
  Dont deflect much more than δ_o otherwise the wipers will not contact the surface.

Fuel System Diagrams

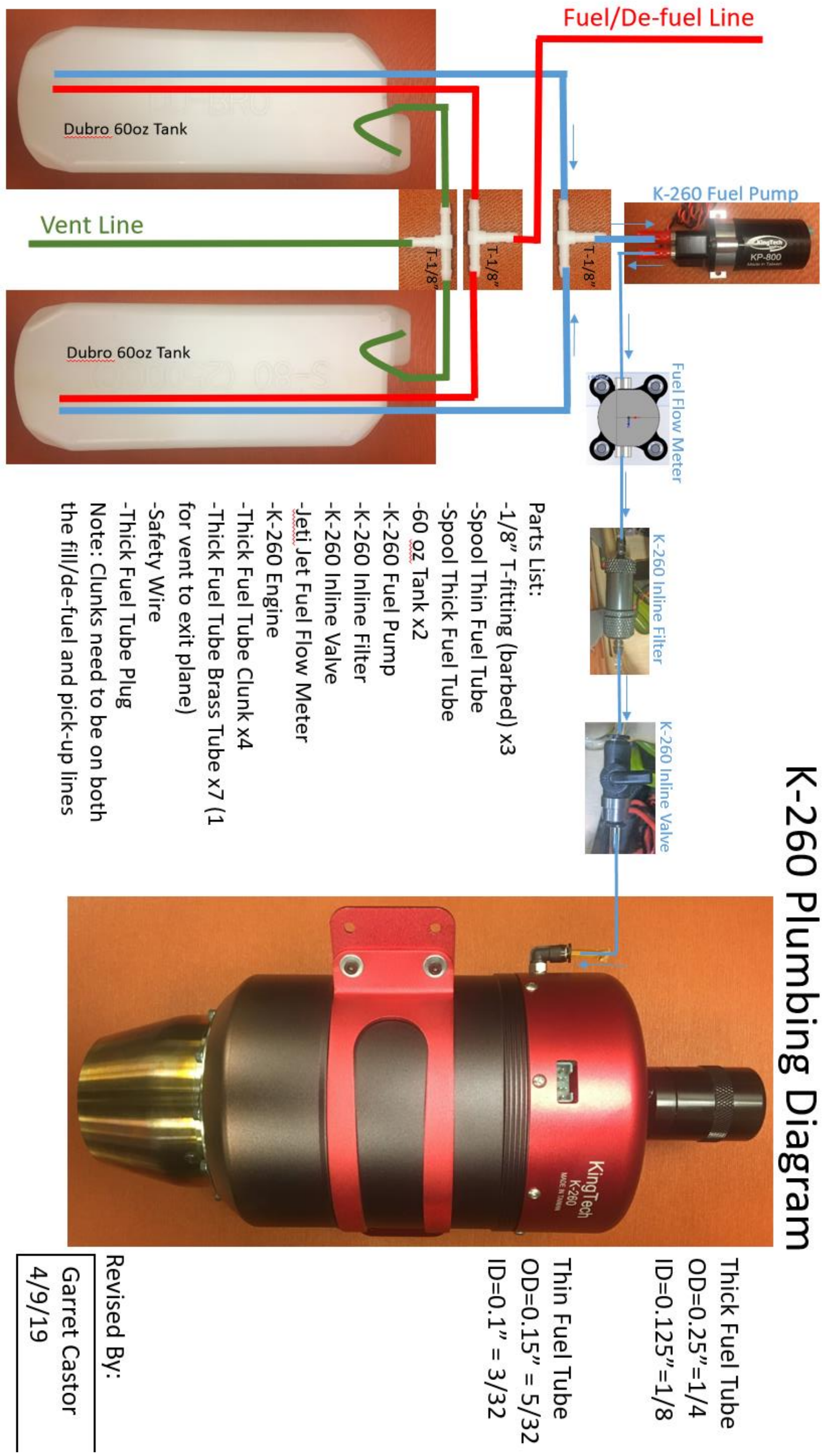

DA-120 Plumbing Diagram

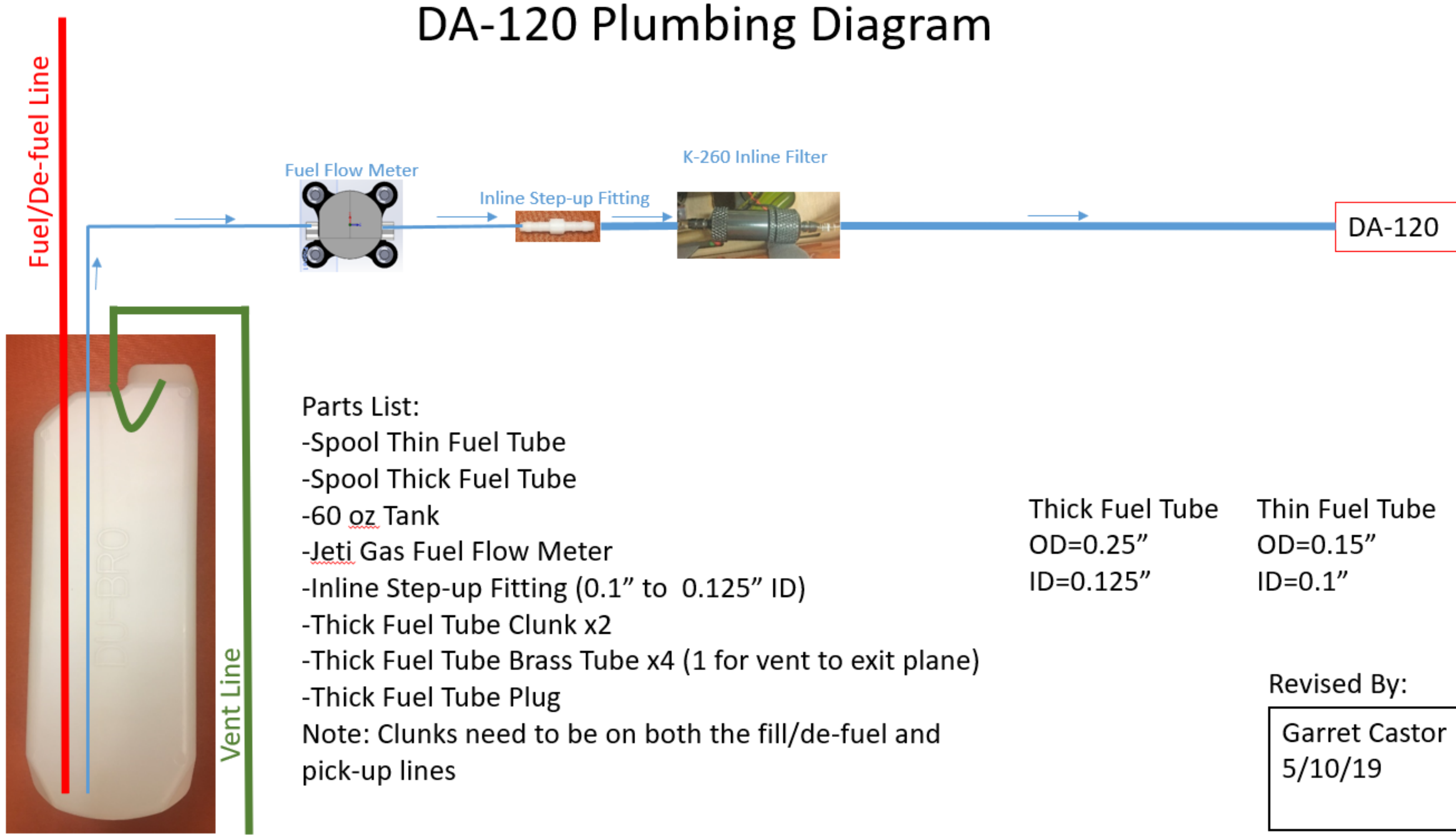

Parts List:
-Spool Thin Fuel Tube
-Spool Thick Fuel Tube
-60 oz Tank
-Jeti Gas Fuel Flow Meter
-Inline Step-up Fitting (0.1” to 0.125” ID)
-Thick Fuel Tube Clunk x2
-Thick Fuel Tube Brass Tube x4 (1 for vent to exit plane)
-Thick Fuel Tube Plug
Note: Clunks need to be on both the fill/de-fuel and pick-up lines

Thick Fuel Tube	Thin Fuel Tube
OD=0.25”	OD=0.15”
ID=0.125”	ID=0.1”

Revised By:

Garret Castor
5/10/19

VITA

Garret Oakley Castor

Candidate for the Degree of

Master of Science

Thesis: DESIGN AND DEVELOPMENT OF A CONTROLLABLE WING LOADING UNMANNED AERIAL SYSTEM

Major Field: Mechanical and Aerospace Engineering

Biographical:

Education:

Completed the requirements for the Master of Science in Mechanical and Aerospace Engineering at Oklahoma State University, Stillwater, Oklahoma in 2019.

Completed the requirements for the Bachelor of Science in Mechanical Engineering Magna Cum Laude at Oklahoma State University, Stillwater, Oklahoma in 2017.

Completed the requirements for the Bachelor of Science in Aerospace Engineering Magna Cum Laude at Oklahoma State University, Stillwater, Oklahoma in 2017

Experience:

Graduate Research Assistant to Dr. Andy Arena, Department of Mechanical and Aerospace Engineering, Oklahoma State University, August 2017 – December 2019. Responsibilities included: designing, manufacturing, and testing composite unmanned aerial vehicles and their accompanying systems.